Molecular characterization of the organelle contact facilitating protein Pex30 and its role in peroxisome dynamics in *Saccharomyces cerevisiae*

A Thesis

submitted in partial fulfilment of the requirements for the degree of

Doctorate of Philosophy

by

NAYAN MONI DEORI

(156106035)

Under the supervision of

Dr. Shirisha Nagotu (Main Supervisor)

Dr. Rajkumar P. Thummer (Co-Supervisor)

Department of Biosciences and Bioengineering
Indian Institute of Technology Guwahati
Guwahati-781039, Assam, India

January 2023

Dedicated to
Family and Friends

INDIAN INSTITUTE OF TECHNOLOGY GUWAHATI

Department of Biosciences and Bioengineering

Assam, Guwahati-781039

DECLARATION

I do hereby declare that the research findings in this thesis is the result of research work carried out by me in the Department of Biosciences and Bioengineering, Indian Institute of Technology Guwahati, India, under the supervision of **Dr. Shirisha Nagotu** and **Dr. Rajkumar P. Thummer.**

I also declare that the contents of this thesis have not been the basis for award of any other degree, diploma, fellowship or any other similar title of any other University or Institution.

As per general norms of reporting research findings, due acknowledgments have been made, whenever findings of other researchers have been cited in this thesis.

Date: 16-02-2023

Place: IIT Guwahati

Nayan Moni Deori

Nayan Moni Deori

INDIAN INSTITUTE OF TECHNOLOGY GUWAHATI

Department of Biosciences and Bioengineering

Assam, Guwahati-781039

CERTIFICATE

This is to certify that the work described in the thesis entitled **"Molecular characterization of the organelle contact facilitating protein Pex30 and its role in peroxisome dynamics in *Saccharomyces cerevisiae***" is an authentic record of the results obtained from the research work carried out by **Nayan Moni Deori** in the Department of Biosciences and Bioengineering, Indian Institute of Technology Guwahati, Assam, India, under my supervision and this work in part or as a whole has not been submitted elsewhere for the award of any other degree.

Dr. Shirisha Nagotu
Assistant Professor
Department of Biosciences and Bioengineering
Indian Institute of Technology Guwahati
Guwahati 781039, Assam, INDIA

Dr. Shirisha Nagotu

(Main Supervisor)

Dr. Rajkumar P. Thummer

(Co-supervisor)

Date: 16-02-2023

Place: IIT Guwahati

ACKNOWLEDGEMENTS

The work presented in this Ph.D thesis is the outcome of contribution extended by several individuals. It gives me immense pleasure to express my sincere appreciation for their support and encouragement throughout my Ph.D tenure.

First and foremost, I would like to take this opportunity to express my humble gratitude to my supervisor, **Dr. Shirisha Nagotu** for her guidance, expert suggestions and supervision that helped in successful completion of the undertaken research objectives. I thank her for providing the required facilities and a conducive environment to share and discuss several research ideas. Her expertise and willingness to share knowledge and experience has contributed immensely in improving quality of the research work. The intense brainstorming sessions and prolonged discussions on numerous research topics have encouraged the development of intellectual capability needed to carry out my research work. I am fortunate enough to have the opportunity to work as a student under her supervision.

I would also like to thank my co-supervisor **Dr. Rajkumar P. Thummer** for his valuable suggestions in overcoming the frequent hiccups encountered during the execution of many crucial experiments. His genuine feedbacks and advices have served as an inspiration to excel in many endeavours all through my Ph.D tenure.

I would like to express my sincere thanks to the doctoral committee members: **Prof. Sachin Kumar**, **Dr. Priyadarshi Satpati** and **Prof. Debapratim Das** for their critical suggestions, valuable discussions and scrutinization of the work carried out as part of this Ph.D thesis. I would also like to thanks **Dr. Avinash Kale** (University of Mumbai-Department of Atomic Energy, Centre for Excellence in Basic Sciences, Mumbai) for allowing me to work in his lab.

I acknowledge the past and present Heads of the Department of Biosciences and Bioengineering, **Prof. V. Venkata Dasu**, **Prof. Kannan Pakshirajan**, **Prof. Latha Rangan** and **Prof. Rakhi Chaturvedi** for providing all the departmental facilities during their tenure. I also acknowledge the Department of Biosciences and Bioengineering, IIT Guwahati and the institute as a whole for providing the infrastructural facilities required to carry out my research work. I am thankful to the office staff members of BSBE for their technical support.

I would like to acknowledge the Ministry of Human Resource Development, India (MHRD) and Indian Institute of Technology Guwahati for providing financial assistance during my Ph.D tenure.

I extend my warm and generous appreciation to the past and present members of **Organelle Biology and Cellular Ageing Lab (OBCAL)** for their constant support and encouragement. I would like to acknowledge my colleague **Rachayeeta** (a batch-mate / lab-mate / friend) for embarking on this journey together and sharing the ecstasy and agony of an adult life that we've experienced throughout this journey. Those therapeutic-esque conversations were indeed a necessity to declutter and rekindle my focus after repeated failed experiments. I would like to thank my juniors **Riddhi**, **Neha**, **Suchetana**, **Tanveera** and **Isha** for their cooperation that eventually helped me to meticulously execute many of the lab experiments. I would also like to extend my regards to **Sahaya** and **Terence** with whom I have worked as their lab supervisor and shared many remarkable moments (shenanigans *per se*) worthy of becoming folklores. I will profoundly cherish all those moments shared in the lab with **Ganesh, Agradeep, Abhigna, Jyoti, Atchaya, Jitika, Rishi, Hridayesh and others.** I would also like to acknowledge all lab members of **Stem Cell Engineering and Regenerative Medicine (SCERM)** for their support and cooperation.

Expressing a token of appreciation to my batchmates (Ph.D batch of December 2015) especially **Manas**, **Renu**, **Bhagyashree**, **Christy** and **Krishna** for making this Ph.D journey a wholesome one. Together we lived some precious moments while creating many memories that I shall be reminiscing for many long years to come.

Last but not the least, I would like to acknowledge the blessings and support of my family. Their love and trust provided me the strength in the relentless pursuit of my dreams and goals.

Finally, I submit my heartfelt gratitude to the Almighty Nature who governs everything.

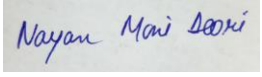

Date: 16-02-2023

Place: IIT Guwahati

Nayan Moni Deori

TABLE OF CONTENTS

ABSTRACT

Peroxisomes are single membrane-bound organelles found in most eukaryotes. They perform diverse cellular functions depending on the metabolic requirements of the cell. Scavenging harmful reactive oxygen species and β-oxidation of fatty acids are the most well-characterized functions of peroxisomes. They are dynamic in nature whose number and function may vary according to the need of the cell. Peroxisomes interact with other surrounding organelles like mitochondria, lipid droplet, endoplasmic reticulum (ER) *etc* to optimize their multiple cellular functions. Several peroxisomal proteins (Pex) have been identified with a role in various facets of peroxisome biogenesis and functions. Pex30 is one such peroxisomal protein that resides in the ER and associates with peroxisomes to regulate their biogenesis. It is a 58 KDa protein that consists of an N-terminal reticulon homology domain (RHD) and an uncharacterized C-terminal dysferlin domain. Recent studies have elucidated the role of Pex30 in the formation of pre-peroxisomal vesicles (PPVs) and lipid droplets (LDs) from the ER. Interestingly, it also associates with the ER reticulon proteins and functions in the maintenance of ER morphology. In this study, we aim to characterize the mechanism involved in the dual distribution of Pex30 and its function in peroxisome biogenesis. For this, we have looked at the role of uncharacterized interacting proteins of Pex30, the role of post-translational modifications and the role of various domains of the protein in its distribution and functions.

The distribution and expression of GFP-tagged Pex30 in *Saccharomyces cerevisiae* using a yeast expression vector was analyzed. We generated two constructs GFP-Pex30 and Pex30-GFP to confirm the correct terminal for tagging. Fluorescence microscopy revealed an interesting difference in phenotype and localization pattern for both the fusion proteins. Pex30-GFP displayed both punctate and reticulate distribution of the protein as reported in previous studies whereas GFP-Pex30 cells exhibited only the reticulate phenotype suggesting that N-

terminal tagging with GFP disrupted the punctate distribution of Pex30. Further our microscopic analysis revealed an interesting difference in the distribution of Pex30-GFP in cells grown in YND and oleic acid (OA) media. Reticulate distribution of GFP around the cell periphery along with discrete GFP puncta was observed in almost all the cells cultured in YND media. On the other hand, cells grown in OA medium exhibited two distinct phenotypes viz. only reticulate and both reticulate and punctate. In line with this, western blot analysis revealed reduced expression of Pex30 in OA as compared to YND. We further analyzed the distribution and expression of the protein in strains deleted for Pex30 interacting proteins such as Pet10, Erg6 and Mdm10. Our data indicates that the distribution and expression levels of Pex30 remains unaltered in the deletion strains. Quantification data indicates that cells lacking Mdm10 exhibits significant increase in peroxisome number as compared to WT cells.

Further, to understand the role of post-translational modifications (PTMs) in targeting and function of the protein, Pex30 was purified and the secondary structure was determined by far-UV circular dichroism (CD) spectroscopy. Our *in silico* analysis of CD spectroscopy data indicates that purified Pex30 retained its secondary structure which predominantly comprises of α-helices. Mass spectrometry analysis of the purified protein identified three residues at Threonine 60, Serine 61 and Serine 511 that are phosphorylated. The significance of phosphorylation status of Pex30 and its contribution in localization of the protein was then studied by modification of the phosphorylated residues to non-phosphorylatable and phosphomimetic mutant variants. Microscopy analysis of the mutant variants indicated that alteration in the phosphorylation status did not change the localization of the protein to peroxisomes and ER. Notably, a decrease in peroxisome number was exhibited cells expressing the phosphomimetic variants in OA media. This indicates that phosphorylation of Pex30 may be crucial in regulation of peroxisome abundance but not important for its targeting to peroxisomes and ER.

To understand whether the domains of Pex30 influence the sub-cellular localization of the protein and the regulation of peroxisome number, we constructed six different truncated versions of the protein. The growth kinetics of cells expressing the truncated variants did not differ significantly in comparison to cells expressing the full-length (FL) protein. Interestingly, each of these truncations showed distinct distribution patterns such as punctate, reticulate and cytosolic fluorescence. In addition, variable expression and localization of the truncated variants in both peroxisome-inducing and non-inducing growth conditions was observed. The absence of the entire dysferlin domain or only the C-Dysf leads to an increase in peroxisome number similar to that exhibited by cells lacking the FL protein. However, our data indicates that the dysferlin domain does not contribute to the reticulate distribution of Pex30.

In conclusion, our study sheds light on some interesting aspects of the regulation of Pex30 mediated peroxisome biogenesis.

LIST OF ABBREVIATIONS

Abbreviations

ACOX	Acyl-Coenzyme A Oxidase
ANOVA	Analysis of Variance
ATP	Adenosine triphosphate
CD	Circular Dichroism
CIAP	Calf Intestinal Alkaline Phosphatase
CoA	Coenzyme A
Dlp	Dynamin-like protein
Dysf	Dysferlin
ER	Endoplasmic Reticulum
ERMES	Endoplasmic Reticulum and Mitochondria Encounter Structure
FAD	Flavin Adenine Dinucleotide
GAPDH	Glyceraldehyde 3-phosphate dehydrogenase
H_2O_2	Hydrogen peroxide
IMAC	Immobilised Metal Ion Affinity Chromatography
LB	Luria-Bertani
LD	Lipid Droplet
MCS	Membrane Contact Site
MDV	Mitochondria Derived Vesicle
MS	Mass Spectrometry
OA	Oleic Acid
PBD	Peroxisome Biogenesis Disorder
PBS	Phosphate Buffer Saline

PCR	Polymerase Chain Reaction
PDH	Pyruvate Dehydrogenase
pER	Peroxisome-ER
Pex	Peroxin
PMP	Peroxisomal Membrane Protein
PPV	Pre-peroxisomal Vesicle
PTM	Post-Translational Modification
PTS	Peroxisomal Targeting Sequence
RHD	Reticulon Homology Domain
ROS	Reactive Oxygen Species
SAM	Sorting and Assembly Machinery
SDM	Site-Directed Mutagenesis
SDS-PAGE	Sodium Dodecyl Sulphate – Polyacrylamide Gel Electrophoresis
SGD	Saccharomyces Genome Database
SSB	SDS-Sample Buffer
TAE	Tris-acetate-EDTA
TAG	Triacylglycerol
TBS	Tris-buffered saline
TCA	Trichloro Acetic acid
WT	Wild Type

LIST OF FIGURES

LIST OF TABLES

Chapter 1

Introduction and Review of Literature

Abstract

Peroxisomes are highly dynamic organelles present in most eukaryotic cells. They also play an important role in human health and the optimum functioning of cells. An extensive repertoire of proteins is associated with the biogenesis and function of these organelles. Two protein families that are involved in regulating peroxisome number in a cell directly or indirectly are Pex11 and Pex30. Interestingly, these proteins are also reported to regulate the contact sites between peroxisomes and other cell organelles such as mitochondria, endoplasmic reticulum (ER) and lipid droplets (LDs). In this chapter, we review our current knowledge of the role of these proteins in peroxisome biogenesis in various yeast species. Further, we also discuss in detail the role of these protein families in the regulation of inter-organelle contacts in yeast.

Parts of this chapter are published as

1. **Deori NM**, Nagotu S (2022) Peroxisome biogenesis and inter-organelle communication: an indispensable role for Pex11 and Pex30 family proteins in yeast. Current Genetics 68, 537–550. https://doi.org/10.1007/s00294-022-01254-y
2. **Deori NM**, Kale A, Maurya PK, Nagotu S (2018) Peroxisomes: role in cellular ageing and age-related disorders. Biogerontology 19:303-324. https://doi.org/10.1007/s10522-018-9761-9

1.1 Introduction

A eukaryotic cell compartmentalizes its functions in membrane-bound structures called organelles. A huge amount of literature exists with respect to biogenesis, structure-function and degradation of these structures. Interestingly, a role for several organelles in various human diseases has been identified in the last decade. This has garnered incredible interest in understanding these essential structures. One such metabolically active organelle fondly referred to as "Cinderella" is the peroxisome [1]. Interest in peroxisome research comes from their two-fold importance: Lack of peroxisomes or absence of essential peroxisomal enzymes is associated with lethal disorders in humans and secondly, the interesting architecture of these organelles makes them very suitable for several biotechnological applications that need compartmentalization [2, 3].

Peroxisomes are single membrane-bound organelles present in almost all eukaryotes that perform a plethora of diverse cellular functions as a response to the metabolic requirements of the cell. Of all their functions, peroxisomes are well-characterized for their role in neutralizing harmful reactive oxygen species (ROS) produced by the cell and for β-oxidation of fatty acids [4, 5]. Peroxisomal β-oxidation is required for the oxidation of very long (>C20) and branched chain fatty acids. This culminates in the mitochondria where the shortened fatty acids subsequently undergo complete oxidation or act as precursors for the biosynthesis of lipids [6]. Peroxisomal β-oxidation is however not coupled to oxidative phosphorylation for the production of ATP. The oxidase enzymes involved in peroxisomal β-oxidation lead to the production of ROS such as superoxide radicals, hydroxyl radicals and hydrogen peroxide (H_2O_2) [7]. Unlike β-oxidation, α-oxidation is exclusively localized to peroxisomes in mammalian cells. Phytanic acid and long chain fatty acids like 2-hydroxy fatty acids and 3-methyl branched fatty acids are first converted to their CoA esters. After further decarboxylation and oxidation it enters the β-oxidation pathway [8]. Synthesis of ether lipids

such as plasmalogens, that act as ROS-protecting lipids is another major function of peroxisomes [9]. The synthesis of ethanolamine plasmalogens which are major constituents of most biological membranes are initiated in peroxisomes [10]. The peroxisomal enzyme dihydroxyacetone phosphate acyltransferase (DHAPAT) facilitates the esterification of dihydroxyacetone phosphate (DHAP) with a long chain acyl CoA ester [11]. The acyl chain of acyl-DHAP is then substituted by alkyl-DHAP synthase (ADHAP-S) to form alkyl DHAP linkage [10]. The subsequent steps involved in the synthesis of plasmalogen are catalyzed by enzymes localized in the ER [12, 13].

Peroxisomes in mammalian cells house several oxidases that generate different ROS species like superoxide radicals, hydroxyl radicals and H_2O_2. In mammalian cells, the oxidative breakdown of fatty acids, purines, amino acids and polyamines catalyzed by oxidases results in the transfer of hydrogen from the substrates directly to O_2 thereby generating H_2O_2. Peroxisomal fatty acid oxidation begins with the conversion of fatty acids into acyl-CoA (catalysed by acyl-coenzyme A oxidase (ACOX)). This conversion happens in the cytosol in yeast and mammalian cells and the fatty acyl CoA is imported via membrane transporters into the peroxisome [14, 15]. This reaction leads to transfer of electrons from FAD to oxygen thereby generating H_2O_2 and is the common source of H_2O_2 in all organisms [7]. The metabolism of primary amines like methylamine or ethylamine are catalyzed by the peroxisomal enzyme amine-oxidase. Peroxisome also harbors enzymes such as urate oxidase and d-amino acid oxidase that aids in the metabolism of d-alanine [16, 17]. Plant peroxisomes are involved in the regulation of glyoxylate cycle that enables growth in the absence of glucose; where the two carbon compounds such as ethanol and acetate are the only available source of carbon [17]. The key enzymes involved in glyoxylate cycle are isocitratelyase (Icl1) and malate synthase (Mls1). Mls1 is localized to peroxisomes and cells devoid of either Mls1 or Icl1 are unable to utilize ethanol or acetate as carbon sources [18, 19]. Peroxisomes also play a

significant role in methylotrophic yeast species such as *Hansenula, Pichia, Candida, etc* which can utilize methanol as the sole source of carbon [17, 20]. In these methylotrophs, the oxidation of methanol leads to the accumulation of harmful and toxic components such as formaldehyde and hydrogen peroxide [21]. The peroxisomal ROS scavenging enzymes functions in the proper metabolism of formaldehyde generated from methanol preventing further toxicity caused by the production of formaldehyde [20, 21]. Peroxisomes also act as site for neutralization of the highly reactive hydrogen peroxide.

A role for peroxisomes in antiviral signaling upon infection of reovirus and influenza virus was recently reported [22, 23]. Noise-induced hearing loss, a type of hearing impairment is characterized by increased oxidative stress in the cochlear sensory hair cells and auditory neuron of the inner ear. Enhanced proliferation of peroxisomes in these cells lead to redox homeostasis and buffers against the harmful effects caused by oxidative stress [24]. Studies reveal a role for peroxisomes in brain development and functioning. Patients lacking peroxisomes or specific peroxisomal functions show an aberrant development of the brain and also may develop neurodegenerative disorders [25]. Abnormalities in brain development are also characteristic of peroxisome biogenesis disorders (PBD) caused due to defects in peroxisomal biogenesis proteins [25, 26]. Peroxisomal dysfunction as a result of altered organelle assembly has also been linked to the early onset of many age-related diseases like Psoriasis, Type-II Diabetes, Hypertension, Alzheimer's and Parkinson's disease [27, 28]. Peroxisome abundance changes during brain development and also the number of peroxisomes vary in different regions of the brain and may contribute to an imbalance in ROS levels upon ageing. A role for neurodegeneration in several brain related diseases/disorders is under investigation. [29]. Patients lacking either all peroxisomal functions or a single enzyme or transporter function are reported to exhibit neurological defects. These defects can be typically associated with aberrant development of the brain, demyelination and loss of axonal integrity,

neuro inflammation or other neurodegenerative processes [25]. Several recent studies suggest a role for peroxisomes in the development of neurodegenerative diseases [25, 30]. A common aspect to most neurodegenerative disorders is their association with oxidative stress irrespective of different pathological and clinical features. Type 2-diabetes mellitus is caused due to defects in insulin action and generally remains undiagnosed for many years because symptoms of high blood glucose level or hyperglycemia are not easily noticeable. Ageing, obesity, familial predisposition, a prior history of gestational diabetes, impaired glucose homeostasis and physical inactivity are some of the major risk factors for type 2-diabetes [31]. As mentioned above peroxisomes participate in lipid metabolism, and are a major source of cellular ROS. Reduced expression/repression of catalase in β-cells may be considered as one of the reasons for their vulnerability to oxidative stress [32]. Overexpression of catalase in peroxisomes and not in mitochondria reduced the oxidative stress and resulted in the protection of β-cells from lipotoxicity [33]. Long chain saturated fatty acids also exhibit strong cytotoxic effects on insulin producing β cells [34]. Increased plasma concentrations of non-esterified fatty acids (NEFAs) resulting in pancreatic β-cell dysfunction and apoptosis are associated with Type 2-diabetes. Generation of harmful H_2O_2 during peroxisomal β-oxidation of long-chain saturated NEFAs in rat β-cells was reported to be prevented by unsaturated NEFAs [35, 36]. A role for peroxisomal H_2O_2 and not H_2O_2 generated from mitochondria in lipotoxicity was also reported [33, 34]. Several studies also suggest a role for peroxisomal H_2O_2 in the development of diabetic neuropathies and osteoarthritis [37-39]. Reduced activity of GNPAT, a peroxisomal enzyme required for plasmalogen synthesis at the onset of insulitis also highlights the role of peroxisomes [40]. Growing evidence now suggests a direct or indirect role for peroxisomes in the development of cancer [41]. Altered expression of peroxisomal proteins, mislocalization of essential peroxisomal enzymes, altered ROS production include factors that may contribute to cancer. Reduced catalase levels have been reported in various cancers [42, 43]. An association

between ether lipid synthesis - a peroxisomal metabolic process and cancer is signified by the upregulation of ether lipids in several cancers. Studies also identified up regulation of AGPS (Alkyl-glycerone phosphate synthase) an essential enzyme of ether lipid synthesis across several cancers [44]. Enzymes like monocarboxylate transporter (MCT) 2, α-methylacyl-CoA racemase (AMACR) localized to peroxisomes also exhibit altered expression levels in various cancers [45-48]. Uyama and colleagues have reported mislocalization of peroxisomal proteins and decrease in ether lipid levels upon overexpression of the tumor suppressor H-rev107 in cells [49]. Later, it was also reported that H-rev107 interacts with Pex19, a peroxisomal membrane protein and inhibits its function [50]. Another observation that points towards a role for peroxisomes, is the upregulation of α-methyl-CoA racemase (AMACR) that is localized to both mitochondria and peroxisomes in cancer cells [51]. Recent studies identified that the tumor suppressors, ATM and TSC involved in the mTORC1 pathway are localized to peroxisomes. The authors reported a role for these proteins in regulating peroxisome numbers by modulating pexophagy [52]. Therefore, an adequately functioning peroxisome is a pre-requisite for healthy cell.

Recently artificial peroxisome that mimics the antioxidant properties of a natural peroxisome was designed and has been shown to have a therapeutic effect in conditions like Ischemic stroke [53]. On the other hand, peroxisomes are also explored as the new cellular hub for metabolic engineering and the production of compounds of interest in yeast [54].

Important features that distinguish peroxisomes from other cell organelles are import of fully folded matrix proteins that contain specific targeting sequences, two accepted pathways of membrane protein trafficking to the organelles – direct and via the ER, semi-autonomous nature of the organelles and extensive collaboration with other cellular structures to maintain cellular homeostasis.

1.2 Protein targeting and import: matrix and membrane proteins

Peroxisomal matrix proteins are composed of two different peroxisomal targeting signals PTS1 and PTS2 that are recognized by the receptors Pex5 and Pex7, respectively (Fig. 1.1A) [55, 56]. Most peroxisomal matrix proteins consist of a PTS1 which is a carboxy-terminal tripeptide with the consensus sequence [S/A/H/C/E/P/Q/V] [K/R/H/Q] [L/F] in yeast [57]. A smaller subset of peroxisomal matrix proteins consists a PTS2 which is an amino-terminal nonapeptide consisting of the consensus sequence (R/K) (L/V/I)-X_5-(H/Q) (L/A) [58]. In addition, Pex5 recognizes a PTS3 signal responsible for sorting acyl-CoA oxidase to peroxisomes in *S. cerevisiae* (Fig. 1.1A) [59]. Unlike PTS1 and PTS2 that are linear sequences, PTS3 was identified as a signal patch comprising of amino acid residues that are distant from each other in the primary protein sequence. However, these amino acid residues align close to each other in the folded protein [59]. Recent studies identified Pex9 as a paralog of Pex5 that functions as a PTS1 receptor in *S. cerevisiae* (Fig. 1.1C). Import of PTS1 proteins such as malate synthases Mls1 and Mls2 requires Pex9 [60, 61]. Some peroxisomal proteins that lack any recognizable PTS signal are transported to peroxisomes by a mechanism called "piggy-backing" [62]. Some examples of such import are Malate dehydrogenase 2 (Mdh2), nicotinamidase (Pnc1), hydrolase (Lpx1) *etc* [62, 63]. The receptor-cargo complexes interact with the docking complex at the membrane and subsequently translocate into the matrix and release the cargo. Following this, the receptor is recycled for another round of import [64].

The sorting mechanism of peroxisomal membrane proteins (PMPs) is less elucidated compared to the matrix protein import and both these pathways seem to be independent of each other. Mutants incompetent of importing peroxisomal matrix proteins can still target the PMPs resulting in the formation of empty peroxisomal structures called "ghosts" [65, 66]. PMPs are either targeted to the peroxisomal membrane directly or can traffic through the ER in the form of vesicles (Fig. 1.1B) [67, 68]. A role for Pex19 as either a receptor or chaperone in the direct

targeting of PMPs to peroxisome membrane has been reported (Fig. 1.1B) [69, 70]. Pex3 is suggested to act as a docking partner at the membrane in this pathway [71]. Surprisingly, not much is known regarding the mechanism of insertion of these proteins into the membrane [68]. A recent study highlights localized translation as an important means of accurate targeting of membrane proteins to peroxisomes [72]. An alternative route, where PMPs are targeted to the ER and subsequently are sorted into specialized regions called peroxisomal-ER (pER) also exists in yeast (Fig. 1.1B) [73]. Further, these PMPs are pinched off from the ER in the form of heterogenous vesicles called pre-peroxisomal vesicles (PPVs) and undergo fusion [67, 74]. An important role for Pex19 and Pex3 in pinching off these vesicles has been reported [67, 74]. Interestingly, recent studies identified the presence of vesicular structures in cells lacking Pex19 and Pex3, emphasizing that multiple routes of trafficking may exist that may also vary in the cargo that is transported [75, 76].

1.3 Peroxisomes: semi-autonomous in nature

An interesting feature of peroxisomes is their ability to increase in number in response to external cues. This increase in the number in yeast is either by the division of existing organelles or by *de novo* formation from the ER, making them semi-autonomous in nature (Fig. 1.1).

De novo formation has been extensively studied and reported in several model organisms (Fig. 1.1C) [74, 77]. Functional peroxisomes are undetectable in yeast mutant cells that lack PMPs such as Pex3 [67, 70, 78]. However, upon reintroduction of these PMPs, appearance of import-competent peroxisomes in the mutant cells was reported [78, 79]. As mentioned above (section 1.2), PMPs are targeted to the ER and further exit the ER as PPVs in the absence of functional peroxisomes in a cell [67, 76]. The PPVs either fuse together or invariably develop into nascent peroxisome and subsequently mature by importing matrix proteins and other PMPs (Fig. 1.1C) [67, 76, 80]. Evidence from *in vitro* and *in vivo* experiments from various yeast

models suggests that different subtypes of PPVs exist [67, 75, 76]. A role for the ESCRT-III complex in the formation of functional peroxisomes has also been reported [81]. Interestingly, yeast cells impaired in peroxisome inheritance also exhibit *de novo* biogenesis [82, 83]. In mammals, the role of mitochondria in peroxisome biogenesis has also come to light in recent years. Mitochondria-derived vesicles (MDVs) that can ferry selected cargoes, fuse with the peroxisome and may aid in peroxisome biogenesis [84]. In patients with Zellweger syndrome, distinct vesicles from the mitochondria and the ER fuse together to form new peroxisomes [85].

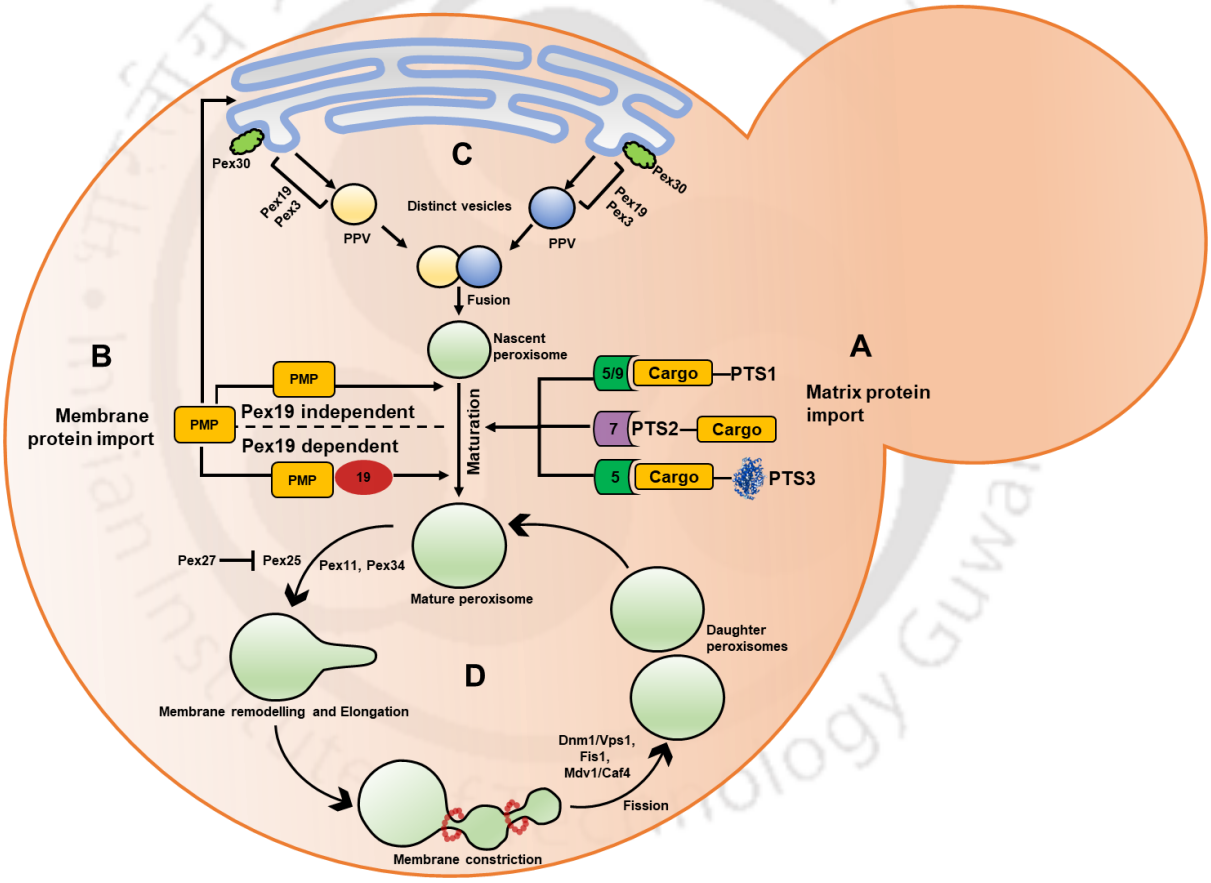

Fig. 1.1 An overview of various pathways involved in the biogenesis of peroxisomes in yeast
The figure depicts fours important aspects of peroxisome biogenesis: growth and division, *de novo* formation, matrix protein import and membrane protein trafficking. **(A)** Matrix proteins and PMPs are subsequently targeted to the nascent peroxisome resulting in the formation of a mature peroxisome. Import of peroxisomal matrix proteins containing PTS1 and PTS2 is facilitated by the receptor proteins Pex5 and Pex7 respectively [55, 56]. Peroxisomal proteins containing a PTS3 signal patch are also recognized and translocated to peroxisomal matrix by Pex5 [59]. In addition, Pex9 also acts as a receptor for a limited set of PTS1 containing proteins [60]. **(B)** PMPs can either be targeted to peroxisome membrane directly or alternatively are first targeted to the ER and then inserted into peroxisome membrane via the vesicular transport [68]. In the direct pathway, the PMP targeting sequences (mPTS) are recognized by Pex19 and the Pex19-PMP complex interacts with Pex3 that results in the docking of receptor-cargo protein complex on the peroxisome membrane. PMPs can also be targeted directly to

peroxisome in a Pex19-independent mechanism [86]. **(C)** An alternative mode of peroxisome biogenesis called *de novo* formation that involves ER has been reported. In the absence of functional peroxisomes, PMPs are trafficked through the ER in the form of PPVs [67]. The ER-resident protein Pex30 is enriched at the site of PPV formation and acts in concert with the reticulon proteins and aids in regulating the tubular structure of ER [87]. The PPVs are pinched off from the ER with the help of Pex19 and Pex3 [68]. Biochemically distinct PPVs fuse to form a nascent peroxisome [67]. **(D)** Peroxisomes are predominantly formed by growth and division in yeast cells. Three mechanistic steps – elongation of the membrane, constriction and fission constitute the division process. Elongation of the membrane of a pre-existing peroxisome requires proteins belonging to the Pex11 family (Pex11 and Pex25) [88, 89]. Antagonistic role for Pex27 has also been reported [89]. Pex34 on the other hand functions as a positive regulator of peroxisome number and can act independently or in association with the Pex11 family proteins [90]. The elongated membrane undergoes constriction whose mechanistic details are unknown. In the final step, proteins involved in peroxisomal fission (Dnm1, Vps1, Fis1, Mdv1 and Caf4) assemble at the site of constriction [91, 92]. Fis1 together with the adapter proteins Mdv1 and Caf4 recruits Dnm1 to the peroxisomal membrane [92, 93]. The GTPase activity of Dnm1 is stimulated by Pex11 resulting in scission of the elongated membrane thereby forming new daughter peroxisomes [92, 94, 95].

In the growth and division model, new peroxisomes are formed by elongation of the membrane of a pre-existing peroxisome followed by constriction and final scission separating the daughter peroxisomes (Fig. 1.1D) [96, 97]. Proliferation by fission is also coupled with retention and inheritance of peroxisomes dependent majorly on Inp1 and Inp2 in yeast cells [98, 99]. The central player required for membrane elongation is Pex11, followed by fission by dynamin-related proteins (DRPs) [88, 95, 100-102]. We refer the readers to a recent paper that discusses in detail about the various facets of Pex11 in different organisms [103]. Similar to Pex11 a conserved role for Dnm1 and its homologs in peroxisome fission has been reported [92, 94]. Interestingly, the complex of proteins associated with Dnm1 required for mitochondrial fission is also required for the division of peroxisomes in yeast [93, 97].

1.4 Regulation of peroxisome number in yeast: two multifaceted protein families

To date several proteins are identified that regulate the formation of peroxisomes and are involved in the import of matrix and membrane proteins required for the maturation of nascent peroxisomes [104, 105]. Interestingly, the abundance, size or dynamics of peroxisomes are influenced by distinct set of proteins whose deletion leads to abnormal peroxisome number or size. In this section we discuss two such protein families: Pex11 and Pex30 (Fig. 1.2).

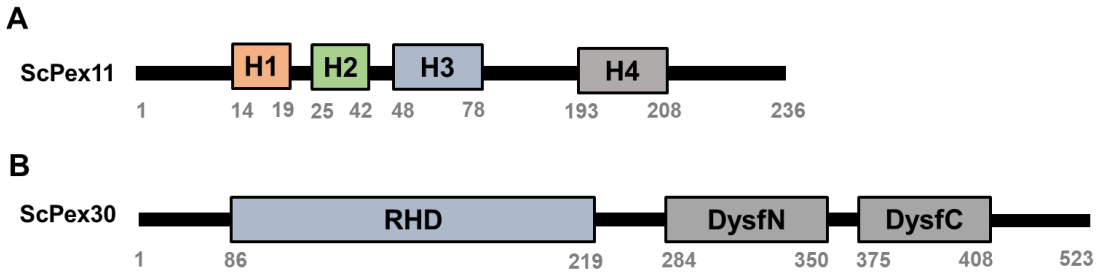

Fig. 1.2 Graphical representation of the *S. cerevisiae* Pex11 and Pex30
(A) *S. cerevisiae* Pex11 is a 236 amino acid membrane protein. Four helical domains, three at the N-terminus (H1, H2 and H3) and one at the C-terminus (H4) have been identified in the protein. A role for the H3 helical domain in the membrane remodelling has been reported [86, 88]. **(B)** Pex30 is a 523 amino acid protein and consists of two distinct domains: Reticulon homology domain (RHD) and the dysferlin domain. A role for the RHD domain in the ER membrane tubulation and the dyferlin domain in Pex30-dependent peroxisome and LD biogenesis has been reported [87, 106].

1.4.1 Pex11 family

Proteins that are the main regulators of peroxisome proliferation and maintenance in all studied model organisms belong to Pex11 family [107, 108]. These proteins are highly conserved in different yeast species [109]. In *S. cerevisiae*, this family comprises of Pex11/Pex25/Pex27 whereas in *Yarrowia lipolytica*, *Ogataea polymorpha* and *Komagataella phaffii* paralogs Pex11, Pex25 and Pex11C are identified [90, 109-111]. *S. cerevisiae* Pex34 was also reported to have a weak homology with Pex11 [90]. A novel peroxin Pex36 identified in *K. phaffii* shows functional homology to *S. cerevisiae* Pex34 [112].

Pex11 is the most extensively studied protein in this family. Interestingly, unlike other PMPs that consist of multiple Pex19 binding sites, Pex11 harbors a single Pex19 binding site that also functions as mPTS for its peroxisome targeting in *K. phaffii* [86]. Interestingly, an additional Pex19-independent mPTS that is sufficient for trafficking to peroxisomes has also been identified in Pex11, suggesting that its interaction with Pex19 may not be essential for peroxisomal localization in *K. phaffii* [86].

Reduction in peroxisome number and an increase in organelle size are reported in cells lacking Pex11 in most yeast models, whereas overexpression results in increased number of comparatively smaller peroxisomes [98, 101, 113]. Loss of Pex11 also results in other

phenotypes associated with peroxisomes and specifically identified in certain yeast species. For instance, *Y. lipolytica* cells lacking Pex11 depict loss of morphologically identifiable peroxisomes resulting in mislocalization of matrix proteins and enhanced degradation of membrane proteins [102]. A defect in peroxisome retention in mother cells lacking Pex11 and a role in the re-distribution of PMPs on the peroxisome membrane was also identified in *O. polymorpha* [98, 114].

The conserved amphipathic α-helix at the N-terminus of Pex11 imparts the membrane remodelling property to the protein that aids in the elongation of the peroxisome membrane prior to fission [88] (Fig. 1.2A). Molecular dynamics simulations indicate that the amphipathic region of Pex11 (H3) oligomerizes on the peroxisomal membrane to induce membrane curvature [115]. Mutations disrupting the oligomerization of Pex11 were associated with loss of membrane remodelling property of the protein, thereby indicating a direct link between the oligomerization and the function of Pex11 [115]. In addition, the amino-terminal region of Pex11 was also reported to stimulate the GTPase activity of Dnm1 resulting in the final scission of peroxisomal membranes [95]. Pex11 has also been implicated in the formation of non-selective membrane channels in peroxisomal membranes [116]. Mutations in the channel-forming region of the protein affects the rate of peroxisomal β-oxidation highlighting its role in the transfer of metabolites across the membranes [116].

Available literature does not provide a mechanistic understanding of the role of Pex25 and Pex27 in the regulation of peroxisome biogenesis. The triple deletion cells (*pex11pex25pex27*) in *S. cerevisiae* are characterized by reduced number of peroxisomes highlighting their role in peroxisome formation [89, 117]. Earlier studies identified a role for Pex25 in actin assembly on the peroxisome membrane by recruiting the GTPase Rho1 to the peroxisome membrane [118]. A role for Pex25 in the *de novo* biogenesis of peroxisomes in cells lacking functional peroxisomes was reported in *S. cerevisiae* [89]. In addition, deletion of

Pex11C or Pex25 resulted in fewer and enlarged peroxisomes in *Y. lipolytica* [102]. Transcriptome analysis indicated upregulation of the expression levels of Pex11 and Pex25 when *O. polymorpha* cells were cultured in peroxisome-inducing growth conditions (methanol) whereas Pex11C was reported to be downregulated [111]. Interestingly, a role for Pex25 in Pex19 mediated interaction with PMPs has been suggested in *K. phaffii*. Using various C and N-terminal truncations of Pex19, the authors reported that Pex25 strengthens the interactions between Pex19 and certain PMPs and thereby aids in peroxisome biogenesis [119].

A variable effect of phosphorylation of Pex11 on its function in various yeast species has been reported [120]. Phosphomimetic mutants of Pex11 resulted in enhanced peroxisome proliferation in *S. cerevisiae* [121]. Phosphorylation of the protein promoted its interaction with the peroxisome fission protein, Fis1 in *K. phaffii* [101]. However, the phosphorylation status of Pex11 in *O. polymorpha* did not have any effect on peroxisomal fission, indicating the role of an alternate mechanism to regulate the function of Pex11 in *O. polymorpha* [100].

1.4.2 Pex30 family

The second set of proteins that regulate peroxisome number and size in yeast belong to the Pex30 family. Interestingly, the number of proteins in this family and their nomenclature is largely variable among different yeast species [109]. The methylotrophic yeasts *O. polymorpha* and *K. phaffii* consist of four proteins Pex23/24/29/32 and Pex24/29/30/31 respectively [109, 122]. In *Y. lipolytica*, Pex23/24/29 and five homologs Pex28/29/30/31/32 have been identified in *S. cerevisiae* [106, 109]. Proteins of the Pex30 family invariably share similar domain architecture comprising of transmembrane domains in the N-terminus and a dysferlin domain at the C-terminus [106, 123] (Fig. 1.2B). A recent study describes a phylogenetic analysis of these proteins [124].

Interestingly, the phenotype of yeast cells lacking proteins belonging to this family is variable in different yeasts studied. All data, however points towards an important role of these

proteins in peroxisome biogenesis. Cells lacking Pex30 or Pex31 depicted fewer and enlarged peroxisomes in *K. phaffii* cells [123]. Similar peroxisome morphology was observed in *S. cerevisiae* cells lacking the homologs Pex31 or Pex32 [125]. In contrast, an increase in the number of peroxisomes was reported in cells deleted for Pex28, Pex29 or Pex30 in *S. cerevisiae* [125, 126]. *O. polymorpha* cells lacking Pex24 and Pex32 are characterized by the presence of small-sized peroxisomes and cells lacking Pex32 displayed cytosolic localization of peroxisomal matrix proteins [122]. A similar observation was also reported in *Y. lipolytica* lacking Pex23 or Pex24 [127, 128]. In addition, mutants devoid of Pex24 in *O. polymorpha* displayed a defect in the inheritance of peroxisomes [122].

Combination deletion of members of the Pex30 family revealed that Pex28 and Pex29 function upstream of Pex30, Pex31 and Pex32 and regulate peroxisome number and size in *S. cerevisiae* [125]. Interestingly, in *S. cerevisiae,* deletion of Pex30 in cells already lacking Pex11 leads to the restoration of peroxisome number to the WT level. This suggested that Pex30 can function as a negative regulator of peroxisome abundance [129]. Experiments in *K. phaffii* revealed an important role for the dysferlin domain in the regulation of peroxisome number in OA cultured cells [123]. Intriguingly, in cells lacking Pex30 or Pex31 abnormal peroxisome morphology was observed only in oleate-containing media, whereas cells cultured in methanol exhibited peroxisome morphology similar to that of the WT cells in *K. phaffii* [123].

In justification to their name, most PMPs are largely localized to peroxisomes. Interestingly, proteins of the Pex30 family do not fall in this category and show significant localization to ER [124]. However, it is still not decisive under what conditions these are exclusively localized to ER or show dual localization to ER and peroxisomes [122, 123, 129, 130]. On the other hand, a role for Pex19 interaction in the localization of Pex30 and Pex32 to peroxisomes in *S. cerevisiae* has also been reported [131].

After the initial studies in various yeasts that suggested a role for proteins of Pex30 family in the regulation of peroxisome number and morphology, further studies identified a very interesting role for these proteins in the formation of peroxisomes from the ER. However, the exact mechanistic details as to how these proteins aid in the regulation of peroxisome number is still not clear. Interaction of Pex29 and Pex30 with a subset of ER-resident proteins (Rtn1, Rtn2 and Yop1) has been reported in *S. cerevisiae* [130]. Electron micrographs demonstrated that the overexpression of Pex30 and Pex31 in *rtn1rtn2yop1* cells restores the ER morphology indicating the role of these proteins in maintaining the tubular structure of ER [87]. Further, the Pex30 enriched regions on the ER were demonstrated to be the site of origin of nascent PPVs in *S. cerevisiae* [87]. On the other hand, loss of Pex30 and Pex31 resulted in clustered PPVs and further reduced the rate of *de novo* peroxisome formation [87]. In *O. polymorpha* all the members of the family were reported to localize to ER. Interestingly, only Pex24 and Pex32 were observed to be localized to a distinct domain on the ER [122].

1.5 Peroxisome membrane contact sites: contribution of Pex11 and Pex30 family proteins

The majority of the metabolic pathways occurring in a cell are compartmentalized in different organelles. Organelles harbour unique enzymes and physiological conditions specific to a metabolic pathway. However, interaction with the surrounding organelles is essential to optimize their functions and for the exchange of resulting products of these pathways [132, 133]. For efficient transfer of metabolites, organelles must establish close-range interactions where the membranes of two juxtaposed organelles are in physical contact [133]. This point of interaction between two neighbouring organelles, termed as membrane contact site (MCS), is facilitated via proteins that act as tethers or by protein-lipid interactions leading to the formation of tethering structures. Peroxisomes interact dynamically with various cellular structures such as plasma membrane, vacuole, ER, mitochondria and LDs [134-136]. However,

in this section, we focus on those peroxisome-organelle contacts that are mediated by Pex11 and Pex30 families.

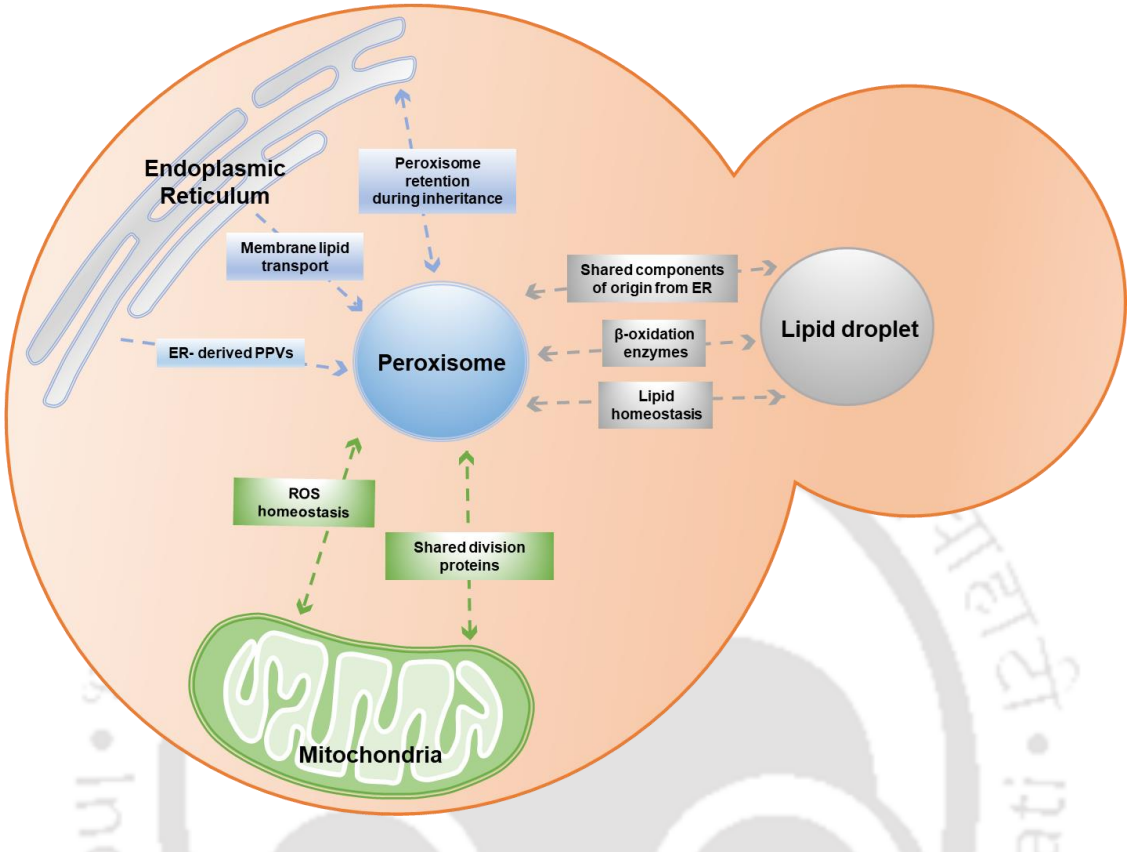

Fig. 1.3 Functional interplay between peroxisomes and neighboring organelles in yeast
It is now well accepted that peroxisome interacts with several other cellular organelles and aids in maintaining cellular homeostasis. The ER is an indispensable contributor to peroxisome biogenesis. *De novo* formation of peroxisomes especially in mutant cells lacking a pre-existing functional peroxisome has been reported [137]. In addition, membrane lipids required for expansion of peroxisomal membranes are either transported via vesicles or directly from the ER to peroxisomes [138]. Retention of peroxisomes by the mother cell during cell division, also depends on the association between peroxisomes and ER [98]. Peroxisomes and mitochondria are closely associated with each other in maintaining redox homeostasis. Peroxisomal catalase, Cta1 can localize to mitochondria during ROS accumulation under respiratory growth conditions and facilitates the detoxification of mitochondrial derived H_2O_2 [139]. Peroxisomes are juxtaposed to the site of mitochondrial PDH complex possibly for the efficient transfer of metabolites between the organelles [140]. In addition, peroxisomes and mitochondria share common division proteins such as the Dnm1, Fis1, Mdv1 and Caf4 [92, 94, 97]. Under peroxisome-inducing conditions, a membrane protrusion called pexopodium that extends from the peroxisome and fuses with the LDs was observed [141]. These structures act as a connecting link enabling the flux of free fatty acids and β-oxidation enzymes between peroxisomes and LDs [135, 141]. In addition, peroxisomes and LDs originates from specific ER subdomains enriched with proteins such as Pex30 that mediates the formation of both these organelles [87, 142].

1.5.1 Peroxisome-mitochondria contact sites

An important role for the intimate association of mitochondria and peroxisomes in fatty acid β-oxidation and ROS homeostasis is reported [7]. In higher eukaryotes, the peroxisomal β-oxidation does not lead to the complete degradation of fatty acids but results in the shortening

of chain length [143]. The resulting products of peroxisomal β-oxidation are subsequently transported into mitochondria for further oxidation and generation of ATP via the tricarboxylic acid cycle (TCA) [140]. Interestingly, a defect in peroxisomal catalase activity results in enhanced ROS levels in mitochondria. This observation is concomitant with a decrease in mitochondrial enzymatic activity, indicating that ROS produced in peroxisome imparts a significant effect on mitochondrial function (Fig. 1.3) [144]. Therefore a balanced interplay between these two organelles is a pre-requisite for cellular ROS homeostasis [145]. A recent study highlights that peroxisome proliferation, division and biogenesis in *K. phaffii* relies on functional oxidative phosphorylation [146].

In addition, peroxisomes and mitochondria also coordinate their biogenesis by sharing key proteins involved in their division. In *S. cerevisiae*, under peroxisome-proliferating conditions, the fission proteins Dnm1 and Fis1 along with the adapter proteins Mdv1 and Caf4 are involved in the division of peroxisomes [92, 93, 96]. Homologs of these proteins are also reported to regulate mitochondrial and peroxisomal division in *O. polymorpha* [94, 97]. In *S. cerevisiae*, peroxisomes are distributed in close proximity to mitochondrial subdomains, which are in contact with the ER suggesting a three-way junction of association between these organelles [140]. Interestingly, localization of peroxisomes in proximity to the sites of mitochondrial matrix enriched with the pyruvate dehydrogenase (PDH) complex that dehydrogenates pyruvate to generate acetyl CoA was reported [140]. The proximity of peroxisomes to the PDH complex was proposed to serve as an alternative source of acetyl-CoA for mitochondria or as a site for the accumulation of acetyl-CoA to maximize its entry into the TCA cycle [135].

Three peroxisome-mitochondria tethering proteins have been identified in *S. cerevisiae.* Interestingly, it has been proposed that different tether complexes may have different functions. Also, the characteristic of a true tether can be identified by its effect on the function of the

contact site. In *S. cerevisiae*, Pex11 was reported to interact with Mdm34, a component of ER-mitochondria encounter structure (ERMES) and act as a peroxisome-mitochondria tether (Fig. 1.4A) [147]. This tethering was reported to be important for pexophagy [148]. Close proximity of peroxisomes to the ER-mitochondria contact site during pexophagy was reported in this study. Mutations in Mdm34 that disrupt the formation of ERMES complex were also reported to result in reduced interaction with Pex11 that in turn leads to defects in pexophagy [148]. Interestingly, a role for ERMES complex proteins on regulating peroxisome abundance has been reported recently [149].

Further studies have also reported Pex34 and Fzo1 to function as peroxisome-mitochondria tethers (Fig. 1.4B). Interestingly, the authors propose that these tethers may function independently and that Pex34 is a more specific tether required for the transfer of β-oxidation intermediates from mitochondria to peroxisomes. Upon overexpression of Pex34 enhanced association between peroxisomes and mitochondria was also reported [150]. Fzo1 is a homolog of mitofusin 1 and 2 and was reported to be enriched at the peroxisome-mitochondria contact site. Interestingly, constitutively expressed Fzo1 did not localize to peroxisomes but on overexpression was found to localize to peroxisomes. Overexpression of Fzo1 also resulted in enhanced sites between peroxisome and mitochondria [150]. The tethering partner of Fzo1 on peroxisomes is however not yet reported. The authors speculate a homotypic interaction or an unidentified partner (Fig. 1.4B).

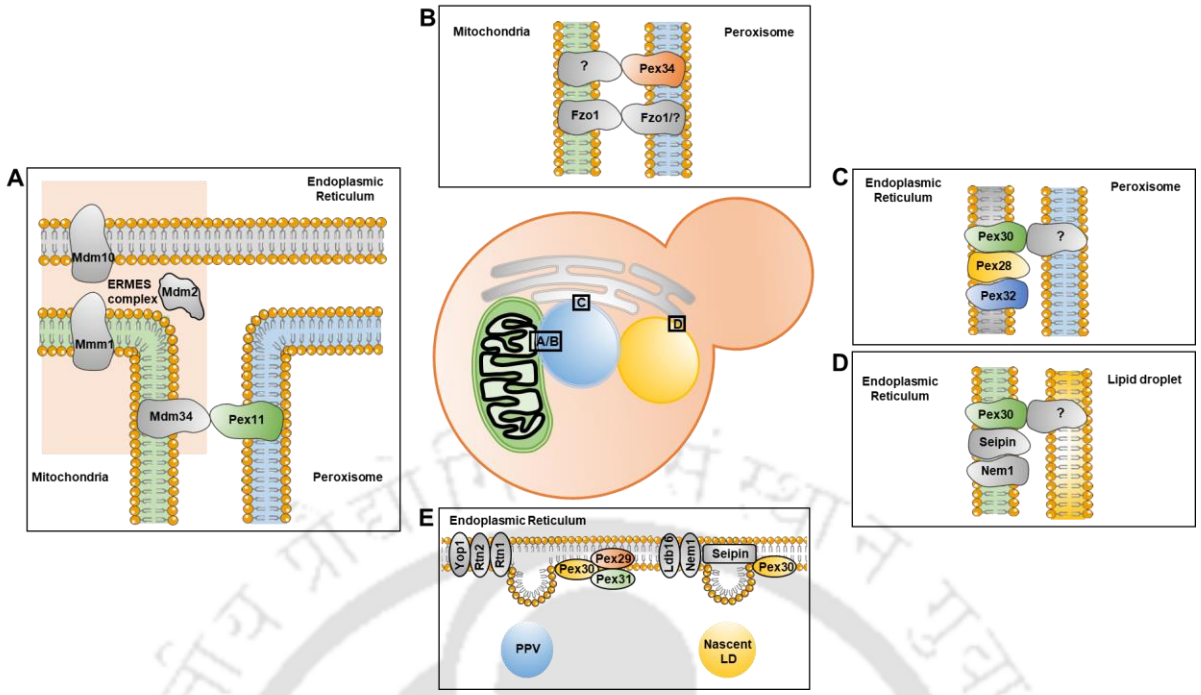

Fig. 1.4 Organelle contact sites mediated by Pex11/Pex30 family and their associated proteins
(A) Pex11 interacts with Mdm34 of the ERMES complex resulting in the formation of a tethering complex [147]. **(B)** In addition, the peroxisomal protein Pex34 acts as a tether and binds to a yet unknown protein at the mitochondrial membrane. The mitochondrial protein Fzo1 is a part of the tethering complex of mitochondria and peroxisomes. Fzo1 may form the contact site either by a homotypic interaction with Fzo1 present on peroxisomes or by binding to an unknown tethering protein [150]. (**C)** Pex30 together with members of proteins of the same family, Pex28 and Pex32 at the ER are required for the formation of peroxisome-ER contact site. Their interacting partner at the peroxisome is not known yet [106]. **(D)** Pex30 associates with Seipin and Nem1 at the ER and aids in the formation of ER-LD contact sites. The interacting partner on LDs is yet to be identified [106, 151]. **(E)** Biogenesis of peroxisomes and LDs occurs at specific ER subdomains. The ER site enriched with RHD-containing proteins such as Pex29, Pex30 and Pex31 that interacts with the ER reticulons (Rtn1, Rtn2 and Yop1) marks the site of PPV formation [87, 130]. PPVs emanate from these sites and eventually mature to form functional peroxisomes. The LD biogenesis protein, Seipin and Nem1 co-ordinate with Pex30 to initiate the formation of nascent LDs from the ER [151].

1.5.2 Peroxisome-ER contact sites

Electron micrographs from early studies have demonstrated that peroxisomes and ER are placed in close proximity to each other, with the tubular structure of ER surrounding the peroxisomes [152]. The adjacent distribution of these two organelles in a cell may be required for the coordination of several cellular and metabolic events [135]. As described in the earlier sections, peroxisomes are formed *de novo* from the ER in the absence of a pre-existing functional peroxisome [74, 77]. Moreover, the maturation of peroxisomes also requires essential membrane lipids and other peroxisomal proteins transported from the ER to peroxisomes (Fig. 1.3) [153]. PMPs required for the increase in size and maturation of nascent

peroxisome are reported to be transported via the PPVs [64, 154]. On the other hand lipids required for the growth of newly formed peroxisomes are transported from the ER via vesicles or by non-vesicular mode [138]. Retention of peroxisomes in *S. cerevisiae* was reported to depend on the intricate association between ER and peroxisomes [155]. Knoblach and colleagues reported an interaction of Inp1 with Pex3 present on the membrane of both ER and peroxisomes forming a bridge that facilitates the retention of peroxisomes via interaction with ER in the mother cell [155].

As mentioned in section 1.4.2, *S. cerevisiae* contains five members of the Pex30 family: Pex28/Pex29/Pex30/Pex31 and Pex32 [106]. All these proteins are reported to be localized to the ER by the membrane shaping RHD [87, 106, 130]. These proteins also interact with the RHD containing ER-resident proteins Rtn1, Rtn2 and Yop1, most likely at the ER-peroxisome MCS [87, 106, 129, 130]. Interestingly, Pex30 is identified as the central player in the formation of different MCS at the ER and its interactions with other family members result in the formation of different Pex30 complexes. These Pex30 complexes are unique for distinct ER-organelle MCS. For example, the RHD of Pex30 aids in the interaction and complex formation with Pex28 and Pex32 at the ER-peroxisome MCS in *S. cerevisiae* (Fig. 1.4C) [106].

The localization of Pex30 family proteins to the ER is also linked to PPV formation [156]. Pex30, Pex31 and Pex29 are reported to localize to specific subdomains on the ER identified as the site for the formation of PPVs in *S. cerevisiae* [87, 129, 130]. Loss of Pex29, Pex30 and Pex31 resulted in an altered number of PPVs per cell [87, 130]. The cells also exhibited the formation of less mobile and highly clustered PPVs at the ER membrane suggesting the role of these proteins in the regulation of PPV biogenesis [87]. Interestingly, deletion of Pex30 and Pex31 in *rtn1rtn2ypo1* cells was associated with reduced formation of mature peroxisomes [87]. Taken together, these observations suggest that members of Pex30

family are involved in the formation of PPVs at the ER and thereby influence the formation of peroxisomes *de novo* from the ER.

In *O. polymorpha*, Pex23, Pex24 and Pex32 localize to discrete subdomains on the ER membrane and aid in the formation of peroxisome-ER MCS [122]. The most severe defect in the formation of the MCS was reported in cells lacking Pex32 and a much lesser role for Pex23 and Pex29 in the formation of ER-peroxisome MCS was reported [122]. The authors report that cells lacking Pex24 and Pex32 exhibited a reduction of the peroxisomal membrane surface. This further resulted in a reduction in the extent of physical contact between these two organelles. However, the loss of these proteins did not completely abolish their physical interaction mediated by MCS. These defects were suppressed by the introduction of an artificial tether protein that facilitated the re-association between ER and peroxisomes and restored peroxisome function [122]. A role for the conserved lipid transfer protein Vps13 involved in multiple MCS formation in the peroxisome membrane expansion was reported [157]. *O. polymorpha* double deletion mutants *pex23vps13* and *pex24vps13* exhibit small peroxisomes and compromised matrix protein targeting. On the other hand, the *vps13* single deletion strains harbours normal functional peroxisomes [157]. An interesting role for Vps13 in the growth of peroxisomes in cells with reduced peroxisome-ER MCSs was proposed [157].

1.5.3 Peroxisome-LD contact sites

Peroxisomes and LDs share the common function of maintaining lipid homeostasis in a cell. LDs store neutral lipids such as triacylglycerol (TAG) and sterol esters (SE), whereas peroxisomes degrade lipids. Peroxisomes also lack enzymes required for the biosynthesis of membrane lipids and therefore, the expansion of peroxisomal membranes requires the transfer of lipids from the ER or LDs [135]. Interestingly, in *Y. lipolytica* cells lacking Pex3, accumulation of peroxisome clusters that enclose the surface of LDs under peroxisome-inducing conditions was reported [158]. This observation indicates the existence of membrane

contacts for the efficient transfer of lipids between the two organelles. Peroxisomes were reported to stably adhere to the surface of LDs in peroxisome-inducing growth conditions in *S. cerevisiae*, indicating the presence of an intricate physical association to facilitate the transfer of lipids between the organelles [141]. Electron micrographs demonstrated that membrane-bound protrusions called pexopodia emerge from peroxisomes, extends to the core of LDs and results in a direct physical contact required for the transfer of fatty acids. Interestingly, it has been reported that the site of interaction between peroxisome and LD is enriched with enzymes involved in β-oxidation, indicating the breakdown of lipids at these sites (Fig. 1.3) [141].

Though experimental evidence confirms a physical association between these two organelles, the protein that might act as a physical tether between them has not yet been identified [135, 156]. Interaction between peroxisomal and LD proteins has been identified using proteomics in *S. cerevisiae* (Fig. 1.4D). Interestingly, Pex30 was identified as one of the interaction partners of the LD proteins Erg6 and Pet10 [159].

The ER subdomain at which Pex30 accumulates and aids in PPVs formation is also reported as the site of origin of nascent LDs in *S. cerevisiae* (Fig. 1.4E) [160]. Interestingly, Pex30 localizes to the domains enriched in the ER-resident proteins Seipin (Fld1) and Nem1 that regulate the formation of LDs by recruiting yeast TAG-synthases Lro1 and Dga1 [142, 151]. Cells devoid of Lro1 and Dga1 are characterized by the absence of neutral lipids and hence lack morphologically recognizable LDs that can store the synthesized lipids [161]. On the other hand, loss of Pex30 results in the absence of Lro1 at the ER subdomains in *S. cerevisiae* [142, 151, 160]. This indicates that the loss of Pex30 results in failure to recruit the necessary LD biogenesis proteins to the ER site of LD formation [151]. Interestingly, this role of Pex30 in the LD biogenesis from the ER is reported to be independent of its interaction with other Pex30 family proteins [106].

1.6 Perspectives on future work

Extensive recent studies on peroxisome biogenesis have put Pex11 and Pex30 family members in the forefront of regulation of various aspects of peroxisome biogenesis in yeast. A definite role for these proteins in membrane alteration, regulating peroxisome numbers and establishing organelle contacts in yeast has been reported. The statement "organelles contact each other and interact in a dynamic fashion" is now a consensus in the field. Evidence that shows a role for such interactions in human health and disease is also now ample. Development of novel methods such as high-resolution microscopy, split fluorophore interactions, *etc* has provided insights into the organelle contact sites and their interactions. Peroxisome contacts that effect important organelle functions such as β-oxidation are also expected to have a great influence on human health. Peroxisome biogenesis and functions seem to be greatly dependent on such interactions and proteins involved in forming these contact sites called tethers have been identified.

Several questions that are still to be answered for the mechanistic understanding of the role of Pex30 family proteins in peroxisome dynamics are as follows:

- How is Pex30 targeted to multiple locations in a cell?
- Is the expression and function of Pex30 dependent on its interacting proteins?
- Is Pex30 regulated by post-translational modifications?
- What is the exact mechanistic role of Pex30 family proteins?

In conclusion, we think excellent recent studies have highlighted the role of Pex30 family proteins in various aspects related to peroxisome biogenesis. However, the intricate details of how these proteins regulate the structure and function of peroxisomes is yet to be deciphered.

1.7 Motivation of the research work

In eukaryotic cells, proteins can be targeted to more than one subcellular location, a phenomenon termed dual targeting, dual localization, or dual distribution. As mentioned in section 1.4.2, the peroxisomal protein Pex30 not only associates with peroxisomes but also localizes to the ER from where it regulates *de novo* biogenesis of peroxisome. Pex30 also associates with its interacting proteins, the ER reticulons Rtn1, Rtn2 and Yop1, in maintaining the tubular morphology of ER. Till date, several independent studies have demonstrated diverse functions of Pex30 across different organisms, but the mechanism by which Pex30 regulates peroxisome number in a cell still remains to be investigated. In addition, it is also intriguing to explore the role of different interacting partners of Pex30 in the function or localization of the protein.

In *S. cerevisiae*, the differential identification of phosphorylated proteins when cultured in peroxisome-inducing and peroxisome-repressing conditions emphasizes the relevance of phosphorylation on peroxisome dynamics. Several phospho-proteomic studies have revealed multiple phosphorylation sites in Pex30 that caters for possibilities to characterize the effect of these phospho-sites on the function of the protein.

The RHD and dysferlin domain of Pex30 are conserved among its family members. Membrane tubulation property of Pex30 depends on the RHD domain whereas the role of dysferlin domain in the function of the protein is unknown. Functional characterization of different domains of Pex30 is not investigated. Therefore, a holistic study deciphering the role of these domains might unravel important facets associated with the targeting and function of the protein.

1.8 Objectives of the thesis

Based on the literature available and the scope for further studies in deciphering the role of post-translational modifications (PTMs) like phosphorylation and different domains of Pex30 in its targeting and function, the following objectives were formulated:

1. To characterize the expression and localization of Pex30 and its role in regulating peroxisome number in WT and in Δpet10, Δerg6 and Δmdm10.
2. To characterize post-translational modifications of Pex30
   A. Expression, purification and determination of secondary structure of Pex30.
   B. Identification of phosphorylation and its characterization in localization and function of Pex30.
3. Characterization of different domains of Pex30 required for its targeting and function.

1.9 Organization of the Ph.D thesis

Chapter 1 provides an overview of recent developments involved in peroxisome biogenesis and the role of Pex11 and Pex30 family proteins in regulation of peroxisome size and abundance. This chapter also encapsulates the importance of proteins belonging to these groups in the formation of MCSs of peroxisomes with other organelles.

Chapter 2 comprises description of the materials and methods used in performing the experiments. The composition of the materials used is outlined and the steps involved in each method are described in detail.

Chapter 3 describes the cloning of GFP to both the N and C-terminal of Pex30 followed by characterization and expression of the protein in various deletion strains in *S. cerevisiae*. In addition, peroxisomal phenotype was studied in Δerg6, Δpet10 and Δmdm10 cells.

Chapter 4 deals with the biochemical characterization of Pex30 and the identification of phosphorylation sites by mass spectrometry analysis. Further, the phosphorylated residues

were mutated to both non-phosphorylated (alanine) and phosphomimetic (aspartic acid) variants to understand the importance of this PTM in the function and localization of the protein.

In ***chapter 5***, multiple GFP-tagged truncations of Pex30 were generated to characterize the domains required for targeting of the protein to ER and peroxisomes. The role of Pex30 domains on the regulation of peroxisome number was also evaluated.

Chapter 6 is the conclusion and future perspective that summarizes and highlights the significant findings of the research work. This chapter also provides an insight on the future scope towards understanding the mechanism by which Pex30 regulates peroxisome dynamics in a cell.

Chapter 2

Materials and Methods

2. 1 Materials

2.1.1 Strains and plasmids

All yeast strains used in this study are listed in Table 2.1. Deletion strains used in this study were obtained from the gene deletion library (Dharmacon) and were confirmed by polymerase chain reaction (PCR). Plasmids generated and used in this study are listed in Table 2.2.

2.1.2 Primers

The primers used in the study are listed in Table 2.3. Primers for gene cloning and site-directed mutagenesis (SDM) were constructed by using the clone-manager software. The primer pairs used in SDM are listed in Table 2.4.

2.1.3 Culture media

All yeast and bacterial growth media components were purchased either from Himedia (Himedia Laboratories Pvt. Ltd., India) or SRL (Sisco research Laboratories Pvt. Ltd., India). Culture media for cell growth were sterilized by autoclaving at 121 ^{0}C, 15 psi for 20 mins. Heat labile components like antibiotics were filter sterilized using 0.22 µM membrane filter. The composition of different media used are described below.

2.1.3.1 Bacterial media

Luria Bertani (LB)

0.5% Yeast extract, 1% Tryptone, 1% NaCl. To prepare LB agar plates, 2% agar was added to the media components. The final volume was adjusted before autoclaving.

LB media were supplemented with ampicillin or kanamycin 100 µg/ml and 50 µg/ml respectively. Stock solutions of 100 mg/ml and 50 mg/ml were prepared for ampicillin and kanamycin respectively. The antibiotic stocks were filter sterilized and added to the cooled LB agar media before pouring plates. The autoclaved media should be moderately warm as high temperature could degrade the antibiotics.

Super-optimal broth (SOB)

2% Bactotryptone, 0.5% Yeast extract, 2% Peptone, 10 mM NaCl, 2.5 mM KCl, 10 mM $MgCl_2$, 10 mM $MgSO_4$.

SOC media

SOC media was derived from the SOB media. The SOB media was supplemented with 20 mM glucose (from a stock of 2 M).

2.1.3.2 Yeast media

Yeast extract-Peptone-Dextrose (YPD)

1% yeast extract, 1% bacteriological peptone and 1% glucose

Minimal medium (YND)

0.17% yeast nitrogen base without amino acids and ammonium sulphate, 0.5% ammonium sulphate, 2% glucose and pH adjusted to 6.0. Whenever necessary, media was supplemented with leucine (3 mg/ml), lysine (10 mg/ml) and histidine (10 mg/ml). For growth on plates, 2% agar was added to the media.

RYTKA: Oleic-acid (OA) containing media

0.17% yeast nitrogen base without amino acids and ammonium sulphate, 0.5% ammonium sulphate, 0.1% glucose, 0.1% yeast extract, 0.1% OA, 0.05% Tween-80 and pH adjusted to 6.0.

Raffinose-containing media (YNR)

0.17% yeast nitrogen base without amino acids and ammonium sulphate, 0.5% ammonium sulphate, 2% raffinose, isoleucine (30 mg/L), valine (150 mg/L), arginine (20 mg/L), adenine (20 mg/L), histidine (20 mg/L), leucine (30 mg/L), lysine (30 mg/L), methionine (20 mg/L), phenylalanine (50 mg/L), tryptophan (20 mg/L) and tyrosine (30 mg/L). pH adjusted to 6.0.

Galactose-containing media (YNG)

3X yeast-extract and peptone (YP) supplemented with 6% galactose.

2.1.4 Buffers and solutions

2.1.4.1 Buffers for protein extraction

Lysis Buffer

50 mM Tris-HCl (pH 7.3), 300 mM NaCl, 0.1% Triton X-100, 0.1% β-mercaptoethanol, 1 mM PMSF, 1X protease inhibitor cocktail without EDTA and 1X phosphatase inhibitor cocktail. The protease and phosphatase inhibitor cocktail were added just before use.

TCA buffer

50 % (w/v) Tri-chloro acetic acid

cold 80 % (v/v) acetone

1% (w/v) SDS in 0.1 N NaOH

2.1.4.2 Buffers for protein purification

Equilibration buffer

50 mM Tris-HCl (pH 7.3), 300 mM NaCl, 0.1% Triton X-100, 30 mM imidazole.

Wash buffer

50 mM Tris-HCl (pH 7.3), 300 mM NaCl and varying concentration of imidazole such as 40 mM, 60 mM and 80 mM.

Elution buffer

50 mM Tris-HCl (pH 7.3), 300 mM NaCl and 250 mM imidazole.

2.1.4.3 Buffers and solutions for SDS-PAGE (sodium dodecyl sulphate-polyacrylamide gel electrophoresis)

30% Acrylamide solution

29 g Acrylamide, 1 g Bis-acrylamide dissolved in 100 ml water

10% Sodium Dodecyl Sulphate (SDS)

10 g SDS dissolved in 100 ml water

Resolving gel mix (10%, 10 ml)

4 ml Tris-Cl (1 M, pH 8.8), 1 ml SDS (1%), 3.3 ml acrylamide: bis-acrylamide (29:1), 1.7 ml H_20, 100 µl ammonium persulphate (APS) (10%), 10 µl TEMED.

Stacking gel mix (4%, 5 ml)

0.6 ml Tris-Cl (1 M, pH 6.8), 0.5 ml SDS (1%), 0.7 ml acrylamide: bis-acrylamide (29:1), 3.2 ml H_20, 50 µl ammonium persulphate (APS) (10%), 5 µl TEMED.

SDS sample buffer (SSB)

0.1 M Tris-Cl (pH 6.8), 20% Glycerol (v/v), 4% SDS (w/v), 0.002% bromophenol blue, 10% β-mercaptoethanol. The SDS sample buffer was prepared as a 2X concentrate and used at 1X final concentration.

SDS-PAGE electrophoresis buffer

0.25 M Tris-Cl (pH 8.0), 1.92 M Glycine, 1% SDS. The stock was prepared as a 10X concentrate and used at 1X final concentration.

Coomassie Brilliant Blue (CBB) staining solution

0.1% Coomassie Brilliant Blue R-250, 50% Methanol, 10% Glacial acetic acid

Destaining solution

40% Methanol, 10% Glacial acetic acid, 50% water

2.1.4.4 Buffers for Western blotting

Transfer buffer (10X stock solution)

0.25 M Tris-Cl (pH 8.0), 1.92 M Glycine, 1% SDS. Transfer buffer was prepared as a 10X concentrate and used at 1X final concentration.

1X Transfer buffer (100 ml)

20 ml Methanol, 10 ml transfer buffer (10X), 70 ml water

Tris-Buffered Saline (TBS)

50 mM Tris, 150 mM NaCl, final pH was adjusted to 7.4 with HCl. TBS buffer was prepared as a 10X concentrate used at 1X final concentration.

Wash buffer (TBS-T)

TBS (1X final concentration), 0.1% Tween-20. The desired volume was prepared in water.

Blocking buffer

TBST (1X final concentration), 5% skim milk, 0.1% Tween-20

Ponceau 3S staining solution

0.25% Ponceau S, 40% Methanol, 15% Acetic acid

2.1.4.5 Other buffers

Phosphate-Buffered Saline (PBS)

137 mM NaCl, 2.7 mM KCl, 10 mM Na_2HPO4, 2 mM KH_2PO4. Final pH was adjusted to 7.3 with HCl. PBS buffer was prepared as a 10X concentrate used at 1X final concentration.

Tris-acetic acid EDTA (TAE) buffer

40 mM Tris base, 0.5 M EDTA. Final pH was adjusted to 8 with glacial acetic acid. TAE buffer was prepared as a 10X concentrate used at 1X final concentration.

Bacterial competent cell preparation buffer

10 mM Pipes, 15 mM $CaCl_2$, 250 mM KCl, 55 mM $MnCl_2$. pH adjusted to 6.7 with KOH. The buffer was filter sterilized and stored at 4 ^{0}C.

Yeast transformation buffer

1 M Lithium acetate (LiOAc), 50% Polyethylene glycol (PEG), 100 mM Tris-Cl pH 7.5 with 10 mM EDTA.

2.2 Methods

2.2.1 Microbiological techniques

2.2.1.1 Bacterial culture

Escherichia coli strain DH5α was used for cloning purpose and was grown at 37 °C in LB (Luria-Bertani) medium and was supplemented with 100 µg/ml ampicillin whenever required. The bacterial strains were stored in 87% glycerol at -80 ^{0}C. Cells from the glycerol stocks were revived by first streaking into agar plates containing antibiotic markers.

For plasmid isolation, bacterial cells were inoculated in LB media containing the appropriate antibiotic selection marker and allowed to grow overnight at 37 °C, 200 rpm. The overnight grown cells were then harvested by centrifugation and plasmids were isolated from the cell pellets.

2.2.1.2 Bacterial transformation

$CaCl_2$ method

DH5α, was grown to saturation in LB media. The overnight grown cells were then shifted to fresh LB media and allowed to grow till they reach an OD_{600} of 0.3-0.5. After that, the cells were harvested by centrifugation at 14,000 rpm for 30 secs. The cell pellet was resuspended in 1 ml ice-cold $CaCl_2$ and incubated for 45 mins on ice followed by centrifugation at 14,000 rpm for 30 secs. The harvested cells were very carefully resuspended in 100 µl 0.1M ice-cold $CaCl_2$ while keeping the cells on ice. Plasmid DNA was then added and the cell-DNA mixture was incubated in ice for 30 mins followed by a brief heat shock of 105 secs at 42 ^{0}C. The cells were then immediately transferred to ice and kept for 1 min followed by addition of 1 ml LB media and incubated with agitation at 37 ^{o}C for 1 hr. Cells were then plated on selective plates with the appropriate antibiotic (1%, 10% and 89%).

Preparation of *E. coli* DH5α chemical-competent cells

The *E. coli* strain, DH5α, was grown to saturation in LB media at 37 ^{o}C. 250 µl of overnight grown cells was then inoculated into 250 ml SOB (Super Optimal Broth) and allowed to grow at 18 ^{0}C to an OD_{600} of 0.6 (for approximately 50 hrs). The cells were harvested at 4400 rpm, 4 ^{0}C for 10 mins followed by resuspending the cells in 80 ml ice-cold TB (Transformation Buffer) and incubated for 10 mins on ice. The cells were then centrifuged 4400 rpm, 4 ^{0}C for 10 mins. In the next step, the pellet was resuspended in 20 ml ice-cold TB. This was followed by the addition of DMSO to a final concentration of 7% (1.4 ml for 20 ml cells) and incubation on ice for 10 mins. The cells were then aliquoted in 1.5 ml centrifuge tubes and flash-freezed by the use of liquid nitrogen. The competent cells thus obtained were then stored at -80 ^{0}C.

2.2.1.3 Yeast culture

In brief, cells were grown at 30 °C and 200 rpm overnight and shifted to fresh medium and subsequently grown at 30 °C till they reached exponential growth phase. Cells were further shifted to fresh medium two times. All microscopic experiments were performed by analyzing exponentially growing cells. To induce peroxisomes, cells were grown in OA-containing media and were cultured for a minimum of 8 hrs and subsequently analyzed.

The yeast cells were stored in 87% glycerol at -80 ^{0}C (600 µl culture and 400 µl glycerol). Cells from the glycerol stocks were revived by first streaking into agar plates containing amino acids. WT BY4742 and the strains with gene deletion were streaked onto YPD plates. Colonies from plates were grown overnight in liquid media to stationary phase (pre-culture). Cells grown till the stationary phase were subsequently shifted to fresh media and cultured till exponential phase for further experiments.

2.2.1.4 Yeast transformation

A loop-full of yeast cells were taken with a sterile loop or toothpick from a freshly streaked yeast strain and put in a sterile eppendorf tube. After that, 5-6 µl of denatured herring sperm DNA and 2-3 µl of plasmid DNA was added. 500 µl of 40% PEG (3350) in LiAc/TE was added

to the mixture and either mixed with pipette or vortexed for few secs. The cell mixture was then incubated for 30 mins at 30 ^{0}C with shaking followed by the addition of 40 µl DMSO and a heat shock for 5 mins at 42 ^{0}C. The cells were harvested by centrifugation at 5000 rpm for 2 mins. After decanting the supernatant, the pellet was resuspended in 100 µl of 1 M sorbitol and the complete suspension was plated on selective plates.

2.2.2 Molecular biology techniques

2.2.2.1 Yeast colony PCR

Yeast genomic DNA was first extracted from a freshly streaked plate by using a loopfull of cells and mixed with 30 µl of 0.2% SDS. The cell-SDS solution was then vortexed for 15 mins and incubated in a heat block for 4 mins at 90 ^{0}C. After centrifugation at 4000 rpm for 1 min, the supernatant (gDNA) was isolated to a new tube and stored at -20 ^{0}C.

Colony PCR was performed by using Taq DNA polymerase and 10 ng of template DNA for a 50 µl reaction mixture to amplify the desired product. After amplification, 10 µl of PCR product was visualized on an agarose gel.

2.2.2.2 Plasmid isolation

The Macherey-Nagel nucleospin plasmid isolation kit (Table 2.6) was used for isolation of plasmids from bacterial cells. The *E. coli* DH5α cells bearing the plasmids were stored as glycerol stocks and revived on an LB-agar plate containing the appropriate antibiotics. Single colony from the agar plate was then inoculated in LB broth and allowed to grow overnight at 37 ^{0}C, 200 rpm. The overnight cultured cells were centrifuged at 11,000 g for 30 secs and plasmid DNA was isolated as per the manufacturer's instructions.

(https://www.mn-net.com/media/pdf/45/51/02/Instruction-NucleoSpin-Plasmid.pdf)

2.2.2.3 Gel extraction and PCR clean-up

DNA extraction from excised agarose gel fragments and purification of PCR reaction mix was performed by using the Macherey-Nagel nucleospin gel and PCR clean-up kit (Table 2.6). All procedures were followed as per the manufacturer's instructions. (https://www.mn-net.com/media/pdf/02/1a/74/Instruction-NucleoSpin-Gel-and-PCR-Clean-up.pdf)

2.2.2.4 Restriction digestion and ligation

Cloning of desired genes into plasmids was performed by digesting the amplified product and the vector with the same set of restriction enzymes (Table 2.6). The digested product was either purified by using PCR purification kit or extracted from excised agarose gel fragments by the use of gel extraction kit. Both the digested PCR product and plasmids were then ligated by using T4 DNA ligase. The vector: insert ratio was calculated by using the NEBiocalculator. The ligation mixture consisting of vector, insert, ligase and reaction buffer was incubated at 16 ^{0}C for 16 hrs and then transformed to DH5α cells.

2.2.2.5 Site-directed mutagenesis

To generate non-phosphorylatable variants of Pex30, targeted mutations were introduced by following a two-stage PCR method using the Pfu Turbo DNA polymerase (Agilent Technologies, USA) as described by Wang and Malcom [162]. Briefly, the stage-1 PCR involves two separate extension reactions performed in two separate tubes, one containing the forward primer and the other containing the reverse primer. A 20 ng template plasmid DNA was amplified by the following thermal cycler conditions: 2 mins, 95 °C initial denaturation; 30 secs, 95 °C denaturation step; 30 secs, 60 °C, 62 °C and 65 °C annealing step followed by 16 mins extension step. The two independent reactions were performed for 10 cycles. Subsequently, the two reactions were mixed and further amplification was performed for another 20 cycles. Finally, the terminal extension was performed for 10 mins, 72 °C. Primers and template DNA used for generation of the plasmids carrying desired mutations is given in

Table 2.4. The resulting plasmids containing phosphomimetic and non-phosphorylatable variants of Pex30 were confirmed by restriction digestion using specific restriction enzymes followed by DNA sequencing analysis. All the obtained plasmids were then separately transformed into *S. cerevisiae* Δpex30 cells by lithium-acetate transformation method and the recombinant clones were selected based on auxotrophy [163].

2.2.2.6 Generation of Pex30 truncations

The Pex30 gene was amplified using the primer pair pr-NMD001 and pr-NMD002 and *S. cerevisiae* BY4742 genomic DNA as a template. The amplified product was then fused to GFP at the C-terminus and expressed under the *MET25* promoter of the pUG35 vector. Using yeast genomic DNA as template, truncated versions of the protein were generated by PCR amplification using specific primers for each truncation. Pex30 truncations encoding for the regions (1-87), (1-250) and (1-352) were cloned into the pUG35 vector between *Xba*I and *Bam*HI site using restriction endonucleases and the primers: pr-NMD001, pr-NMD016, pr-NMD018 and pr-NMD20. Moreover, the truncations encoding for the regions (88-523), (251-523) and (353-523) were cloned into the vector by using *Sma*I and *Bam*HI restriction endonucleases and the primers pr-NMD002, pr-NMD017, pr-NMD019 and pr-NMD021. All the inserts were tagged with GFP at the C-terminus and expressed under the control of MET25 promoter. Further, the fusion of GFP to the inserts were confirmed by DNA sequencing.

2.2.3 Proteomics

2.2.3.1 Purification of His-tagged Pex30 from yeast

S. cerevisiae cells expressing Pex30 tagged to hexa-histidine at its C-terminus under the control of an inducible galactose promoter were cultured in YND liquid medium supplemented with amino acids. Cells were grown at 30 °C and 200 rpm overnight and were subsequently shifted to a fresh medium containing 2% raffinose. These cells were cultured till 1.2 OD_{600} units in raffinose media after which 3X yeast extract-peptone (YP) with 6% galactose was added to the

media and incubated for 6 hrs in growth conditions as per instructions provided in Yeast ORF collection manual (https://horizondiscovery.com/-/media/Files/Horizon/resources/Technical-manuals/yeast-orf-collection-manual.pdf). The induced cells were then harvested by centrifugation at 10,000 rpm for 10 mins and subsequently, the pellet was resuspended in lysis buffer with protease and phosphatase inhibitors. The resuspended cells were transferred to a screw-capped microcentrifuge tube to which zirconia beads corresponding to 1/3rd volume of the cell suspension were added. The cells were disrupted by vortexing for 15-20 cycles of 30 secs beating and 1 min rest (for cooling). The cell lysate was subjected to mild centrifugation at 2000 rpm, 4 °C for 5 mins. The supernatant was collected and mixed with Ni-NTA-charged resin pre-calibrated with equilibration buffer containing 30 mM imidazole. The matrix-bound His-conjugated Pex30 protein was eluted with two different concentrations of imidazole viz. 300 mM and 500 mM. Stringent washing of the column with 40 mM, 60 mM and 80 mM imidazole concentrations was performed prior to elution. The eluted samples were run on a conventional 10% SDS-PAGE gel and stained with Coomassie brilliant blue G-250 and the purified Pex30 band was excised for mass spectrometry (MS) analysis. The MS analysis was performed by the Proteomics Facility, Institute of Bioinformatics (IOB), Bangalore, India.

2.2.3.2 Circular dichroism spectroscopy

The eluted protein samples were pooled and desalted in 20 mM phosphate buffer using PD10 columns (GE healthcare) according to manufacturer's instructions prior to circular dichroism (CD) spectroscopy. Far-ultraviolet (UV) CD spectroscopy was performed to analyze the secondary structure of Pex30 as described previously [164]. Briefly, J-1500 spectropolarimeter (Jasco, Japan) equipped with a thermoelectric cooling-based temperature control unit was used under continuous nitrogen purging. The far-UV CD spectrum was recorded from 260-190 nm wavelength at a scan rate of 100 nm/min with a data integration time of 1 sec. The spectrum was determined as an average of ten accumulations in a quartz cuvette of pathlength 0.1 cm.

The phosphate buffer in which the protein was desalted, was used as a blank for background subtraction and the resulting spectrum was analyzed using BeStSel online tool [165, 166].

2.2.3.3 Mass Spectrometry (MS)

In-gel digestion

The excised gel fragment was subjected to a destaining solution of 40 mM ammonium bicarbonate (Sigma-Aldrich) and 40% (v/v) acetonitrile (Merck Millipore). Once the gel fragments were completely destained, 0.5 ml of 100% acetonitrile was added and incubated for 10-15 mins until the gel slice shrunk and became opaque. After destaining, a reduction solution of 5 mM dithiothreitol (Sigma-Aldrich) in ammonium bicarbonate was added to the gel fragment and incubated at 60 °C for 30 mins. This was followed by incubation of the gel fragment in an alkylation solution consisting of 20 mM iodoacetamide (Sigma-Aldrich) in 40 mM ammonium bicarbonate for 10 mins at room temperature in the dark. The gel fragment was then dehydrated in 100% acetonitrile solution followed by digestion with trypsin (Promega) overnight at 37 °C. Following overnight digestion, the peptides were extracted using an extraction buffer consisting of 5% formic acid (Merck Millipore) and 40% acetonitrile. The final peptide extraction was performed in 100% acetonitrile solution, followed by subjecting the pooled extract to vacuum-dry in a SpeedVac.

LC-MS/MS analysis

Reconstitution of the dried peptides was performed in 0.1% formic acid. The reconstituted peptides were then analyzed using Orbitrap Fusion Tribrid™ (Thermo Scientific™, Bremen, Germany) mass spectrometer coupled with Proxeon Easy nLC system (Thermo Scientific™, Bremen, Germany). Peptide enrichment was achieved by allowing the protein fragments to pass through at a flow rate of 3 µL/min on to an Acclaim™ PepMap™ trap column (2 cm x 75 µm, Magic C18AQ, 5 µm, 100 Å, Michrom Biosciences Inc.). Peptides were separated on an analytical column (10 cm x 75 µm, Magic C18AQ, 3 µm, 100 Å, Mi-chrom Biosciences Inc.)

at a flow rate of 350 nL/min employing a linear gradient of 5–32% acetonitrile for 40 mins with a total run time of 60 mins. MS and MS/MS scan acquisitions were executed in the Orbitrap mass analyzer at a mass resolution of 120,000 and 15000 at 200 m/z, respectively. MS spectra were acquired in a data-dependent manner targeting the twenty most abundant ions with charge state ≥2 in each survey scan in the m/z range of 350 to 1600. Fragmentation was carried out using higher-energy collisional dissociation mode with normalized collision energy of 34. Isolation width was set to 1.6 m/z with 0.5 m/z offset. Precursor ions selected for MS/MS fragmentation were dynamically excluded for 30 secs. The automatic gain control for full MS and MS/MS was set to 4 x 105 and 1 x 105 ions, respectively. The maximum ion injection time for full MS and MS/MS was set to 50 ms and 75 ms, respectively. Internal calibration was carried out by enabling lock mass option using polydimethylcyclosiloxane (m/z, 445.1200025) ions [167].

Data analysis

The mass spectrometry data was searched against NCBI *S. cerevisiae* RefSeq protein database (version 2.4 containing 6118 protein sequences and known contaminants) and analyzed using Mascot (version 2.2.0, Matrix Science, London, UK) and SequestHT algorithm and Proteome Discoverer software (Version 1.4.0.288, Thermo Fisher Scientific). The analyzing criteria were set as oxidation of methionine and phosphorylation modification of serine, threonine and tyrosine as variable modifications and carbamidomethyl modification of cysteine as fixed modification. A 10 ppm of precursor mass tolerance, 0.02 Da of fragment mass tolerance and a maximum of two missed cleavages were allowed. The spectral match hits were screened with 1% false discovery rate at the peptide level.

2.2.3.4 Phosphatase treatment, Phos-tag SDS PAGE

The purified Pex30 was treated with three units of calf intestinal alkaline phosphatase (CIAP) (Promega) and incubated at 37 °C for 30 mins. Elution fractions of Pex30 without CIAP

treatment were taken as control. Further these proteins were separated using a 10% SDS-PAGE containing 50 µM Phos-tag (Wako Chemicals) and 100 µM $MnCl_2$ in the resolving gel [168]. Electrophoretic separation was carried out at 80 volts for 4 hrs in an ice-tank. After electrophoresis, the gel was soaked with gentle agitation first in transfer buffer (25 mM Tris, 192 mM glycine, 10% methanol, pH 8.3) with 1 mM EDTA for 10 mins, and subsequently with transfer buffer without EDTA. Proteins were transferred onto a nitrocellulose membrane at 20 volts for 30 mins.

2.2.3.5 Western blotting

For protein expression studies, cells corresponding to 3 OD_{600} units of each strain were lysed by trichloroacetic acid (TCA) method and this crude yeast extract was used for SDS-PAGE [169]. Briefly, cell pellet from culture corresponding to 3 OD_{600} units was resuspended in 50% TCA and incubated for 30 mins at -80 °C. The cells were then washed twice with ice-cold 80% acetone. After air-drying the pellet at room temperature, the pellet was finally dissolved in 1% SDS/0.1 N sodium hydroxide solution. Lowry's method of protein estimation was used to estimate the amount of protein and an equal amount of protein was loaded onto each well [170]. The gels were run at a constant voltage of 130 volts and transferred onto nitrocellulose membrane using Bio-Rad Trans-Blot®TurboTM. The membrane was first incubated with a blocking solution (5% skimmed milk) at room temperature for 2 hrs. The blots were probed with rabbit anti-GFP polyclonal antibody (1:5000) (Biobharti Life Science, Kolkata, India) and incubated overnight at 4 °C. For detection of his-tagged protein, blots were probed with an anti-his polyclonal antibody (1:5000) (Biobharti Life Science, Kolkata, India). Detection of GAPDH and β-actin were done by probing the blot with anti-GAPDH (1:5000) (Biobharti Life Science, Kolkata, India) and anti-β-actin polyclonal antibody (1:5000) (Invitrogen, Thermo Fisher Scientific, US). Goat anti-rabbit IgG (1:5000) or anti-mouse IgG (1:5000) conjugated to horseradish peroxidase (Invitrogen, Thermo Fisher Scientific, US) was used as secondary

antibody for detection (Table 2.5). Blots were developed using Bio-Rad ECL substrate and captured using the Bio-Rad ChemiDocTM XRS+ system.

2.2.4 Fluorescence microscopy

Fluorescence microscopy experiments were performed using an Olympus IX83 inverted microscope equipped with DP80 camera. A Plan-APOCHROMAT 100x/1.4 objective was used for image acquisition. Samples were illuminated using pE-300whiteCoolLED light source and GFP was visualized using U-FBNA filter with excitation range: 470-495 nm, dichroic: 505 nm and emission: 510-550 nm. RFP/DsRed was visualized using a brightline triple-bandpass filter 378/474/575 nm (Semrock) with dichroic beamsplitter 409/493/596 nm (Semrock). All images were captured at room temperature and processed using Cellsens software (version 2.3). For co-localization experiments, cells were fixed with 4% formaldehyde in phosphate-buffered saline, pH 7.4 (PBS) for 30 mins on ice. The z-axis stacks were obtained starting from top to bottom of yeast cells with the stacks spaced 0.3 μm apart. The final images were assembled in Adobe Photoshop 7.0. Individual cells in the images were marked by using the "multi-point" tool of ImageJ for quantification. Quantification of the number of peroxisomes was done by counting peroxisomes in 40 random non-budding yeast cells from each experiment. Two independent experiments were considered for the analysis.

2.2.5 Statistical analysis

Quantitative analysis was performed from atleast two independent biological experiments. Student's t-test or two-way analysis of variance (ANOVA) was used for multiple comparisons. Error bar indicates the mean ± SEM. Values of $P < 0.05$ were considered significant (*), $P < 0.01$ very significant (**) and $P < 0.001$ extremely significant (***). The data were analyzed using GraphPad prism 8.2.

Table 2.1 *S. cerevisiae* strains used in this study

Strain	Description	Source
BY4742 WT	MATα *his3*Δ *leu2*Δ *lys*Δ *ura3*Δ	Dharmacon
BY4742 GFP.SKL	BY4742 *URA3*::P$_{MET25}$ *GFP.SKL*	This study
Y258::Pex30-His-HA	MATα *pep4-3 his4-580 leu2-3112. URA3::Pex30-His-HA*	Dharmacon
BY4742 *pex30*Δ	MATα *his3*Δ *leu2*Δ *lys*Δ *ura3*Δ *pex30*Δ::kanMX4	Dharmacon
BY4742 *erg6*Δ	MATα *his3*Δ *leu2*Δ *lys*Δ *ura3*Δ *erg6*Δ::kanMX4	Dharmacon
BY4742 *pet10*Δ	MATα *his3*Δ *leu2*Δ *lys*Δ *ura3*Δ *pet10*Δ::kanMX4	Dharmacon
BY4742 *mdm10*Δ	MATα *his3*Δ *leu2*Δ *lys*Δ *ura3*Δ *mdm10*Δ::kanMX4	Dharmacon
BY4742 *pex30*Δ Pex30-GFP	BY4742 *pex30*Δ *URA3*::P$_{MET25}$ *Pex30-GFP*	This study
BY4742 *pex30*Δ GFP-Pex30	BY4742 *pex30*Δ *URA3*::P$_{MET25}$ *GFP-Pex30*	This study
BY4742 *erg6*Δ Pex30-GFP	BY4742 *erg6*Δ *URA3*::P$_{MET25}$ *Pex30-GFP*	This study
BY4742 *pet10*Δ Pex30-GFP	BY4742 *pet10*Δ *URA3*::P$_{MET25}$ *Pex30-GFP*	This study
BY4742 *mdm10*Δ Pex30-GFP	BY4742 *mdm10*Δ *URA3*::P$_{MET25}$ *Pex30-GFP*	This study
BY4742 *pex30*Δ GFP.SKL	BY4742 *pex30*Δ *URA3*::P$_{MET25}$ *GFP.SKL*	This study
BY4742 *erg6*Δ GFP.SKL	BY4742 *erg6*Δ *URA3*::P$_{MET25}$ *GFP.SKL*	This study
BY4742 *pet10*Δ GFP.SKL	BY4742 *pet10*Δ *URA3*::P$_{MET25}$ *GFP.SKL*	This study
BY4742 *mdm10*Δ GFP.SKL	BY4742 *mdm10*Δ *URA3*::P$_{MET25}$ *GFP.SKL*	This study
BY4742 *pex30*Δ pUG35	BY4742 *pex30*Δ *URA3*::P$_{MET25}$ *GFP*	This study
BY4742 *pex30*Δ pUG35 DsRed.SKL	BY4742 *pex30*Δ *URA3*:: P$_{MET25}$ *GFP HIS: DsRed.SKL*	This study
BY4742 *pex30*Δ pUG35 Sec63-mRFP	BY4742 *pex30*Δ *URA3*:: P$_{MET25}$ *GFP LEU: Sec63-mRFP*	This study
BY4742 *pex30*Δ Pex30-GFP DsRed.SKL	BY4742 *pex30*Δ *URA3*::P$_{MET25}$*Pex30-GFP HIS: DsRed.SKL*	This study
BY4742 *pex30*Δ Pex30-GFP Sec63-mRFP	BY4742 *pex30*Δ *URA3*::P$_{MET25}$*Pex30-GFP LEU: Sec63-mRFP*	This study
BY4742 *pex30*Δ Pex30 1-87 –GFP	BY4742 *pex30*Δ *URA3*::P$_{MET25}$ *Pex30 1-87 –GFP*	This study
BY4742 *pex30*Δ Pex30 1-250 –GFP	BY4742 *pex30*Δ *URA3*::P$_{MET25}$ *Pex30 1-250 –GFP*	This study
BY4742 *pex30*Δ Pex30 1-352 –GFP	BY4742 *pex30*Δ *URA3*::P$_{MET25}$ *Pex30 1-352 –GFP*	This study

BY4742 *pex30*Δ Pex30 88-523 –GFP	BY4742 *pex30*Δ *URA3*::P$_{MET25}$ *Pex30 88-523 –GFP*	This study
BY4742 *pex30*Δ Pex30 251-523 –GFP	BY4742 *pex30*Δ *URA3*::P$_{MET25}$ *Pex30 251-523 –GFP*	This study
BY4742 *pex30*Δ Pex30 353-523 –GFP	BY4742 *pex30*Δ *URA3*::P$_{MET25}$ *Pex30 353-523 –GFP*	This study
BY4742 *pex30*Δ Pex30 1-87 –GFP DsRed.SKL	BY4742 *pex30*Δ *URA3*::P$_{MET25}$ *Pex30 1-87 –GFP HIS: DsRed.SKL*	This study
BY4742 *pex30*Δ Pex30 1-250 –GFP DsRed.SKL	BY4742 *pex30*Δ *URA3*::P$_{MET25}$ *Pex30 1-250 –GFP HIS: DsRed.SKL*	This study
BY4742 *pex30*Δ Pex30 1-352 –GFP DsRed.SKL	BY4742 *pex30*Δ *URA3*::P$_{MET25}$ *Pex30 1-352 –GFP HIS: DsRed.SKL*	This study
BY4742 *pex30*Δ Pex30 88-523 –GFP DsRed.SKL	BY4742 *pex30*Δ *URA3*::P$_{MET25}$ *Pex30 88-523 –GFP HIS: DsRed.SKL*	This study
BY4742 *pex30*Δ Pex30 251-523 –GFP DsRed.SKL	BY4742 *pex30*Δ *URA3*::P$_{MET25}$ *Pex30 251-523 –GFP HIS: DsRed.SKL*	This study
BY4742 *pex30*Δ Pex30 353-523 –GFP DsRed.SKL	BY4742 *pex30*Δ *URA3*::P$_{MET25}$ *Pex30 353-523 –GFP HIS: DsRed.SKL*	This study
BY4742 *pex30*Δ Pex30-GFP Sec63-mRFP	BY4742 *pex30*Δ *URA3*::P$_{MET25}$ *Pex30-GFP LEU: Sec63-mRFP*	This study
BY4742 *pex30*Δ Pex30 1-87 –GFP Sec63-mRFP	BY4742 *pex30*Δ *URA3*::P$_{MET25}$ *Pex30 1-87 –GFP LEU: Sec63-mRFP*	This study
BY4742 *pex30*Δ Pex30 1-250 –GFP Sec63-mRFP	BY4742 *pex30*Δ *URA3*::P$_{MET25}$ *Pex30 1-250 –GFP LEU: Sec63-mRFP*	This study
BY4742 *pex30*Δ Pex30 1-352 –GFP Sec63-mRFP	BY4742 *pex30*Δ *URA3*::P$_{MET25}$ *Pex30 1-352 –GFP LEU: Sec63-mRFP*	This study
BY4742 *pex30*Δ Pex30 88-523 –GFP Sec63-mRFP	BY4742 *pex30*Δ *URA3*::P$_{MET25}$ *Pex30 88-523 –GFP LEU: Sec63-mRFP*	This study
BY4742 *pex30*Δ Pex30 251-523–GFP Sec63-mRFP	BY4742 *pex30*Δ *URA3*::P$_{MET25}$ *Pex30 251-523 –GFP LEU: Sec63-mRFP*	This study
BY4742 *pex30*Δ Pex30 353-523–GFP Sec63-mRFP	BY4742 *pex30*Δ *URA3*::P$_{MET25}$ *Pex30 353-523 –GFP LEU: Sec63-mRFP*	This study
BY4742 *pex30*Δ Pex30^{T60AS61A}-GFP	BY4742 *pex30*Δ *URA3*::P$_{MET25}$*Pex30*^{T60AS61}*GFP*	This study
BY4742 *pex30*Δ Pex30^{S511A}-GFP	BY4742 *pex30*Δ *URA3*::P$_{MET25}$*Pex30* ^{S511A}*GFP*	This study

BY4742 *pex30*Δ Pex30^{T60AS61AS511A}-GFP	BY4742 *pex30*Δ *URA3*::P$_{MET25}$*Pex30^{T60AS61AS511A}GFP*	This study
BY4742 *pex30*Δ Pex30^{T60AS61A}-GFP DsRed.SKL	BY4742 *pex30*Δ *URA3*::P$_{MET25}$*Pex30^{T60AS61A}GFP HIS: DsRed.SKL*	This study
BY4742 *pex30*Δ Pex30^{S511A}-GFP DsRed.SKL	BY4742 *pex30*Δ *URA3*::P$_{MET25}$*Pex30^{S511A}GFP HIS: DsRed.SKL*	This study
BY4742 *pex30*Δ Pex30^{T60AS61AS511A}-GFP DsRed.SKL	BY4742 *pex30*Δ *URA3*::P$_{MET25}$*Pex30^{T60AS61AS511A}GFP HIS: DsRed.SKL*	This study
BY4742 *pex30*Δ Pex30^{T60AS61A}-GFP Sec63-mRFP	BY4742 *pex30*Δ *URA3*::P$_{MET25}$*Pex30^{T60AS61A}GFP LEU: Sec63-mRFP*	This study
BY4742 *pex30*Δ Pex30^{S511A}-GFP Sec63-mRFP	BY4742 *pex30*Δ *URA3*::P$_{MET25}$*Pex30^{S511A}GFP LEU: Sec63-mRFP*	This study
BY4742 *pex30*Δ Pex30^{T60AS61AS511A}-GFP Sec63-mRFP	BY4742 *pex30*Δ *URA3*::P$_{MET25}$*Pex30^{T60AS61AS511A}GFP LEU: Sec63-mRFP*	This study
BY4742 *pex30*Δ Pex30^{T60DS61D}-GFP	BY4742 *pex30*Δ *URA3*::P$_{MET25}$*Pex30^{T60DS61D}GFP*	This study
BY4742 *pex30*Δ Pex30^{S511D}-GFP	BY4742 *pex30*Δ *URA3*::P$_{MET25}$*Pex30 ^{S511D}GFP*	This study
BY4742 *pex30*Δ Pex30^{T60DS61DS511D}-GFP	BY4742 *pex30*Δ *URA3*::P$_{MET25}$*Pex30^{T60DS61DS511D}GFP*	This study
BY4742 *pex30*Δ Pex30^{T60DS61D}-GFP DsRed.SKL	BY4742 *pex30*Δ *URA3*::P$_{MET25}$*Pex30^{T60DS61D}GFP HIS: DsRed.SKL*	This study
BY4742 *pex30*Δ Pex30^{S511D}-GFP DsRed.SKL	BY4742 *pex30*Δ *URA3*::P$_{MET25}$*Pex30^{S511D}GFP HIS: DsRed.SKL*	This study
BY4742 *pex30*Δ Pex30^{T60DS61DS511D}-GFP DsRed.SKL	BY4742 *pex30*Δ *URA3*::P$_{MET25}$*Pex30^{T60DS61DS511D}GFP HIS: DsRed.SKL*	This study
BY4742 *pex30*Δ Pex30^{T60DS61D}-GFP Sec63-mRFP	BY4742 *pex30*Δ *URA3*::P$_{MET25}$*Pex30^{T60DS61D}GFP LEU: Sec63-mRFP*	This study
BY4742 *pex30*Δ Pex30^{S511D}-GFP Sec63-mRFP	BY4742 *pex30*Δ *URA3*::P$_{MET25}$*Pex30^{S511D}GFP LEU: Sec63-mRFP*	This study
BY4742 *pex30*Δ Pex30^{T60DS61DS511D}-GFP Sec63-mRFP	BY4742 *pex30*Δ *URA3*::P$_{MET25}$*Pex30^{T60DS61DS511D}GFP LEU: Sec63-mRFP*	This study

Table 2.2 Plasmids used in this study

Plasmid	Description	Source
pUG35GFP	P_{MET25}*GFP*; amp^R; *Sc-URA*3	From Prof. Johannes Hegemann
pUG36GFP	P_{MET25} *GFP*; amp^R; *Sc-URA*3	From Prof. Johannes Hegemann
pUG34-DsRed.SKL	P_{MET25}*DsRed.SKL*; amp^R; *Sc-HIS*3	[92]
pSM1959	Sec63 mRFP; amp^R; *Sc-LEU2*	Addgene plasmid 41837 [171]
pUG35-Pex30-GFP (pNMD001)	P_{MET25}*Pex30 GFP*; amp^R; *Sc-URA*3	This study
pUG36-GFP-Pex30 (pNMD002)	P_{MET25} *GFP Pex30*; amp^R; *Sc-URA*3	This study
pUG35-Pex30 1-87-GFP (pNMD003)	P_{MET25} *Pex30 1-87 GFP*; amp^R; *Sc-URA*3	This study
pUG35-Pex30 1-250-GFP (pNMD004)	P_{MET25} *Pex30 1-250 GFP*; amp^R; *Sc-URA*3	This study
pUG35-Pex30 1-352-GFP (pNMD005)	P_{MET25} *Pex30 1-352 GFP*; amp^R; *Sc-URA*3	This study
pUG35-Pex30 251-523-GFP (pNMD006)	P_{MET25} *Pex30 251-523 GFP*; amp^R; *Sc-URA*3	This study
pUG35- Pex30 353-523-GFP (pNMD007)	P_{MET25} *Pex30 353-523 GFP*; amp^R; *Sc-URA*3	This study
pUG35- Pex30 88-523-GFP (pNMD008)	P_{MET25} *Pex30 88-523 GFP*; amp^R; *Sc-URA*3	This study
pUG35-Pex30^{T60AS61A}GFP (pNMD0012)	P_{MET25}*Pex30*^{T60AS61A} *GFP*; amp^R; *Sc-URA*3	This study
pUG35-Pex30^{S511A}GFP (pNMD013)	P_{MET25}*Pex30*^{S511A}*GFP*; amp^R; *Sc-URA*3	This study
pUG35-Pex30^{T60AS61AS511A}GFP (pNMD0014)	P_{MET25}*Pex30*^{T60AS61AS511A}*GFP*; amp^R; *Sc-URA*3	This study
pUG35-Pex30^{T60DS61D}GFP (pNMD0015)	P_{MET25}*Pex30*^{T60DS61D}*GFP*; amp^R; *Sc-URA*3	This study
pUG35-Pex30^{S511D}GFP (pNMD016)	P_{MET25}*Pex30*^{S511D}*GFP*; amp^R; *Sc-URA*3	This study
pUG35-Pex30^{T60DS61DS511D}GFP (pNMD0017)	P_{MET25}*Pex30*^{T60DS61DS511D}*GFP*; amp^R; *Sc-URA*3	This study

Table 2.3 Primers used in this study

Primer	**Sequence**
pr-NMD001	5'-TGCTCTAGAATGAGTGGTAACACAACTAACG-3'
pr-NMD002	5'-TCCCCCCGGGTACGGCCTTCTTGCTATCG-3'
pr-NMD003	5'-CGGGATCCATGAGTGGTAACACAACTAACG-3'
pr-NMD004	5'-TCCCCCGGGTCATACGGCCTTCTTGCTAT-3'
pr-NMD012	5'-TGGAGGCCCTTGACATAA-3'
pr-NMD013	5'-GCTAGGGCTGGTTACTAT-3'
pr-NMD014	5'-GTGCTGTCGTCGTTGA-3'
pr-NMD015	5'-GGACAAGCTAATTCCTAGAG-3'
pr-NMD016	5'-CGCGGATCCTTCGTCAATGAGAATTAAATAAGGG-3'
pr-NMD017	5'-CGCGGATCCATGTTCCTAAACGTTGTTAC-3'
pr-NMD018	5'-CGCGGATCCACCAAGGTCTAAACCCGTGA-3'
pr-NMD019	5'-CGCGGATCCATGGGAATAAATAAGGACCAGGG-3'
pr-NMD020	5'-CGGGATCCAGTCATGTCTAGCCTCCATGTC-3'
pr-NMD021	5'-CGCGGATCCATGAATGACGGTGCCATTCAAGTGCC-3'
pr-NMD023	5'-GAAAGTTAACGTAGCTGCAGCGCCGCTTTTGACATC-3'
pr-NMD024	5'-GATGTCAAAAGCGGCGCTGCAGCTACGTTAACTTTC-3'
pr-NMD025	5'-GAAGAGAAAGAGCAAGCAAATCCAACAATTGGTCGCGATAGC-3'
pr-NMD026	5'-GCTATCGCGACCAATTGTTGGATTTGCTTGCTCTTTCTCTTC-3'
pr-NMD027	5'-GGTCATTGGAGAAAGTTAATGTAGCTGATGATCCGCTTTTGACATCA-3'
pr-NMD028	5'-TGATGTCAAAAGCGGATCATCAGCTACATTAACTTTCTCCAATGACC-3'
pr-NMD029	5'-GAAGAGAAAGAGCAAGATAATCCAACAATTGGTCGCGATAGC-3'
pr-NMD030	5'-GCTATCGCGACCAATTGTTGGATTATCTTGCTCTTTCTCTTC-3'

Table 2.4 Primers and template DNA used for SDM

Plasmid	Mutation	Primer pair	Template
pNMD012	T60AS61A	pr-NMD023 pr-NMD024	pNMD001
pNMD013	S511A	pr-NMD025 pr-NMD026	pNMD001
pNMD014	T60AS61AS511A	pr-NMD025 pr-NMD026	pNMD012
pNMD015	T60DS61D	pr-NMD027 pr-NMD028	pNMD001
pNMD016	S511D	pr-NMD029 pr-NMD030	pNMD001
pNMD017	T60DS61DS511D	pr-NMD029 pr-NMD030	pNMD015

Table 2.5 List of antibodies used

Primary antibodies				
Name	**Dilution used**	**Source**	**Clonality**	**Company**
anti-GFP	1:5000	Rabbit	Polyclonal	Biobharti Life Science
anti-His	1:5000	Rabbit	Polyclonal	Biobharti Life Science
anti-GAPDH	1:5000	Rabbit	Polyclonal	Biobharti Life Science
anti-β-actin	1:5000	Mouse	Polyclonal	Invitrogen
Secondary Antibodies				
anti-rabbit IgG (HRP-conjugated)	1:5000	Goat		Biobharti Life Science
anti-rabbit IgG (HRP-conjugated)	1:5000	Mouse		Invitrogen

Table 2.6 List of chemicals used

Chemical	Name	Manufacturer
Enzymes	Taq DNA polymerase	New England Biolabs (NEB)
	Phusion polymerase	New England Biolabs (NEB)
	Pfu Turbo DNA polymerase	Agilent Technologies
	T4 DNA ligase	ThermoFisher Scientific
	RNase A	New England Biolabs (NEB)
	Alkaline phosphatase	Promega
	*Xba*I	ThermoFisher Scientific
	*Sma*I	ThermoFisher Scientific
	*Bam*HI	ThermoFisher Scientific
	*Pst*I	ThermoFisher Scientific
	*Mun*I	ThermoFisher Scientific
	*Hpa*I	ThermoFisher Scientific
	*Eco*RI	ThermoFisher Scientific

	*Hin*dIII	ThermoFisher Scientific
	*Sal*I	ThermoFisher Scientific
Kits	Plasmid isolation Miniprep kit	Macherey-Nagel
	PCR purification kit	Macherey-Nagel
	Gel extraction kit	Macherey-Nagel
	Protein concentration estimation kit	BioRad
Other chemicals	Phos-tag	Wako chemicals
	ECL	BioRad
	protease inhibitor cocktail without EDTA	SigmaAldrich
	1x phosphatase inhibitor cocktail	SigmaAldrich

Chapter 3

Pex30: expression, localization and role in regulating peroxisome number in WT, Δpet10, Δerg6 and Δmdm10 cells

Abstract

Pex30 is a peroxisomal protein that resides in the ER and associates with peroxisomes to regulate their biogenesis. In this study, we aim to understand the importance of this dual localization of Pex30 in both peroxisome-inducing and non-inducing growth conditions. For this, we have constructed *S. cerevisiae* strains expressing Pex30 fused to GFP at both C and N-termini. Interestingly, a difference in localization pattern for both the fusion proteins were observed by fluorescence microscopy. Pex30-GFP exhibits both reticulate and punctate distribution whereas GFP-Pex30 displayed reticulate phenotype with reduced punctate distribution. In addition, a differential expression of Pex30 was observed in peroxisome-inducing and non-inducing growth conditions. Several interacting proteins of Pex30 associated with different organelles have been identified. Cells lacking the LD protein Erg6 and Pet10 and the mitochondrial protein Mdm10 were analyzed for the expression and distribution of Pex30. Lack of these proteins did not alter the expression and distribution of Pex30. However, a significant difference in peroxisome number in cells lacking the Pex30 interacting protein Mdm10 was observed similar to as observed in Δpex30 cells.

3. 1 Introduction

All peroxisomal proteins (termed peroxins) are encoded by the nuclear genome, translated in the cytoplasm, and subsequently targeted to the peroxisomes by specific targeting signals [131]. Pex30 is one such peroxin identified in *S. cerevisiae* which co-fractionated with Pex3, suggesting that it is primarily a PMP [172]. However, recent reports established that Pex30 localizes to multiple organelles such as ER, peroxisome and LDs [123, 160, 172].

In vivo studies for understanding protein activity and function reveal that proteins can very rarely function as isolated moieties [173]. Most biochemically active protein molecules interact with other proteins in a cell and this protein-protein interaction can influence the function of target proteins [174, 175]. Interaction of Pex30 with proteins of the same family has been reported to be essential for its function at various MCS [106]. Pex30 is targeted to the peroxisome-ER MCS when associated with Pex28 and Pex32 and functions independently in LD biogenesis [106]. In addition, Pex30 also associates with LD biogenesis proteins and mitochondrial proteins involved in the formation of ERMES complex [147, 151] (Table 3.1).

Protein-protein interaction studies in *S. cerevisiae* reported that the LD proteins Erg6 and Pet10 interact with the Pex30 family proteins [159]. Pet10 is a LD protein that consists of a PAT domain, which is a characteristic feature of perilipins, a class of LD proteins found in mammals that exerts protection to LDs against lipolysis by regulating the activities of lipases [176]. Pet10 associates with nascent LDs and promotes their formation. In the absence of Pet10, the stability of LDs is severely affected and results in their aggregation [176]. In addition, the loss of Pet10 also leads to the fusion of LDs when cultured in OA-containing media [176]. A role for Erg6 present on the surface of LDs in ergosterol biosynthesis pathway has been reported [177]. This protein is also found to be associated with Pex30 indicating the interconnection between Pex30 and mature LDs [160]. A high-throughput screen in yeast identified subunits of the ERMES complex such as Mdm10, Mdm12 and Mdm34 as potential

candidate proteins that may influence peroxisome formation [140]. The absence of these proteins leads to aberrant peroxisome morphology in stationary phase cells [140]. The ERMES subunit Mdm10, exhibits dynamic distribution as it is associated with both ERMES and the sorting and assembly machinery (SAM) of mitochondria [178]. When associated with SAM complex, Mdm10 facilitates the assembly of outer membrane proteins of mitochondria whereas the ERMES-bound Mdm10 is responsible for maintenance of mitochondria morphology [179]. In addition, Mdm10, Mdm12 and Mdm34 are reported to affect the localization of Pex11, a protein involved in regulation of peroxisome proliferation [147]. It is therefore interesting to investigate whether the interacting proteins of Pex30 have any role in the expression, distribution and function of the protein.

Table 3.1 Pex30 interacting proteins identified in various organelles
Interacting partners of Pex30 identified by various protein-protein interaction studies are listed and the features of protein selected in this study are mentioned.

Sl. No	Organelle harboring Pex30 interacting proteins	Interacting partners of Pex30 investigated in earlier studies	Proteins selected for this study and their features	References
1.	Peroxisome	Inp1, Pex19, Pex28, Pex29, Pex30, Pex31, Pex32	-	[106, 155, 172]
2.	Endoplasmic Reticulum	Rtn1, Rtn2, Yop1	-	[129, 130]
3.	Mitochondria	-	**Mdm10** Mdm10 is a component of ERMES complex and is responsible for efficient phospholipid exchange between organelles and for mitophagy	[179]
4.	Lipid droplet	Dga1, Ldb16, Sei1	**Erg6** Erg6 is involved in the ergosterol biosynthetic pathway **Pln1 (Pet10)** Pet10 is involved in the formation and stability of LDs	[177] [176]

PMPs are trafficked to the peroxisomal membrane either directly from the cytosol or via the ER. A role for Pex19 in the direct trafficking has been proposed [68]. Earlier studies demonstrated that Pex19 binds to Pex30 at amino acids 24-38 and 97-111 [131]. A role for the RHD present at the N-terminus of Pex30 in the interaction with ER-reticulons has been demonstrated [87]. The C-terminus of the protein on the other hand has the characteristic dysferlin domain [106]. GFP tagging at either C or N termini is routinely used for studying the localization of a protein. However, in many instances this has resulted in ambiguous results. Hence, we characterized both the C and N-terminal GFP fusion proteins of Pex30. Additionally, the expression of the protein was analyzed in media containing different carbon

sources. The distribution and expression of the protein in strains deleted for interacting proteins (Erg6, Pet10 and Mdm10) was also analyzed followed by the evaluation of peroxisome number in these strains.

3.2 Results

3.2.1 C and N-terminal GFP fusion of Pex30 exhibits differential phenotype

S. cerevisiae Pex30 is a 523 amino acid (aa) protein and comprises of various functional domains. A role for the membrane protein receptor Pex19 in the trafficking of Pex30 to peroxisomes has been reported. Interaction of Pex30 with Pex19 was identified to be via its N-terminal aa 24-38 and 97-111 [131]. On the other hand, RHD and dysferlin domain of Pex30 extending from amino acids 86-291 and 284-408 respectively are indispensable for distribution and function of the protein. Earlier studies have reported that the assembly of Pex30 complexes at the ER-peroxisome MCSs require the RHD domain and the dysferlin domain is essential in regulation of peroxisome number [106, 129]. We, therefore, sought to study the effect of positioning GFP at either the N or C terminus on the phenotype and distribution of Pex30. The yeast expression vectors pUG35 and pUG36 were used to obtain C-terminal and N-terminal GFP constructs respectively (Fig. 3.1A). Both the constructs were introduced into Δpex30 cells and their expression was examined by fluorescence microscopy (Fig. 3.1B).

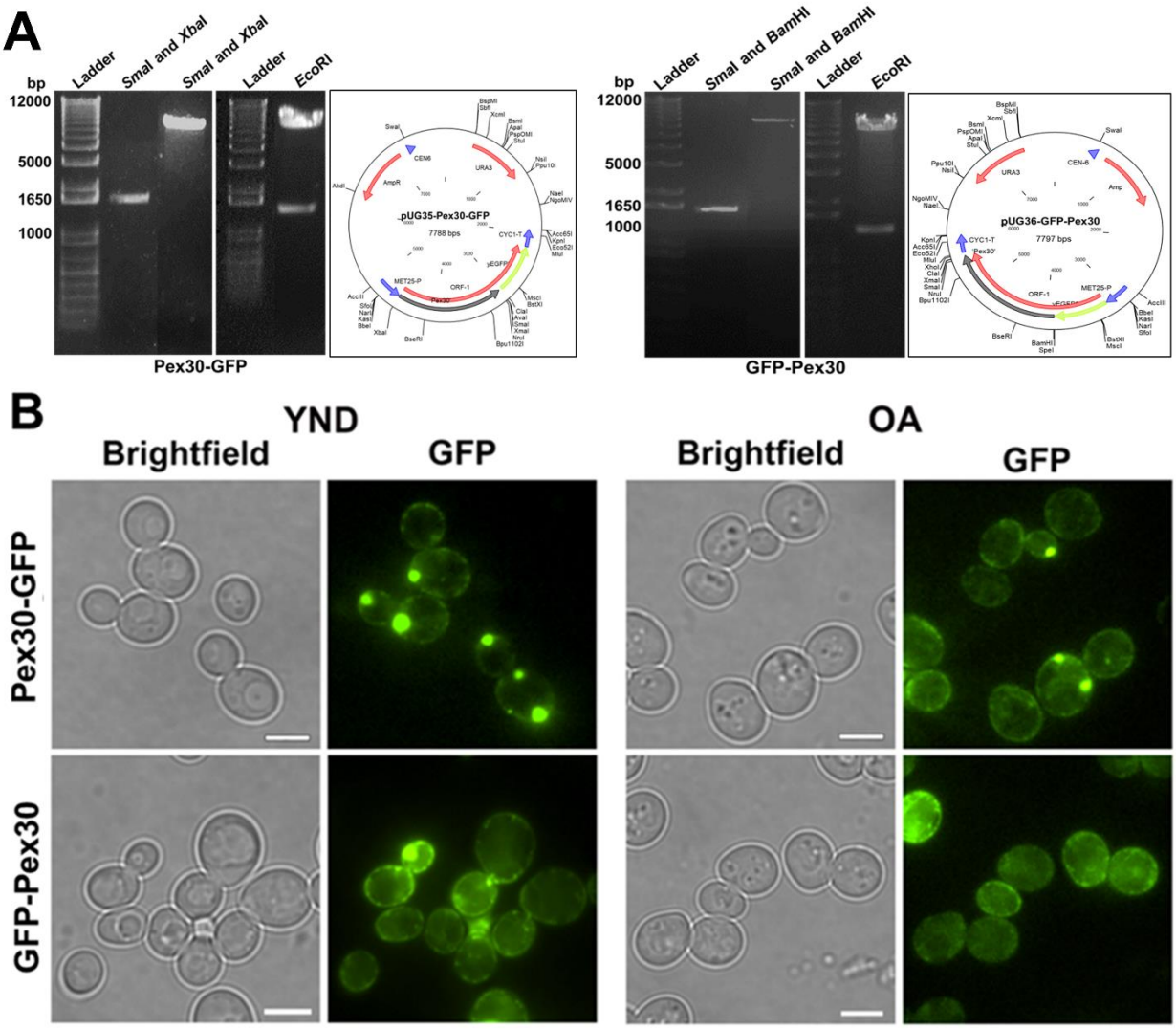

Fig. 3.1 Construction and expression of C and N-terminal GFP-tagged Pex30
(A) Agarose gel electrophoresis image depicting the cloning of Pex30 in the yeast expression vector pUG35 and pUG36. The amplified gene insert was cloned in the pUG35 vector using the restriction endonucleases *Sma*I and *Xba*I. The resulting plasmid pUG35-Pex30-GFP was confirmed by restriction digestion using *Eco*RI. For generation of GFP-Pex30, the amplified gene insert was cloned in the pUG36 vector using the restriction endonucleases *Sma*I and *Bam*HI. The resulting plasmid pUG36-GFP-Pex30 was confirmed by restriction digestion using *Eco*RI. **(B)** Phenotype exhibited by the C and N-terminal constructs, i.e., Pex30-GFP and GFP-Pex30 was examined by fluorescence microscopy. Cells cultured in both YND and OA media were analyzed. Brightfield and fluorescence images corresponding to a group of cells from each strain are represented. Scale bar, 5 μm.

Microscopy analysis indicates that when cultured in YND and peroxisome-inducing OA media, Pex30-GFP exhibits the characteristic puncta and reticulate distribution near the cell periphery which is in accordance with previous studies (Fig. 3.1B) [129, 130, 172, 180]. However, cells expressing GFP-Pex30 exhibited mostly reticulate distribution of the protein in both YND and OA media (Fig. 3.1B). This emphasizes altered interactions of the protein involving the termini and thereby resulting in a change in distribution of the protein. The

punctate as well as reticulate phenotype exhibited by Pex30-GFP is similar to the distribution of Pex30 illustrated in previous studies [87, 129]. Hence, to study the various facets involved in the distribution and function of Pex30, we resorted to the C-terminal GFP-tagged version of the protein for our future experiments.

3.2.2 Expression of Pex30 differs in media containing glucose and OA as carbon source

Peroxisomes are involved in the β-oxidation of fatty acids, and therefore, the function of these organelles can be studied in media containing OA as a carbon source [17, 181, 182]. As it was reported in previous studies that the association between Pex30 and peroxisomes differs in glucose and OA media [130], we sought to analyze the expression of Pex30 in both peroxisome non-inducing (YND) and inducing growth conditions (OA). YND and OA are growth mediums with different carbon source used for culturing yeast. In YND, the main carbon source is glucose whereas in oleate medium, the unsaturated fatty acid, oleic acid is the major carbon source. In yeast, the breakdown of fatty acids solely takes place in peroxisomes via β-oxidation as it harbors the enzymes necessary for fatty acid metabolism. Therefore, peroxisomes are induced in growth media enriched with fatty acids. As Pex30 is involved in the regulation of peroxisome number, we sought to study the function of Pex30 in peroxisome dynamics in a medium containing oleic acid as the sole carbon source. On the other hand, YND is the conventional culture media used for the selection of auxotrophic mutant strains transformed with plasmids.

The Pex30-GFP construct was transformed into Δpex30 cells and subsequently expression was examined by fluorescence microscopy and western blotting. Interestingly, microscopic analysis revealed a difference in the phenotype of Pex30-GFP in cells grown in YND and OA media. Reticulate distribution of GFP around the cell periphery along with discrete GFP puncta was observed in almost all the cells cultured in YND media. On the other hand, cells grown in OA medium exhibited two distinct phenotypes viz. only reticulate and

both reticulate and punctate phenotype (Fig. 3.2A). Quantitative data showed a significant increase in the number of cells exhibiting only reticulate phenotype in OA cultured cells when compared to cells grown in YND (Fig. 3.2A). Sixty random cells were counted from fluorescence images taken of cells grown in YND and OA from two independent experiments. The percentage of cells exhibiting only reticulate phenotype was 5% in YND media as compared to 72% in OA (Fig. 3.2A). Our observation is in line with studies that reported ER localization of Pex30 also in cells grown in OA [129].

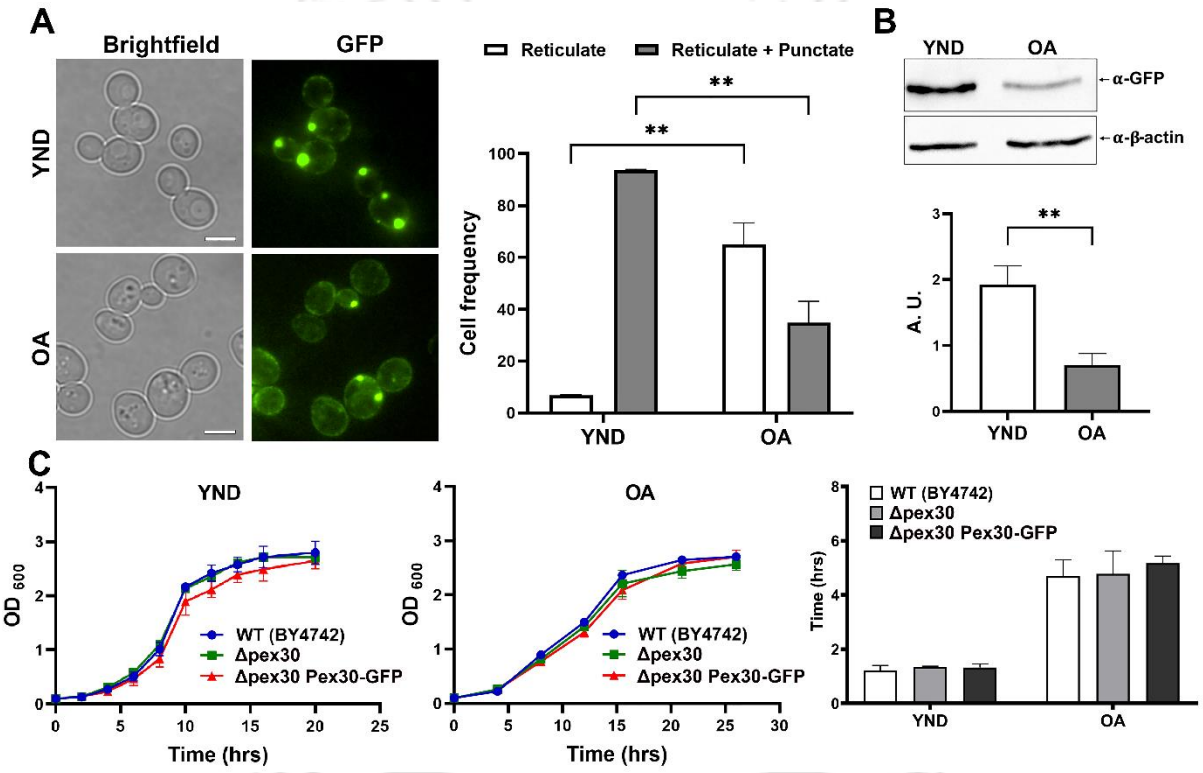

Fig. 3.2 Expression analysis of GFP-tagged Pex30 and its effect on the growth of Δpex30 cells
(A) Fluorescence microscopy images of Δpex30 cells expressing Pex30-GFP cultured in YND and OA medium are depicted. Quantitative analysis of the expression phenotype in YND and OA cultured cells is represented as bar diagrams. Sixty cells were analyzed from each experiment and error bars indicate the SEM from two independent experiments. The significance of the difference between the observed phenotypes was assessed using student's t-test (paired). Values of $p < 0.01$ were considered as significant (**). **(B)** Whole cell lysates equivalent to 3 OD_{600} were resolved in a 10% SDS-PAGE gel and protein expression was analyzed by western blotting using an α-GFP antibody. The Pex30-GFP immunoblots were normalized with β-actin for statistical analysis and represented as bar diagrams. Paired student's T-test was used to analyze the significance of the difference. Values of $p < 0.01$ were considered as significant (**). **(C)** The effect of expression of Pex30-GFP on cell growth was assessed by monitoring the growth kinetics of Δpex30, Δpex30 cells expressing Pex30-GFP and WT cells. The growth curve was obtained by plotting absorbance (Y-axis) against time (X-axis). Error bars indicate SEM from two independent experiments. The doubling time of the strains was analyzed and the significance of the difference was determined by using two-way ANOVA (with multiple comparisons)

Furthermore, the expression of Pex30 in YND and OA was analyzed by western blotting using α-GFP antibody (Fig. 3.2B). Quantification analysis of the α-GFP probed band showed reduced expression levels of Pex30 in OA.

To understand if this altered expression level has any effect on the growth of the cells, WT, Δpex30 and Δpex30 expressing Pex30-GFP were analyzed for their growth kinetics (Fig. 3.2C). The doubling time of WT (1.22 hrs in YND and 4.68 hrs in OA), Δpex30 (1.33 hrs in YND and 4.77 hrs in OA) and Δpex30 expressing Pex30-GFP (1.32 hrs in YND and 5.17 hrs in OA) did not alter significantly (Fig. 3.2C).

3.2.3 Distribution and expression of Pex30 does not alter in cells lacking Pex30 interacting proteins

Interaction of Pex30 with the mitochondrial protein Mdm10 and LD proteins Pet10 and Erg6 has been reported. The localization pattern of another peroxisomal protein, Pex11 that is involved in regulation of peroxisomal size and dynamics is significantly altered by the deletion of Mdm10 [147]. This indicates the role of Mdm10 in regulating the localization of peroxisomal proteins and therefore it is equally intriguing to investigate whether the distribution and expression of Pex30 is influenced by the absence of Mdm10. In addition, Pex30 associates with the LD proteins, Seipin, Nem1 and Ldb16, in the formation of LDs from the ER [142]. Although the functional importance of association between Pex30 and proteins present on the surface of LDs such as Pet10 and Erg6 is not yet reported, the role of these proteins in the distribution of Pex30 might unravel important facets in the biogenesis of LDs. Strains deleted for Pet10, Erg6 and Mdm10 were confirmed by PCR and subsequently transformed with Pex30-GFP. The distribution of the protein was analyzed via fluorescence microscopy in cells cultured in both YND and OA media. Pex30 exhibits reticulate and punctate distribution in the mutant strains which is similar to the phenotype exhibited by WT cells cultured in YND media (Fig. 3.3A). Similarly, in OA-cultured cells, the deletion of the

interacting proteins did not affect the distribution of Pex30 when compared to that observed in WT cells. Quantitative analysis from sixty random cells indicates that the OA cultured cells displayed a significant increase in cell expressing the reticulate phenotype as compared to the YND grown cells (Fig. 3.3A).

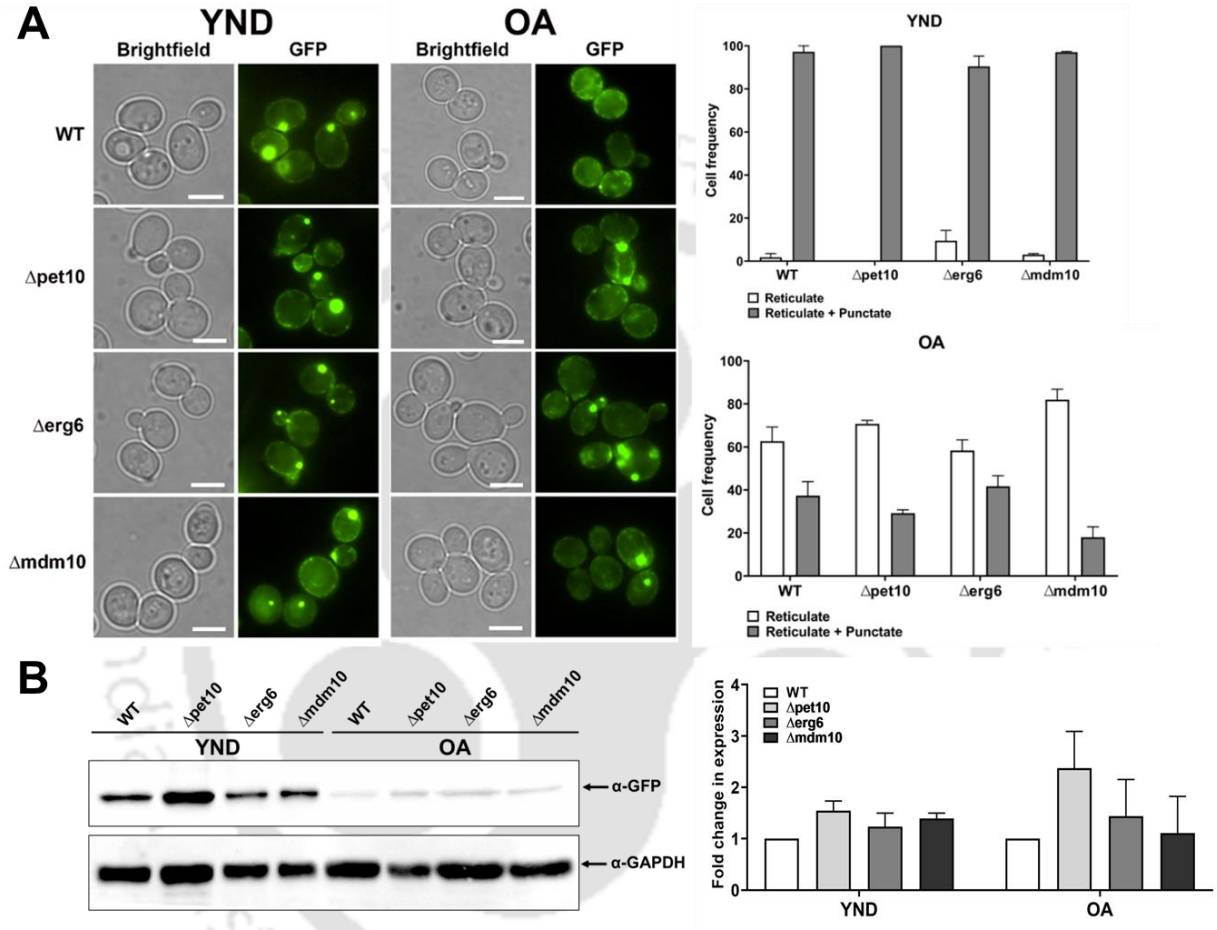

Fig. 3.3 Expression of Pex30 in Δpet10, Δerg6 and Δmdm10 strains
(A) Fluorescence microscopy images of Pex30-GFP expressed in cells deleted for Δpet10, Δerg6 and Δmdm10 are depicted. The mutant cells expressing Pex30-GFP were cultured in both YND and OA media and quantitative analysis of the phenotype exhibited by the cells is represented as bar diagrams. Sixty cells were analyzed from each experiment and error bars indicate the SEM from two independent experiments. The significance of the difference between the observed phenotypes was assessed by using two-way ANOVA (with multiple comparisons). **(B)** Protein expression levels of Pex30 in Δpet10, Δerg6 and Δmdm10 strains cultured in YND and OA-containing media. Cells at the exponential growth phase were harvested by measuring the optical density that corresponds to 3 OD units. The whole cell extracts were separated by SDS-PAGE and subsequently analyzed via western blotting. Equal protein amounts were loaded into each lane. Pex30 was detected by α-GFP and GAPDH, used as a loading control, was probed using α-GAPDH. Quantification of protein expression was performed by normalizing the GFP blots with GAPDH and the obtained data is represented in the form of bar graph. Data from two independent experiments were analysed and the SEM is displayed as error bars. The statistical difference was determined by using two-way ANOVA with multiple comparisons.

Protein expression levels of Pex30 in the deletion strains were analyzed and compared to that of the WT protein via western blotting using an α-GFP antibody (Fig. 3.3B). The difference in expression level was quantified and is illustrated as a fold change in protein expression. The expression of Pex30 in the mutant strains did not differ significantly in comparison to the expression of Pex30 exhibited by the WT cells indicating that expression of Pex30 is independent of its interacting proteins (Fig. 3.3B).

3.2.4 Cells lacking Pex30 and Mdm10 exhibit altered peroxisome number

To determine the role of Pex30-interacting proteins in the regulation of peroxisome number, the total number of peroxisomes in cells lacking Pet10, Erg6 and Mdm10 were analyzed in YND and OA-cultured cells (Fig. 3.4). Fluorescence microscopy and quantification analysis displayed an induction in peroxisome number in WT cells cultured in OA media as compared to YND cultured cells (7.7 ± 1.7 vs 3.6 ± 1.2).

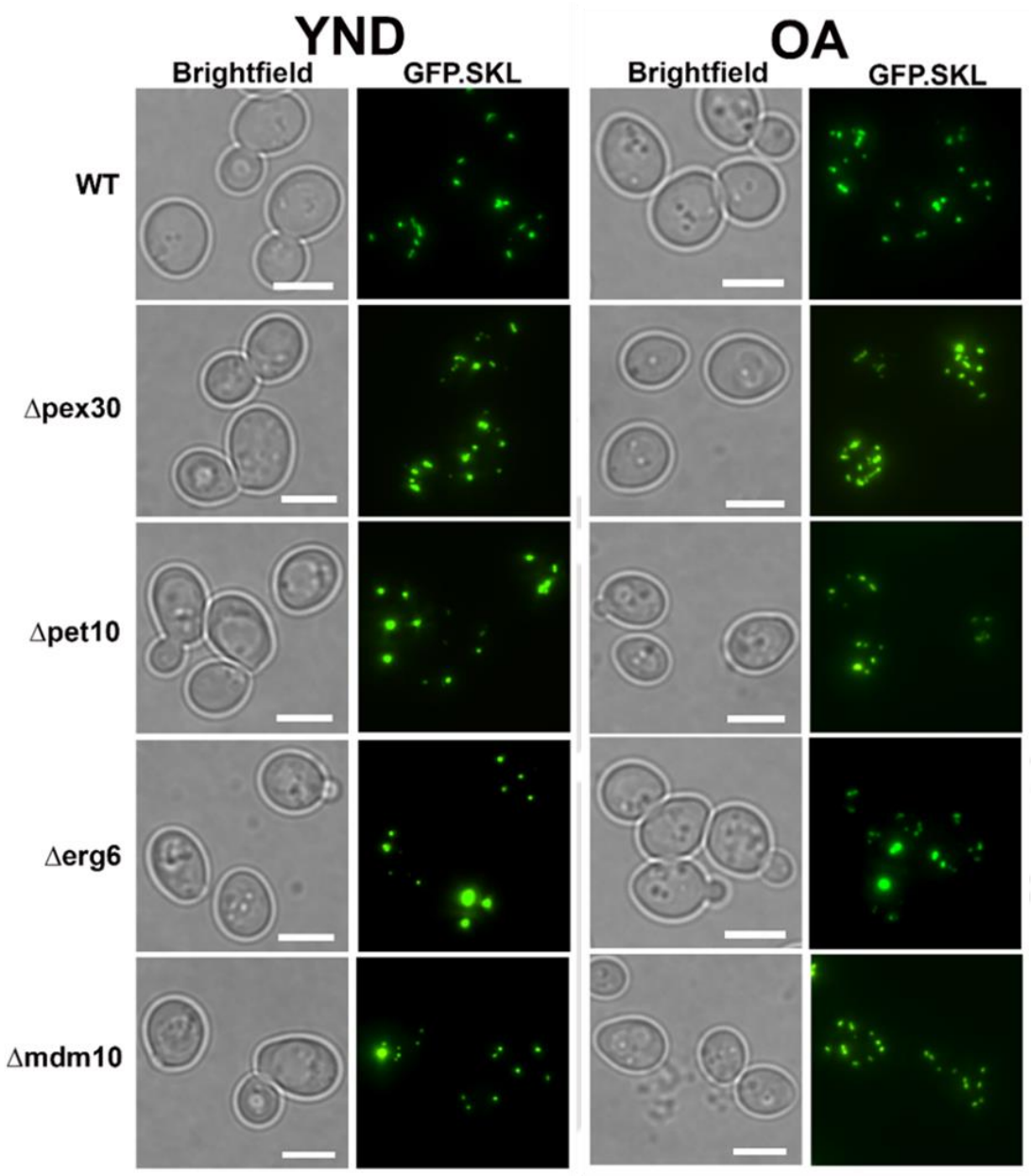

Fig. 3.4 Peroxisome phenotype in Δpet10, Δerg6 and Δmdm10
Fluorescence microscopy images of Δpet10, Δerg6 and Δmdm10 cells cultured in YND and OA are depicted. Cells expressing the peroxisomal marker GFP.SKL were analyzed for peroxisome number in YND and OA media. Brightfield and fluorescence images corresponding to a group of cells from each strain are represented. Scale bar, 5 μm.

Notably, cells lacking Mdm10 displayed a significant increase in peroxisome number whereas cells lacking Pet10 and Erg6 exhibited similar number of peroxisomes as compared to the WT cells. In addition, as reported by previous studies Δpex30 cells exhibited significant increase in peroxisome number thereby substantiating the role of Pex30 as a negative regulator of peroxisome number [172].

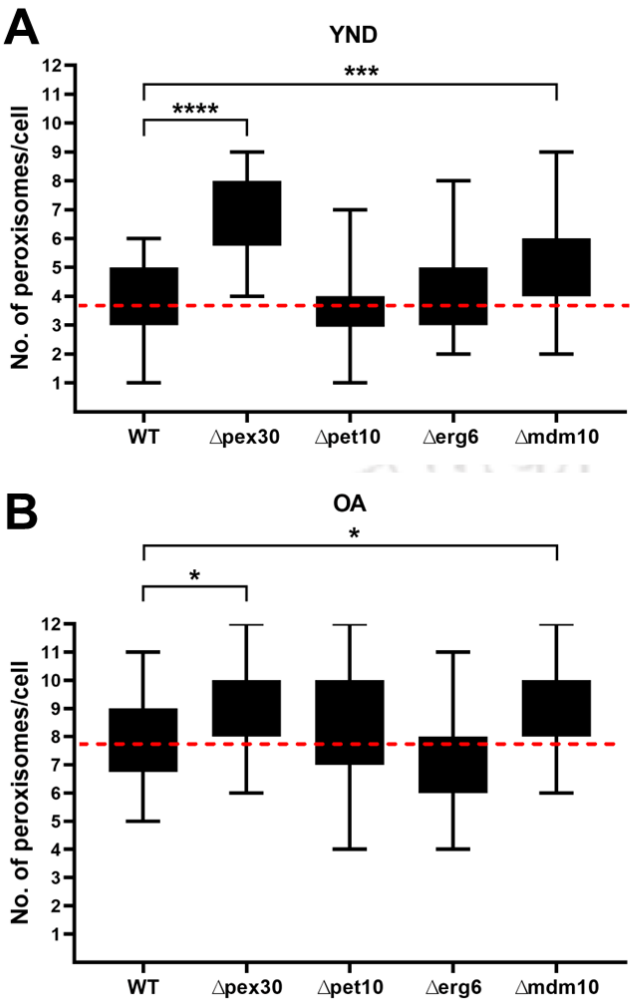

Strain	Mean ± SD
WT	3.6 ± 1.2
Δpex30	6.6 ± 1.3
Δpet10	3.5 ± 1.2
Δerg6	3.8 ± 1.4
Δmdm10	5.1 ± 1.6

Strain	Mean ± SD
WT	7.7 ± 1.7
Δpex30	8.7 ± 1.4
Δpet10	8.1 ± 1.8
Δerg6	7.5 ± 1.6
Δmdm10	8.8 ± 1.7

Fig. 3.5 Quantification of peroxisome number in Δpet10, Δerg6 and Δmdm10 strains
Yeast strains cultured in both YND (A) and peroxisome inducing OA media (B) were analyzed for quantification of peroxisome number. For each yeast strain, peroxisomes were counted by merging the Z-stack and 40 cells were counted from one independent experiment. The data represented is from two such experiments. The box and whisker plot illustrates the diversity of peroxisome number among the yeast strains. The red dashed line denotes the average (mean) number of peroxisomes in WT cells. Values of P <0.05 were considered significant (*), P < 0.001 extremely significant (***).

3.3 Discussion

Previous studies have reported that Pex30 resides in distinct regions of the ER and associates with reticulon family members, Rtn1, Rtn2 and Yop1, that contribute to ER morphology. These specialized ER regions may represent ER-to-peroxisome contact sites required for the formation of peroxisome. The tubular architecture of the ER maintained by the reticulon family proteins seems to be essential to regulate this process. As reported earlier, the C-terminal of the protein contains the dysferlin domain (284-408 aa) and the N-terminal region

has the Pex19 binding site (24-38 and 97-11 aa) and RHD (86-219 aa) [106, 131]. We generated two constructs GFP-Pex30 and Pex30-GFP to confirm the correct terminal for tagging. As shown in Fig. 3.2, Pex30-GFP displayed both punctate and reticulate distribution of the protein, as reported earlier [87, 129]. GFP-Pex30 on the other hand did not alter the reticulate distribution but the punctate distribution was markedly reduced suggesting that N-terminal tagging may alter the distribution. Binding of Pex19 to a peroxisomal protein is essential for its targeting to peroxisomes whereas the RHD domain is indispensable for the assembly of Pex30 complexes at the ER-peroxisome contact sites. The differential phenotype observed between C and N-terminal GFP-tagged Pex30 might be due to an alteration in the interaction of Pex30 with its interacting protein Pex19 caused by the GFP tag at the N-terminus. Similarly, Pex30 shares homology and interacts with the ER reticulon proteins via its RHD domain. Therefore, the hindrance caused by GFP at its N-terminus might alters interaction with the ER proteins and thereby also affect the distribution and phenotype of the protein. We further continued with Pex30-GFP and analyzed the expression of Pex30 in glucose and peroxisome-inducing conditions. OA media is enriched with fatty acid and as peroxisomes in yeast are responsible for the breakdown of fatty acids, the metabolism of fatty acids via the β-oxidation pathway is enhanced when cultured in OA. On the other hand, YND media is devoid of fatty acid and therefore the β-oxidation pathway remains dormant. The glucose in YND media is metabolized via the glycolysis pathway. This suggests that peroxisomal enzymes required for fatty acid metabolism are not induced in the presence of glucose and therefore the number of peroxisomes remains constant. However, upon shifting the YND-cultured cells to OA media, the peroxisomal enzymes involved in β-oxidation such as acyl-CoA oxidase (POX1) are induced concomitant to a significant increase in the size and number of peroxisomes. Interestingly, we have observed reduced expression of Pex30 in OA in comparison to YND. This reduced expression of Pex30 observed in OA conditions may contribute to the reduction

of punctate phenotype. It may also be speculated that the altered expression of Pex30 may influence the induction of peroxisomes in OA.

Further, we analyzed the distribution and expression of Pex30 in strains lacking Pex30-intercating proteins such as Pet10, Mdm10 and Erg6. It was observed that the distribution and expression of Pex30 is independent of its interacting partners as indicated by fluorescence microscopy and western blot analysis (Fig. 3.3). Notably, quantification of peroxisome number indicates that deletion of Mdm10 significantly increases peroxisome number as compared to WT cells (Fig. 3.5). In accordance with previous studies, our microscopy analysis and quantification of peroxisome number clearly demonstrates that cells lacking Pex30 display an increase in the number of peroxisomes. As stated earlier, the distribution of Pex30 was not affected by the deletion of Mdm10 which signifies that Mdm10 might associate with other peroxisomal proteins in the regulation of peroxisome dynamics. An earlier study has demonstrated that in cells lacking Mdm10, the localization of Pex11, a protein that functions as regulator of peroxisome proliferation, is significantly altered [147]. Therefore, it can be speculated that the increase in peroxisome number exhibited by Δmdm10 cells may result from altered interaction with proteins involved in regulation of peroxisome number. However, if Pex30 is involved directly or indirectly has to be further investigated.

The Pex11 family proteins involved in the proliferation of peroxisomes are induced in OA media which results in the increase in peroxisome number. In this thesis work, we have observed a significant increase in peroxisome number in Δpex30 cells in OA cultured cells demonstrating the function of Pex30 as a negative regulator of peroxisome number. However, a basal level of peroxisome proliferation was also observed in cells lacking Pex30 when cultured in YND media. Interestingly, cells lacking the Pex30 interacting protein, Mdm10 also exhibit a similar increase in peroxisome number as observed in Δpex30 cells in both YND and OA media.

Chapter 4

Pex30 undergoes phosphorylation and regulates peroxisome number in *Saccharomyces cerevisiae*

Abstract

Pex30 is a dysferlin domain-containing protein whose role in peroxisome biogenesis has been studied by several research groups. Notably, recent studies have linked this protein to peroxisomes, ER and LDs in *S. cerevisiae*. Phosphoproteome studies of *S. cerevisiae* have identified several phosphorylation sites in Pex30. In this study we expressed and purified Pex30 from its native host. Analysis of the purified protein by circular dichroism spectroscopy showed that it retained its secondary structure and revealed primarily a helical structure. Further phosphorylation of Pex30 at three residues, Threonine 60, Serine 61 and Serine 511 was identified by mass spectrometry in this study. To understand the importance of this post-translational modification in peroxisome biogenesis, the identified residues were mutated to both non-phosphorylated (alanine) and phosphomimetic (aspartic acid) variants. Upon analysis of the mutant variants by fluorescence microscopy, no alteration in the localization of the protein to ER and peroxisomes was observed. Interestingly, reduced number of peroxisomes were observed in cells expressing phosphomimetic mutations when cultured in peroxisome-inducing conditions. Our data suggest that phosphorylation and dephosphorylation of Pex30 may promote distinct interactions essential in regulating peroxisome number in a cell.

This chapter is published as

Deori NM, Infant T, Sundaravadivelu PK, Thummer RP, Nagotu S (2022) Pex30 undergoes phosphorylation and regulates peroxisome number in *Saccharomyces cerevisiae*. Molecular Genetics and Genomics. https://doi.org/10.1007/s00438-022-01872-8

4.1 Introduction

Protein phosphorylation is a ubiquitous PTM that regulates various cellular processes in eukaryotes [183]. Phosphorylation events are dynamic and reversible, mediated by protein kinases and phosphatases [184]. Protein phosphorylation involves introducing a negatively charged phosphate group to the side chain of a specific amino acid residue, mainly serine, threonine, and tyrosine, in a polypeptide chain [185]. The addition of a covalently bound phosphate group results in conformational changes in the structure of the protein that leads to alteration in the binding affinity of the protein with its interacting partners and the regulation of subcellular localization of the protein [186-188]. Approximately 40-50% of yeast proteome is reported to be phosphorylated, indicating the indispensable nature of phosphorylation in the study of eukaryotic biology [189].

Peroxisomes are single membrane-bound organelles ubiquitously present in all eukaryotes whose number and function vary in response to cellular metabolic needs [17]. Peroxisomes are well-characterized for their role in neutralizing harmful ROS produced by the cell and the β-oxidation of fatty acids [17, 190]. The biogenesis of these organelles is regulated by a set of proteins called peroxins (Pex) required for various aspects of biogenesis, such as division and protein import leading to the formation and maturation of new daughter peroxisomes [56, 108]. Previous studies have reported that Pex proteins are also associated with the degradation of peroxisomes termed pexophagy [191, 192]. In *S. cerevisiae*, the differential identification of phosphorylated-proteins when cultured in peroxisome-inducing and peroxisome-repressing conditions emphasizes the relevance of phosphorylation on peroxisome dynamics [193]. Several peroxisomal proteins in various organisms are now reported to be phosphorylated [120]. This modification regulates the import of peroxisomal proteins such as Cit2p (a peroxisomal isoform of citrate synthase) and catalase from the cytosol

into the peroxisomal matrix [194-196]. Phosphorylated forms of the peroxisomal membrane protein Pex11 are also identified in various yeast species [100, 121, 197].

One such interesting protein that is multifunctional and has a role in peroxisome biogenesis, lipid droplet biogenesis, and required for the maintenance of ER shape is Pex30 [87, 142, 172]. Pex30 is a dysferlin domain-containing protein that initially targets to the cortical ER and then traffics to specific subdomains of ER where it associates with proteins responsible for maintaining the tubular structure of ER such as Rtn1, Rtn2 and Yop1 [129]. Earlier studies have reported an increase in peroxisome number in cells lacking Pex30, thereby indicating its role in the regulation of peroxisome number in a cell [172]. However, later studies reported the role of Pex30 in the formation of peroxisomes from the ER [129]. A role for Pex30 in lipid body biogenesis has also been recently demonstrated. Pex30 is reported to associate with the lipid droplet protein, Seipin, in specific subdomains of ER and modulates the exit site of PPVs that eventually leads to the formation of peroxisomes and LDs [160]. The absence of Pex30 is also associated with a delay in the formation of LDs from the ER, underlying the role of Pex30 in LD biogenesis [142].

Several independent phosphoproteome studies have identified 17 putative residues that can undergo phosphorylation. Most of these phosphorylated sites are located at the extreme C-terminus of the protein [198-200]. Although Pex30 is reported to be phosphorylated at multiple residues, detailed studies of these putative sites on the function and localization of the protein are not performed. In this study, we identified the residues that undergo phosphorylation in Pex30. Further we demonstrated that this PTM of the protein is not needed for its expression and localization to peroxisomes and ER. Interestingly, the phosphomimetic variants of the protein exhibit significant reduction in the number of peroxisomes. Our data highlights the role of Pex30 in the regulation of peroxisome number.

4.2 Results

4.2.1 Purified Pex30 retained its secondary structure

In order to investigate the phosphorylation state of Pex30 and the potential effect of this PTM on the protein, purification of Pex30 was performed by immobilized metal ion affinity chromatography (IMAC). *S. cerevisiae* cells expressing His-tagged Pex30 under the control of an inducible galactose promoter were initially cultured in media containing glucose and raffinose as carbon source. Subsequently, the expression of Pex30 was induced by exposing the cells in raffinose-containing medium to a galactose pulse for 6 hrs. Protein expression was further confirmed by western blotting using α-His antibody (Fig. 4.1A). Both SDS-PAGE and western blotting analysis with α-His antibody indicates that Pex30 was purified without any contaminating protein bands (Fig. 4.1B).

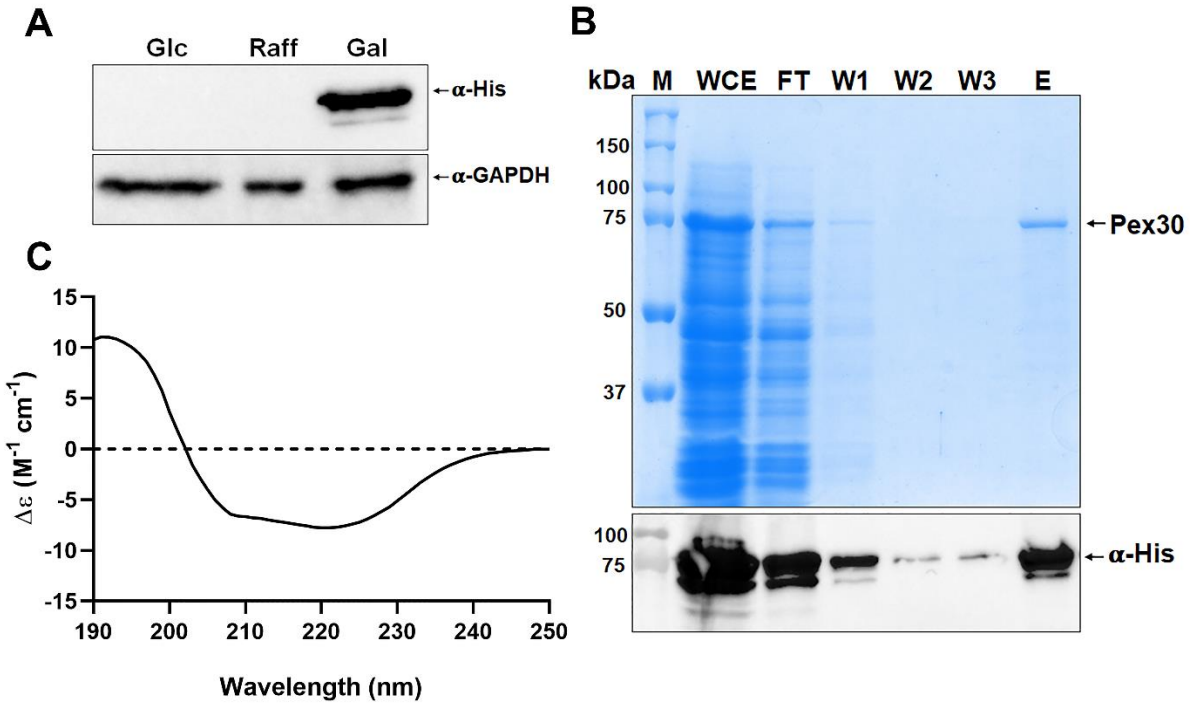

Fig. 4.1 Expression and structural characterization of His-tagged Pex30
(A) Cells pre-cultured in YND media were subsequently cultured in raffinose followed by induction of the Pex30-His-HA cassette by the addition of galactose. The induced cells were then harvested and lysed using zirconia beads. Protein concentrations were measured by the Bradford protein estimation method and GAPDH was used as a loading control. Samples were run on a 10% SDS-PAGE gel and protein expression was confirmed by western blotting using α-His antibody. **(B)** represents affinity purification of galactose-induced Pex30 protein under native conditions. Coomassie-stained 10% SDS-PAGE gel depicting purification of His-tagged Pex30 and confirmed by western blotting using an α-His antibody. M: protein marker (kDa); WCE: whole cell extracts; FT: flow through; W: wash; E: elution. **(C)** Secondary structure determination of Pex30. The purified Pex30 protein was subjected

to a desalting column pre-calibrated with 20 mM PB. The desalted protein eluted in PB was then analyzed via far-UV CD spectroscopy followed by *in-silico* analysis using the BeStSel online tool. The CD spectrum for Pex30 was obtained by plotting the wavelength (nm; Y-axis) against delta epsilon (X-axis).

Experimental data deciphering the secondary structure of Pex30 has not been reported yet. To explore the possibility of determining the secondary structure of Pex30, the purified protein was desalted and then analyzed by far-UV CD spectroscopy (Fig. 4.1C). Previous studies have demonstrated the utility of far-UV CD spectroscopy in the successful determination of secondary structure conformations of proteins [201]. In far-UV CD spectroscopy, the acquired CD spectrum is directly associated with the folding conformation of the protein. The CD spectrum represents the different secondary structure content like α-helix, β-sheets, turns and random coils that depends on the magnitude and characteristic shape of the spectra [201, 202]. Typically, the CD spectrum of a α-helix shows negative peaks at 222 nm and 208 nm and a positive peak at 193 nm [202]. The obtained data from the far-UV CD spectroscopy of purified Pex30 was analyzed *in silico* by using an online tool, BeStSel, that can predict the folds and secondary structure content of proteins [165, 166]. Our *in silico* analysis indicates that the purified Pex30 has retained its secondary structure (Fig. 4.1C) which predominantly comprises of α-helices (51%) followed by a significant proportion of β-sheets (25%) and random coils (17%) and a minor portion of turns (7%). Recently a computational method that can predict 3D structures of proteins to near experimental accuracy was developed [203]. The structure of Pex30 predicted using this method is shown in Fig. 4.2 and primarily comprises of α-helices [203].

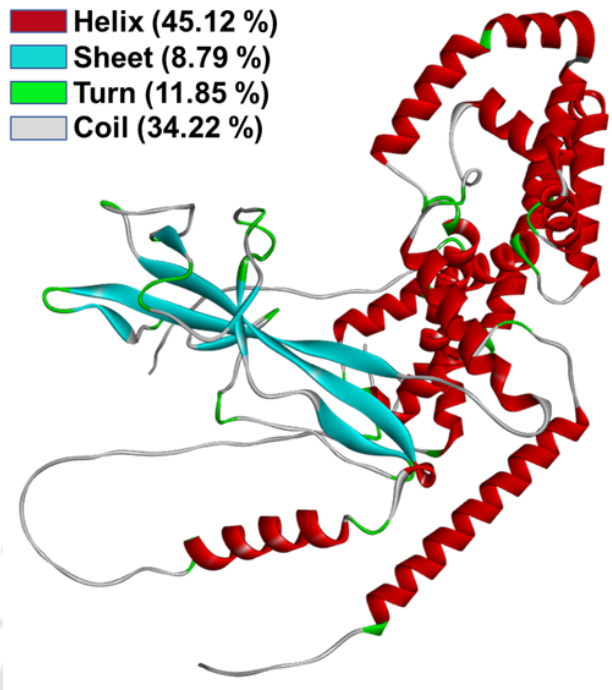

Fig. 4.2 Predicted structure of Pex30
The secondary structure of Pex30 was predicted by the computational method based on the neural network model, AlphaFold [203]. The secondary structure predicted with atomic accuracy comprises mainly of α-helices (45.12 %) followed by other secondary structure components such as random coil (34.22 %), turns (11.85 %) and β-sheets (8.79 %).

4.2.2 Pex30 is phosphorylated at Thr60, Ser61 and Ser511

To gain insights into the phosphorylated state of Pex30, a fraction of the obtained Pex30 eluate from purification was treated with CIAP. The mobility of the CIAP treated sample was analyzed in comparison to the untreated sample in a phos-tag SDS-PAGE gel. A phos-tag is a gel additive that selectively binds to the phosphate groups present in a protein molecule and thereby produces a shift in the electrophoretic mobility making it easier for the PTM to be detected in an SDS-PAGE [168]. The sample incubated with phosphatase (+CIAP) was observed to have slightly increased the migration indicating the removal of phosphate groups from the protein (Fig. 4.3A, lower panel) whereas no difference in migration patterns of the CIAP treated (+CIAP) and untreated (-CIAP) protein samples were observed in a conventional SDS-PAGE gel (Fig. 4.3A, upper panel).

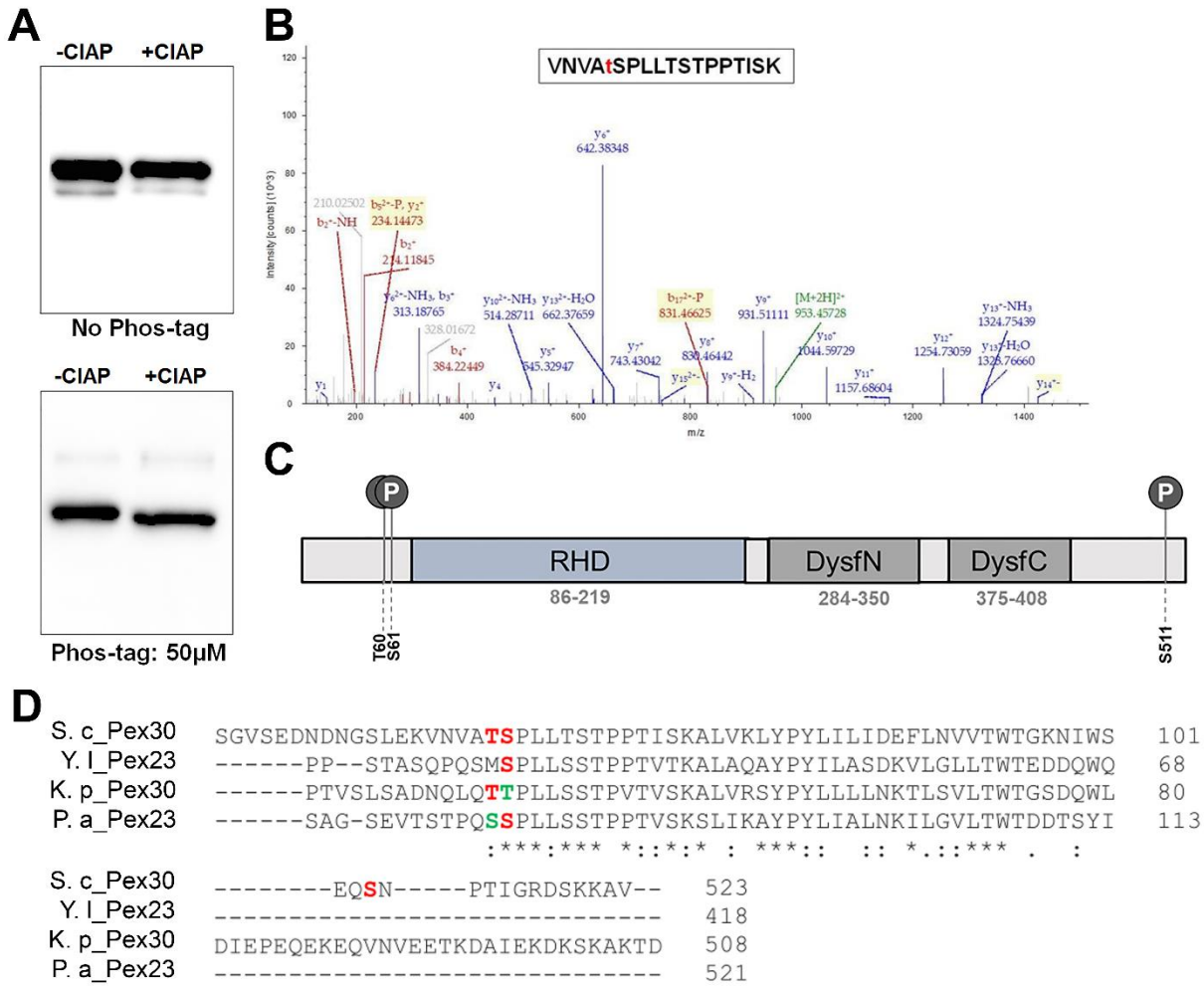

Fig. 4.3 Pex30 is phosphorylated at three residues *in vivo*
(A) His-tagged Pex30 expressed from inducible galactose promoter was affinity purified by the use of Ni/NTA resin and the protein was eluted in tris buffer (pH 7.5). Proteins from CIAP treated and untreated samples were analyzed both by conventional SDS-PAGE and phos-tag SDS-PAGE followed by immunoblotting with α-GFP antibody. **(B)** Representative MS/MS spectrum depicting phosphorylation of Pex30 at Thr60 (VNVAtSPLLTSTPPTISK; m/z 953.500; MH+: 1905.99309 Da; z = +2). **(C)** Schematic representation of Pex30 indicating the position of the identified phosphorylation sites. RHD, reticulon homology domain was predicted by using HH-pred [204]. DysfN/DysfC, N-terminal dysferlin domain and C-terminal dysferlin domain are represented according to Simple Modular Architecture Research Tool (SMART, ID: SM00693 and SM00694). This is taken from Saccharomyces Genome Database, SGD (https://www.yeastgenome.org). **(D)** Sequence alignment of *S. cerevisiae* Pex30 with its homologues in *Y. lipolytica* (Pex23), *K. phaffii* (Pex30) and *O. polymorpha* (Pex23) illustrating the position of the phosphorylated residues identified in this study. Amino acid residues of *S. cerevisiae* Pex30 highlighted in red indicates the identified phosphorylated residues; the conserved phosphorylated residues in other yeast species are also marked in red. Amino acids highlighted in green indicates the presence of residues that are phosphorylatable but not conserved.

To further identify the phosphorylation sites, mass spectrometry was performed on the purified Pex30. Efficient sequence coverage of ~54% was obtained for Pex30 and this included 16 phosphorylation sites reported earlier. However, only two different peptides exhibited a ppm of -0.1 and -0.63 that indicates the presence of additional PTM moiety when compared to the

predicted molecular mass for the peptides. Out of the three sites that we have identified with high confidence Thr60, Ser61 have been reported in phosphoproteome studies [198, 200] and Ser511 has not been reported earlier. The sites with PEP <0.01 were identified to be phosphorylated (Fig. 4.3B and Fig. 4.3C). Further we analyzed if the identified sites are conserved in various yeast species by multiple sequence alignment using Clustal Omega [205]. Of the identified sites, Thr60 is conserved in *S. cerevisiae* and *K. phaffii* whereas Ser61 is conserved in *S. cerevisiae*, *Y. lipolytica* and *O. polymorpha* (Fig. 4.3D). Thus, phos-tag SDS-PAGE and MS analysis data provide evidence for the phosphorylation of Pex30 *in vivo*.

4.2.3 Mutation of the identified phosphorylated residues to non-phosphorylatable or phosphomimetic variants does not alter the expression of the protein and growth of cells

To explore the functional significance of the identified phosphorylation of Pex30, mutant variants of the protein were generated by exchanging the threonine and serine residues with non-phosphorylatable alanine (A) or phosphomimetic aspartic acid (D). Due to the close proximity of the residues Thr60 and Ser61, we generated a variant in which both the phosphorylated sites were changed. Ser511 was also changed to either A or D to create a single mutant variant of the protein. Moreover, a mutant strain with all the three identified sites exchanged with A or D was also generated. The confirmation of all the mutant variants of Pex30 was achieved by restriction digestion with specific enzymes (Fig. 4.4A and Fig. 4.4C) and DNA sequencing of the constructs (Fig. 4.4B and Fig. 4.4D).

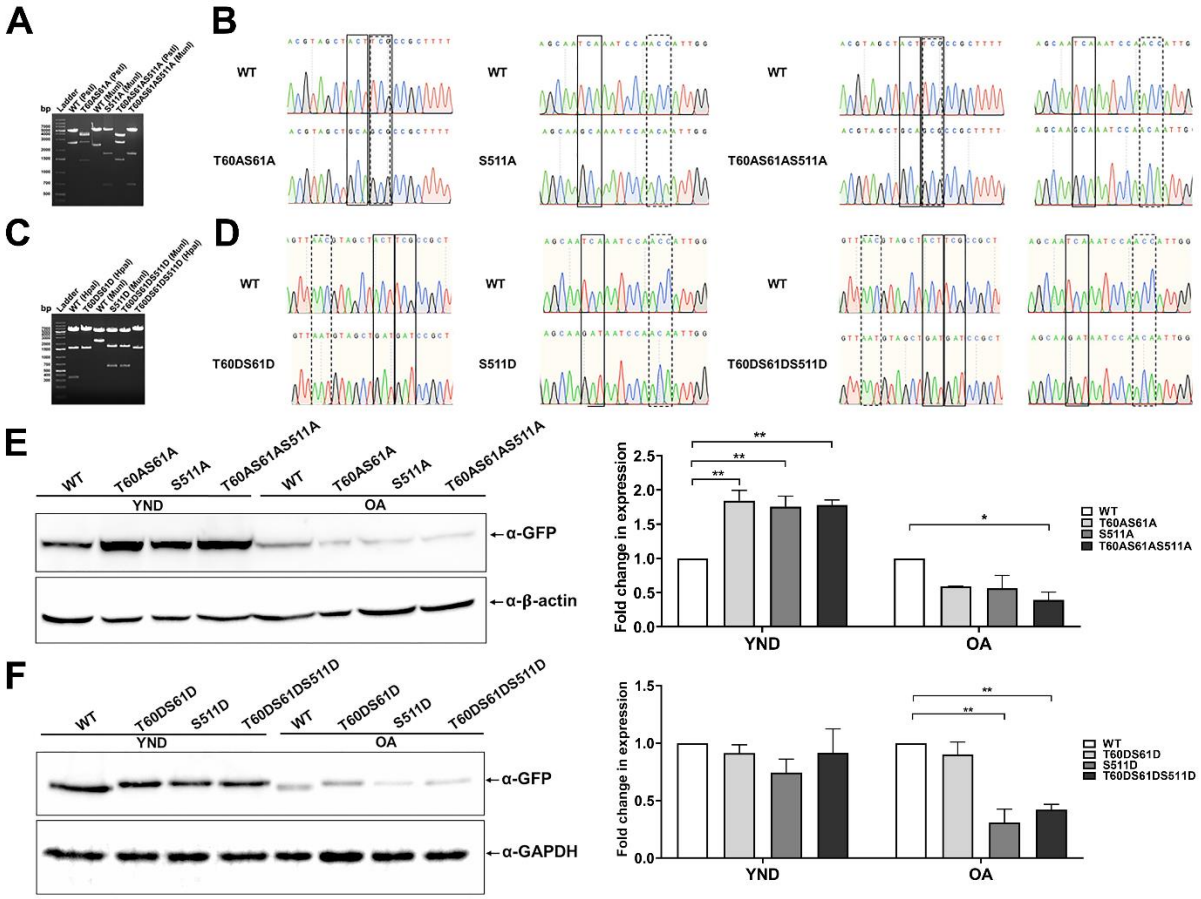

Fig. 4.4 Site-directed mutagenesis and expression of the mutant variants
(A) represents agarose gel images showing restriction digestion profiles to confirm the presence of PCR amplified clones carrying the non-phosphorylatable mutation (left). Site-directed mutagenesis was performed by changing the phospho-sites to non-phosphorylatable alanine. **(B)** The mutations were further confirmed by sequencing analysis. The solid line boxes indicate the desired mutations and the dotted boxes denotes alteration in nucleotide without changing the amino acid to generate a unique restriction site for screening of mutants. Boxes in both solid and dotted line denote the formation of unique restriction sites while generating mutations in the phosphorylated residues. **(C)** and **(D)** represent restriction digestion (left) and sequencing analysis (right) performed to screen and confirm the mutants in which the phospho-sites were exchanged with the amino acid aspartate to generate phosphomimetic variants of Pex30. **(E)** represents expression analysis of the non-phosphorylatable mutants grown in YND and OA medium. Whole cell lysates corresponding to 3 OD_{600} units were resolved by SDS-PAGE and probed with α-GFP antibody. For quantitative analysis, the GFP blots were normalized with β-actin as a loading control and represented as bar diagrams. The error bars indicate SEM obtained from two independent experiments (right). A two-way ANOVA with multiple comparisons was used to determine the significance of difference between the expression levels of WT Pex30 and the non-phosphorylatable mutants. Values of $P < 0.05$ were considered significant (*) and $P < 0.01$ very significant (**). **(F)** depicts expression analysis of the phosphomimetic mutants. 3 OD_{600} units of whole cell lysates were separated by using SDS-PAGE followed by western blotting with α-GFP antibody (left). Quantitative analysis of the immunoblots was performed by normalizing with GAPDH (loading control) and represented as bar diagrams. Error bars denote SEM obtained from two independent experiments (right). The significance of the difference between the expression levels of WT Pex30 and the phosphomimetic mutants were statistically determined by using two-way ANOVA (with multiple comparisons). Values of $P < 0.05$ were considered significant (*) and $P < 0.01$ very significant (**)

The mutant variants were then introduced into Δpex30 cells. The protein expression levels of the mutants were analyzed and compared to that of the WT protein via western blotting using an α-GFP antibody (Fig. 4.4E and 4.4F). The change in protein expression levels was

quantified and is represented as a fold change in expression. In cells cultured in the YND medium, the non-phosphorylatable mutants exhibited significant increase in protein expression in comparison to the WT protein whereas in OA growth conditions, reduced protein expression was observed in cells bearing T60AS61AS511A mutation (Fig. 4.4E). In addition, protein expression levels of the phosphomimetic mutants were unaltered in YND but cells bearing S511D and T60DS61DS511D mutations displayed a significant reduction in protein expression in OA (Fig. 4.4F). Strikingly, a small shift in the band of the phosphomimetic mutants was observed in comparison to WT in both YND and OA (Fig. 4.4F). This change could be due to the change of the overall charge which may affect the electrophoretic mobility of the protein and probable conformational changes in the native structure of Pex30 due to amino acid substitution resulting in a small increase in molecular weight (Fig. 4.4E). Similar decreased electrophoretic mobility upon substitution of aspartate with serine was also reported earlier [206]. This distinct band shift was not observed in the non-phosphorylatable mutants.

Fluorescence microscopy analysis revealed no significant difference between the distribution and expression of the mutant variants and WT protein. Cells expressing both the non-phosphorylatable and phosphomimetic mutant variants exhibited the typical punctate as well as reticulate phenotype as exhibited by WT Pex30 when grown in YND and OA media (Fig. 4.5A and Fig. 4.6A).

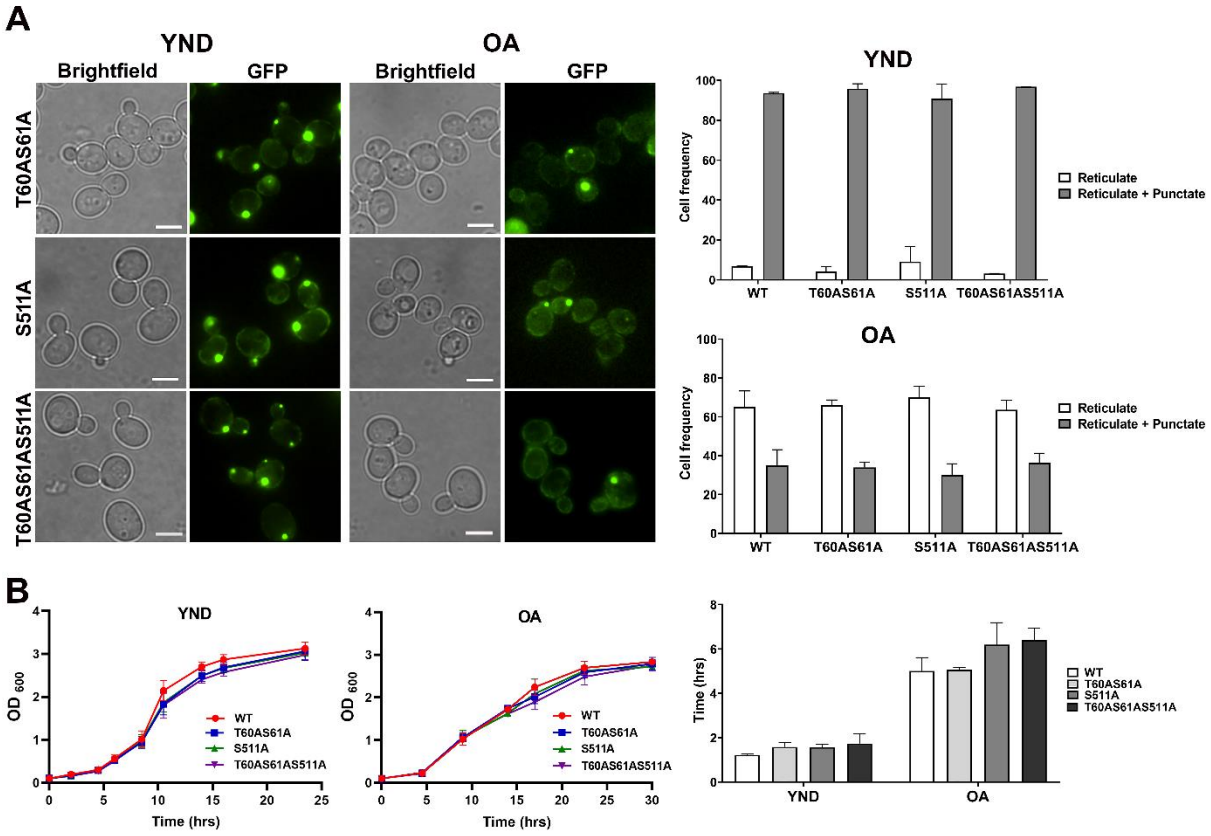

Fig. 4.5 Microscopy analysis of cells expressing the non-phosphorylatable variants of Pex30 and effect on cell growth

(A) Fluorescence microscopy images of Δpex30 cells expressing the GFP-tagged non-phosphorylatable variants of Pex30 (T60AS61A, S511A and T60AS61AS511A). Cells were grown in both YND and peroxisome inducing OA media incubated at 30 ^{0}C. A group of 3-4 cells exhibiting GFP fluorescence from each mutant strain is represented with the corresponding brightfield images. Scale bar represents 5 μm. Quantitative analysis of phenotype exhibited by YND and OA cultured cells is represented as bar diagrams. 60 cells from each experiment were analyzed. Error bars indicate SEM from two independent experiments. The statistical significance was determined by using two-way ANOVA with multiple comparisons. **(B)** The effect of expression of the non-phosphorylatable Pex30 mutants on yeast cell growth was determined by plotting a growth curve. Yeast cells were cultured both on YND (left) and OA media (middle) and the growth kinetics was assessed by measuring the optical density of cells at 600 nm (OD_{600}) over the indicated time. The doubling time of the yeast strains was measured by calculating difference in growth rates during the exponential phase (right). Error bars indicate SEM calculated from two independent experiments. The statistical significance was determined by using two-way ANOVA with multiple comparisons

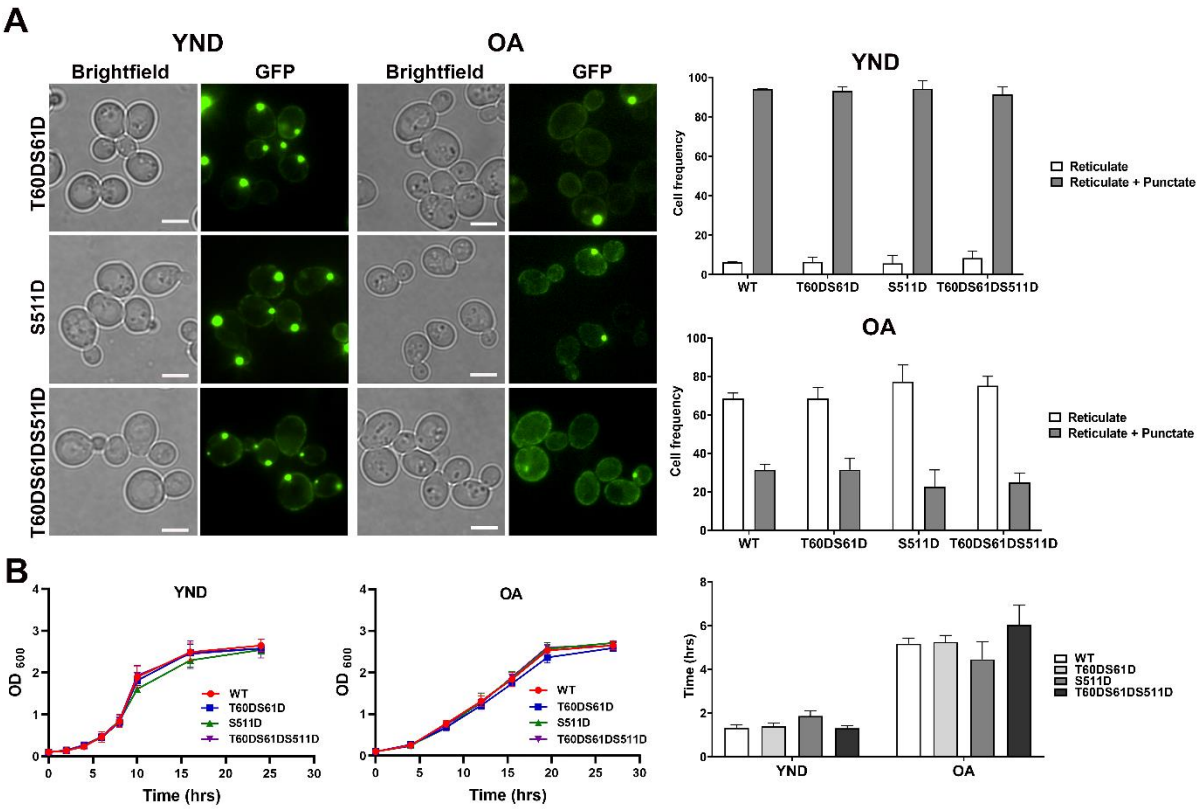

Fig. 4.6 Microscopy analysis of the cells expressing phosphomimetic variants of Pex30 and effect on cell growth **(A)** Fluorescence microscopy images of Δpex30 cells expressing the GFP-tagged phosphomimetic variants of Pex30 (T60DS61D, S511D and T60DS61DS511D). Cells were grown in both YND and OA media. A group of 3-4 cells exhibiting GFP fluorescence from each mutant strain is represented with the corresponding brightfield images. Scale bar represents 5 µm. Quantitative analysis of phenotype exhibited by YND and OA cultured cells is represented as bar diagrams. 60 cells from each experiment were analyzed. Error bars indicate SEM from two independent experiments. The statistical significance was determined by using two-way ANOVA with multiple comparisons. **(B)** The effect of expression of the phosphomimetic mutants on yeast cell growth was determined by plotting a growth curve. Yeast cells were cultured both on YND (left) and OA media (middle) and the growth kinetics was assessed by measuring the optical density of cells at 600 nm (OD_{600}) over the indicated time. The doubling time of the yeast strains was measured by calculating the difference in growth rates during the exponential phase (right). Error bars indicate SEM calculated from two independent experiments. The statistical significance was determined by using two-way ANOVA with multiple comparisons.

Quantification of fluorescence images of these cells also revealed a phenotype comparable to the cells expressing WT Pex30 in YND and OA. Quantitative analysis revealed that most cells grown in YND media exhibited punctate plus reticulate phenotype whereas in OA cultured cells, in addition to this, cells with only reticulate phenotype were also observed. The growth kinetics of yeast cells transformed with the mutant variants and WT Pex30 was monitored. The growth rate of the mutant strains and doubling time did not differ significantly when compared to cells expressing WT Pex30 in both the growth conditions (Fig. 4.5B and Fig. 4.6B).

4.2.4 Mutations in the phosphorylation sites does not alter the localization of the protein

To investigate if the mutant variants exhibit altered subcellular localization, they were co-transformed with plasmids that specifically label peroxisomes or ER. Microscopy analysis revealed that the puncta-like phenotype of WT Pex30 localizes in close proximity to peroxisomes, and in some cells, the GFP puncta were observed to partially co-localize with peroxisomes (Fig. 4.7A and 4.7B). The association between Pex30 puncta and peroxisomes was also analyzed by measuring the fluorescence intensity and is represented as intensity line profiles (Fig. 4.7A and 4.7B).

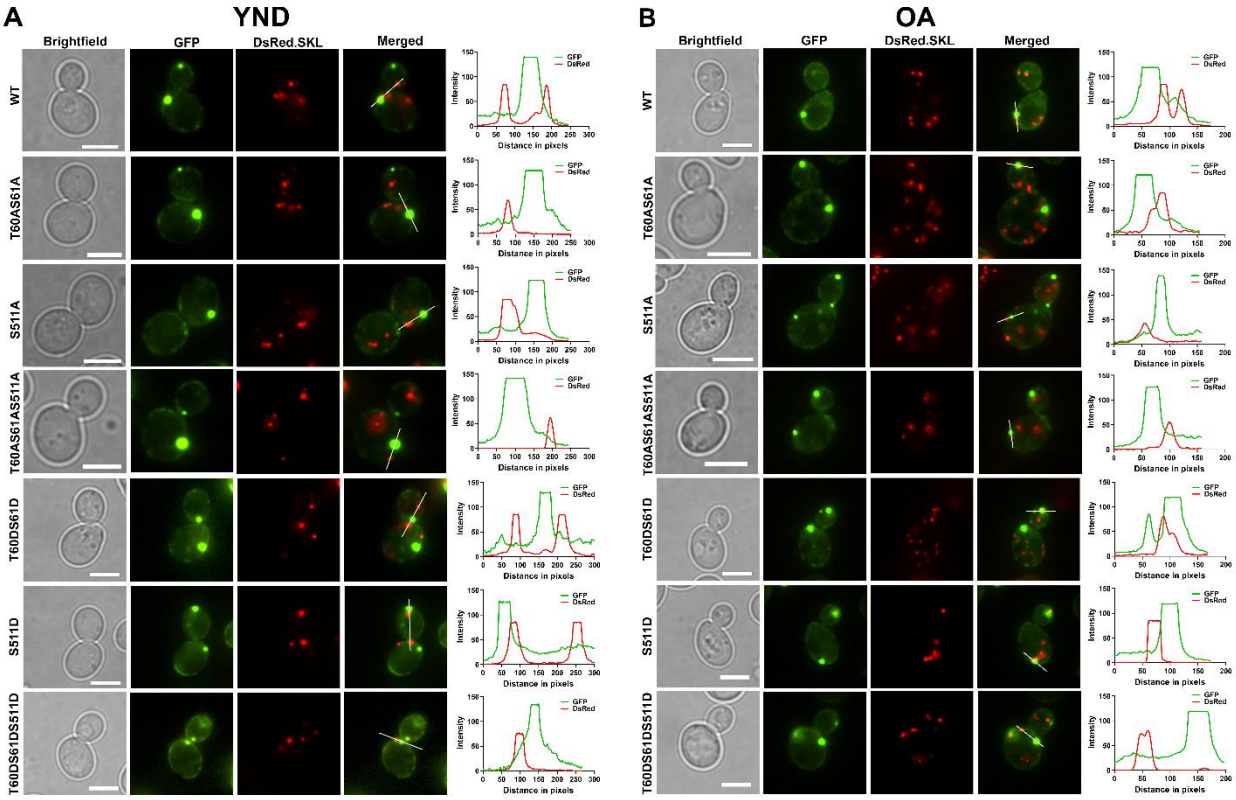

Fig. 4.7 Mutant variants of Pex30 do not show altered localization to peroxisomes
Δpex30 cells consisting of the GFP expressing non-phosphorylatable and phosphomimetic variants of Pex30 was co-transformed with a plasmid containing DsRed.SKL, which specifically targets to peroxisomes. The cells were cultured in YND media **(A)** and OA **(B)** and subsequently co-localization of GFP puncta with DsRed.SKL marked peroxisomes were analyzed by fluorescence microscopy. The extent of co-localization was analyzed by intensity profiles obtained from the regions (line) depicted in the merged panel and is illustrated as graphs. The fluorescence intensity of the green and red fluorophores was measured using ImageJ. Scale bar represents 5 μm

This observation is in line with an earlier study by David and colleagues, where the authors suggest that a small portion of Pex30 targets to peroxisomes and the accumulation of

peroxisomes is juxtaposed to Pex30 puncta [129]. As observed in WT cells, both the non-phosphorylatable and phosphomimetic variants of Pex30 displayed similar co-localization with DsRed.SKL marked peroxisomes which indicates that targeting of Pex30 was not altered in the mutant variants (Fig. 4.7A and 4.7B). The targeting of WT Pex30 and mutant variants to ER was analyzed by co-expressing Sec63-mRFP. As reported earlier [87, 129], our data also indicates that the reticulate structure of WT Pex30 and the mutant variants colocalizes mostly with the cortical ER at the cell periphery (Fig. 4.8). This suggests that phosphorylation of Pex30 at Thr60, Ser61 and Ser511 most likely is not involved in its targeting to peroxisomes and the ER.

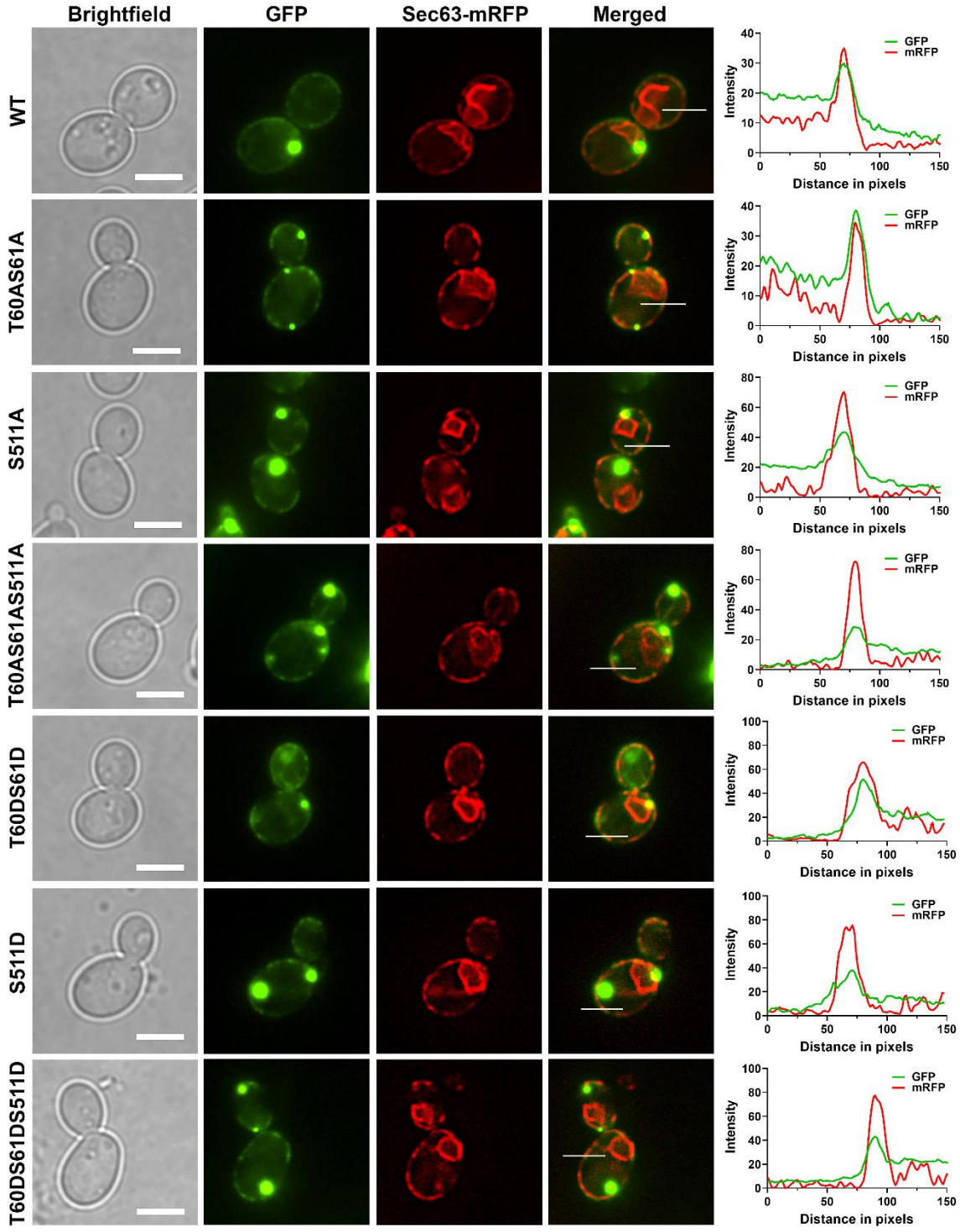

Fig. 4.8 Mutant variants of Pex30 do not show altered localization to ER
Δpex30 cells consisting of the GFP expressing non-phosphorylatable and phosphomimetic variants were co-transformed with the plasmid containing Sec63-mRFP, which specifically targets to ER. The cells were cultured in YND media and subsequently co-localization of the Pex30-GFP with Sec63-mRFP marked ER was analyzed by fluorescence microscopy. The extent of co-localization was analyzed by intensity profiles obtained from the regions (line) depicted in the merged panel and is illustrated as graphs. The fluorescence intensity of the green and red fluorophores was measured using ImageJ. Scale bar represents 5 μm

4.2.5 Peroxisome phenotype in mutant variants of Pex30

To assess whether the non-phosphorylatable and phosphomimetic mutations influence the number of peroxisomes in yeast cells, we analyzed the total number of peroxisomes per cell in the mutant strains cultured in both YND and OA media (Fig. 4.9). Cells expressing WT Pex30 showed a clear induction of peroxisomes when grown in OA media (10.1 ± 3.4 versus 5.9 ± 2.2). In YND, cells bearing non-phosphorylatable mutant variants of Pex30 viz. T60AS61A and T60AS61AS511A displayed a similar number of peroxisomes as in cells expressing WT Pex30 (6.15 ± 2.0 and 5.5 ± 1.5); whereas the number of peroxisomes decreased in cells bearing S511A mutation (5.1 ± 2.3). Similarly, the phosphomimetic variants T60DS61D and T60DS61DS511D exhibited a peroxisome number similar to the WT (5.8 ± 2.5 and 5.6 ± 2.4); whereas a decrease in peroxisome number was observed in the S511D phosphomimetic mutant (4.9 ± 1.9). Upon growth in OA containing media, cells expressing non-phosphorylatable variants T60AS61A and T60AS61AS511A exhibited a similar number of peroxisomes (9.7 ± 3.3 and 10.5 ± 3.3) as compared to cells expressing the WT version of the protein (10.1 ± 3.4); whereas a decrease in peroxisome number was observed in the S511A mutant variant (8.9 ± 2.9). Notably, in peroxisome inducing OA media, all the phosphomimetic variants of Pex30, i.e., T60DS61D, S511D and T60DS61DS511D displayed a decrease in peroxisome number (7.7 ± 2.8, 7.8 ± 3.2 and 7.3 ± 2.5). Hence, our data indicates that mutation at S511 results in decrease of peroxisome number in both YND and OA growth conditions. In addition, under peroxisome proliferating growth conditions, the phosphomimetic variants of Pex30 exhibit a negative effect on the proliferation of peroxisomes.

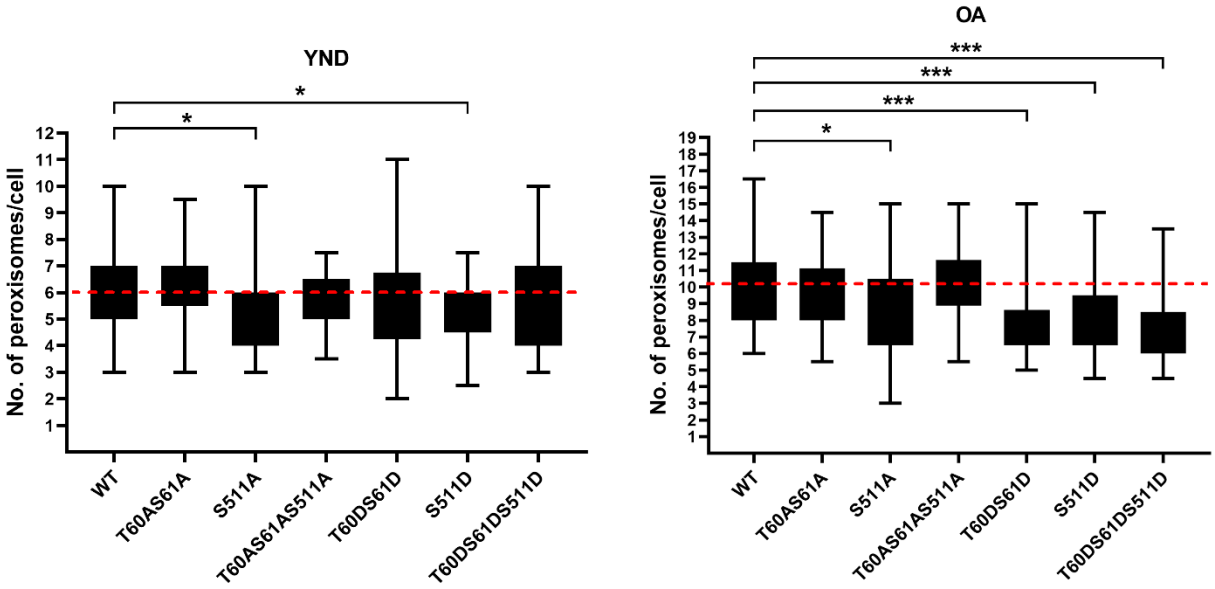

Fig. 4.9 Mutant variants of Pex30 exhibit altered peroxisome number.
WT and mutant variants of Pex30 expressing the peroxisomal marker DsRed.SKL were analyzed for peroxisome number. For quantification of peroxisome number, yeast strains were cultured in both YND and peroxisome inducing OA media. For each yeast strain, peroxisomes were counted by merging the Z-stack and 40 cells were counted from one independent experiment. The data represented is from two such experiments. The box and whisker plot illustrates the diversity of peroxisome number among the yeast strains. The red dashed line denotes the average (mean) number of peroxisomes in WT cells. Values of $P < 0.05$ were considered significant (*), $P < 0.01$ very significant (**) and $P < 0.001$ extremely significant (***).

4.3 Discussion

In this study, we have successfully expressed and purified the full-length Pex30 and structural determination using CD showed that the secondary structure conformation of the purified protein was retained. Analysis of CD data shows that Pex30 has predominantly α-helices followed by β-sheets. At the N-terminus of the protein a RHD that is predominantly α-helical has been predicted. The dysferlin domain in this protein is conserved and is ubiquitously present in other proteins belonging to this family [207]. β-sheet structure for this domain in human dysferlin has been reported [207]. Analysis of the Pex30 structure obtained from AlphaFold also shows a β-sheet structure for this domain. Interestingly, no role for this domain in the interaction of the protein with Pex28, Pex29 and Pex32 has been reported. Cells expressing Pex30 lacking dysferlin domain show a peroxisome phenotype similar to that of Δpex30 cells [106].

Whole proteome studies have identified several residues that are most likely sites for phosphorylation. In this work we have shown that *S. cerevisiae* Pex30 is phosphorylated at three residues Thr60, Ser61 and Ser511. Thr60, Ser61 are present in the N-terminal of the protein and Ser511 is at the extreme C-terminus of the protein. The identified residues were replaced with non-phosphorylatable or phosphomimetic residues and analyzed for variations in protein expression, peroxisome phenotype and the localization of mutant variants to peroxisomes and ER. Our data demonstrates that both non-phosphorylatable and phosphomimetic variants behave similarly to the WT protein. This led us to conclude that phosphorylation most likely does not play an important role in the localization of the protein to peroxisomes or ER. Other cellular mechanisms may be needed for this targeting. Identifying the domains of the protein that particularly interact with proteins on the peroxisomes/ER may help understand this mechanism.

Interestingly, peroxisome number in cells cultured in YND and OA did not alter significantly in non-phosphorylated variants, except for the S511A, which showed a reduced number in OA. Reduced number of peroxisomes in peroxisome-inducing growth conditions was observed when the residues were replaced with phosphomimetic aspartate residue. A role for phosphorylation in the formation of higher-order structures of the protein or to make distinct protein interactions required to regulate peroxisome biogenesis can be envisaged. Our data demonstrate that phospho-mimicking mutant versions of *S. cerevisiae* Pex30 result in altered number of peroxisomes and lead us to conclude that phosphorylation may play a vital role in regulating peroxisome number and does not influence the localization of the protein to ER and peroxisomes.

Other than phosphorylation, ubiquitination and glycosylation are also identified in Pex30 as PTMs by global mass spectrometry analysis. Similar to phosphorylation, both ubiquitination and glycosylation are regulatory mechanisms that mediate the cellular localization and the

function of proteins and are also associated with modulating protein-protein interaction. Although the role of these PTMs in the function of Pex30 has not been explored yet, previous studies have reported that these PTMs regulate the function and targeting of various peroxisomal membrane proteins involved in peroxisome biogenesis. For instance, Pex13 which aids in the translocation of peroxisomal matrix proteins undergoes ubiquitination and is then targeted to proteasomes for degradation. The N-linked glycosylation affects the folding of proteins and enables only the properly folded protein to be trafficked via the ER. It is reported that Pex16 in *Y. lipolytica* which is responsible for peroxisomal division and assembly is targeted to peroxisomes after glycosylation in the ER.

Chapter 5

Characterization of the multiple domains of Pex30 involved in subcellular localization of the protein and regulation of peroxisome number

Abstract

Pex30 is a peroxisomal protein whose role in peroxisome biogenesis via the endoplasmic reticulum has been established. It is a 58 KDa multi-domain protein that facilitates contact site formation between various organelles. The present study aimed to investigate the role of various domains of the protein in its sub-cellular localization and regulation of peroxisome number. For this, we created six truncations of the protein (1-87, 1-250, 1-352, 88-523, 251-523 and 353-523) and tagged GFP at the C-terminus. Biochemical methods and fluorescence microscopy were used to characterize the effect of truncation on expression and localization of the protein. Quantitative analysis was performed to determine the effect of truncation on peroxisome number in these cells. Expression of the truncated variants in cells lacking PEX30 did not cause any effect on cell growth. Interestingly, variable expression and localization of the truncated variants in both peroxisome-inducing and non-inducing medium was observed. Truncated variants depicted different distribution patterns such as punctate, reticulate and cytosolic fluorescence. Interestingly, lack of the complete dysferlin domain or C-Dysf resulted in increased peroxisome number similar to as reported for cells lacking Pex30. No contribution of this domain in the reticulate distribution of the proteins was also observed. Our results show an interesting role for the various domains of Pex30 in localization and regulation of peroxisome number.

This chapter is published as

Deori NM, Infant T, Thummer RP, Nagotu S (2022) Characterization of multiple domains of Pex30 involved in subcellular localization of the protein and regulation of peroxisome number. Cell Biochem Biophys. https://doi.org/10.1007/s12013-022-01122-z

5.1 Introduction

Peroxisomes are dynamic organelles that are involved in a diverse array of cellular functions depending on metabolic requirements of the cell [17, 208]. Among their varied functions, peroxisomes are well studied for their role in β-oxidation of fatty acids and scavenging harmful ROS [182, 190]. Apart from these two major functions, they perform a multitude of functions based on the cell type and organism such as purine metabolism, biosynthesis of glycerolipids, and bile acids [209-211]. They proliferate either by growth and division of pre-existing peroxisomes or by *de novo* formation from the ER [105, 212]. Aberrations in peroxisomal membrane proteins or enzymes lead to multiple disorders in humans such as Zellweger syndrome, neonatal adrenoleukodystrophy, infantile refsum disease, *etc* [213, 214]. Therefore, an adequately functioning peroxisome is a prerequisite for maintaining the homeostasis of the cell.

Peroxisomal proteins (termed peroxins) are encoded by the nuclear genome, translated in the cytoplasm, and are either directly targeted to the peroxisomes by specific targeting signals (PTSs) or enroute via the ER [73, 215]. Pex30 is one such peroxin identified in *S. cerevisiae* which co-fractionated with Pex3, suggesting that it is primarily a peroxisomal membrane protein [172]. However, recent reports established that Pex30 also localizes to ER and lipid bodies [130, 160]. Deletion of Pex30 leads to altered number, function and inheritance of peroxisomes [129, 155]. Pex30 interacts with reticulon homology domain proteins (RHPs) such as Rtn1, Rtn2 and Yop1 and complements their function in maintaining tubular ER structure [87]. Interestingly, a role for Pex30 in promoting the budding of pre-peroxisomal vesicle (PPVs) from the ER was reported [160]. Localization of the protein to the nascent lipid bodies at the ER and its association with mature LDs has also been reported [160]. No significant changes in lipid body or TAG levels were observed upon loss of Pex30 [160]. On the other hand, deletion of Pex30 and the LD protein Seipin leads to dramatic lipidome

remodelling [142]. Whether Pex30 is involved in budding LDs from ER similar to PPVs is still evasive. Although the protein's function is studied to a certain extent, the effect of the different domains of the protein on its function is not properly understood.

Domains are functional, structural and evolutionary units of proteins [216]. A major portion of the eukaryotic proteome consists of multi-domain proteins [217]. Most of these domains are evolutionarily conserved and contributes specifically in regulating the function of proteins [218]. Domains of a protein may have different independent function or the function of one domain may be dependent on other domain(s) [218]. Hence, understanding the different domains may provide insights into the functioning of the protein.

Pex30 is a 523 amino acid protein and comprises of two distinct domains, the RHD (86-219 aa) and the dysferlin domain [87, 106]. The dysferlin domain is further categorized into the N-terminal dysferlin (284- 350 aa) and C-terminal dysferlin domain (375-408 aa) [87, 106]. The RHD and dysferlin domain are conserved across eukaryotes and are associated with different functions depending on the protein and organism [219, 220]. The RHD usually consists of hydrophobic transmembrane segments separated by a hydrophilic loop which help in ER retention and in maintaining high membrane curvature [221]. Interestingly, the dysferlin domain-only protein in *S. cerevisiae*, Spo73 was found to be involved in spore wall formation [222]. Earlier studies have reported that the human dysferlin protein is involved in Ca^{2+}-dependent plasma membrane repair and mutations in this protein result in muscular dystrophy [223]. Previous studies have investigated the role of these domains, but do not give a holistic view on the role of various domains of the protein in the sub-cellular distribution of the protein and on peroxisome biogenesis [106, 131]. In this study, we created GFP-tagged truncations of the protein to analyze the localization of these truncations to ER and peroxisome and also their role in regulating peroxisome number.

5.2 Results

5.2.1 Truncated variants of Pex30 exhibit altered expression and distribution

As mentioned earlier, Pex30 is a multi-domain protein consisting of a RHD, dysferlin domain and a domain of unknown function, DUF4196 [106]. Although studies have shown that Pex30 interacts with the ER reticulon proteins via its RHD domain, the functional characterization of its dysferlin domain has not been reported yet [87, 129]. In addition, contribution of different domains of Pex30 to its localization to peroxisomes and ER remains to be determined. To analyze the domain dependent localization and function of Pex30, six different truncated variants of the protein were constructed. A schematic illustration of the truncations generated in this study is depicted in Fig. 5.1.

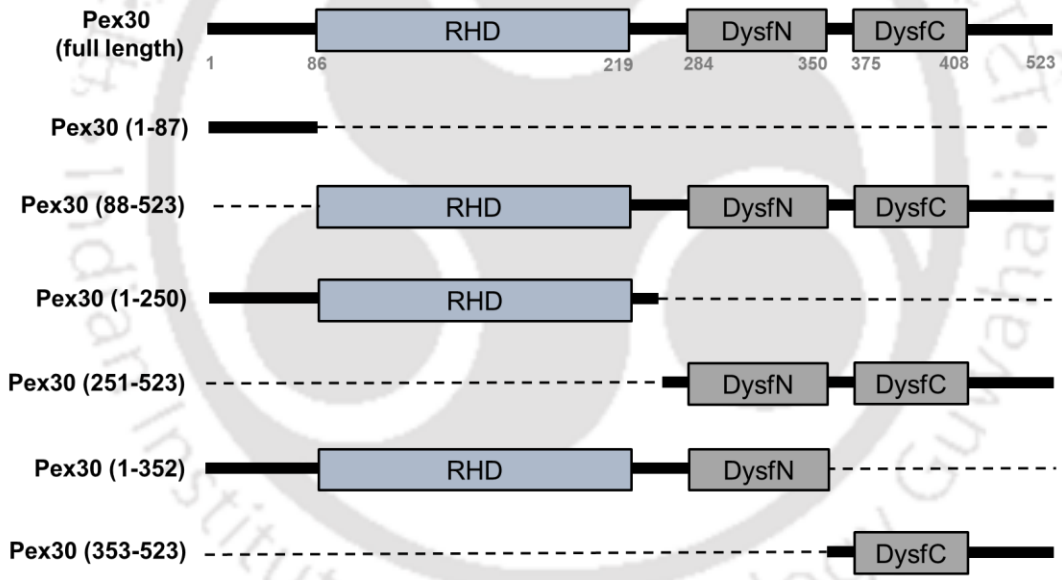

Fig. 5.1 Schematic representing the truncated variants generated in this study
Schematic representation of FL Pex30 and the six truncated variants generated in this study. The dashed line indicates the deleted regions.

The constructs with truncated forms of Pex30 were obtained by using the yeast expression vector pUG35 (Fig. 5.2) resulting in the C-terminal GFP tagging of all the constructs. The resulting plasmids were then introduced into *S. cerevisiae* Δpex30 strain and cultured in both YND and OA containing media.

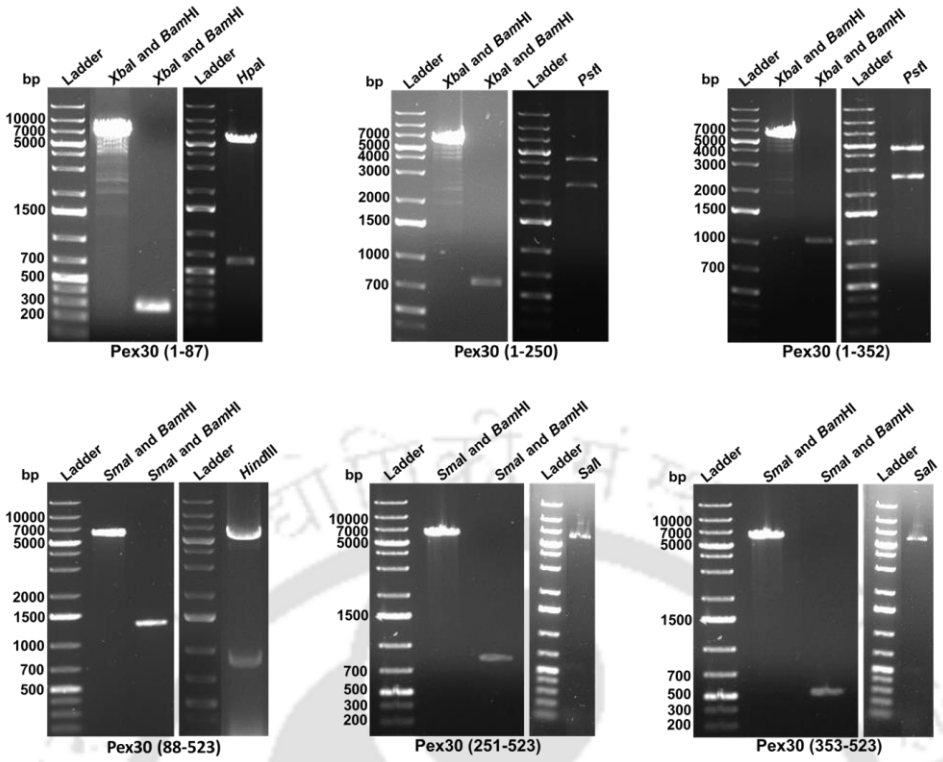

Fig. 5.2 Generation of truncated variants of Pex30
Different truncated variants of Pex30 were cloned in the pUG35 yeast expression vector and the resulting plasmids were confirmed by restriction digestion with specific restriction endonucleases.

The expression of these GFP-tagged truncations was analyzed by fluorescence microscopy and western blotting and compared with the full length (FL) protein. Our microscopy analysis indicates distinct phenotypes exhibited by each of these truncations (Fig. 5.3A and 5.3B).

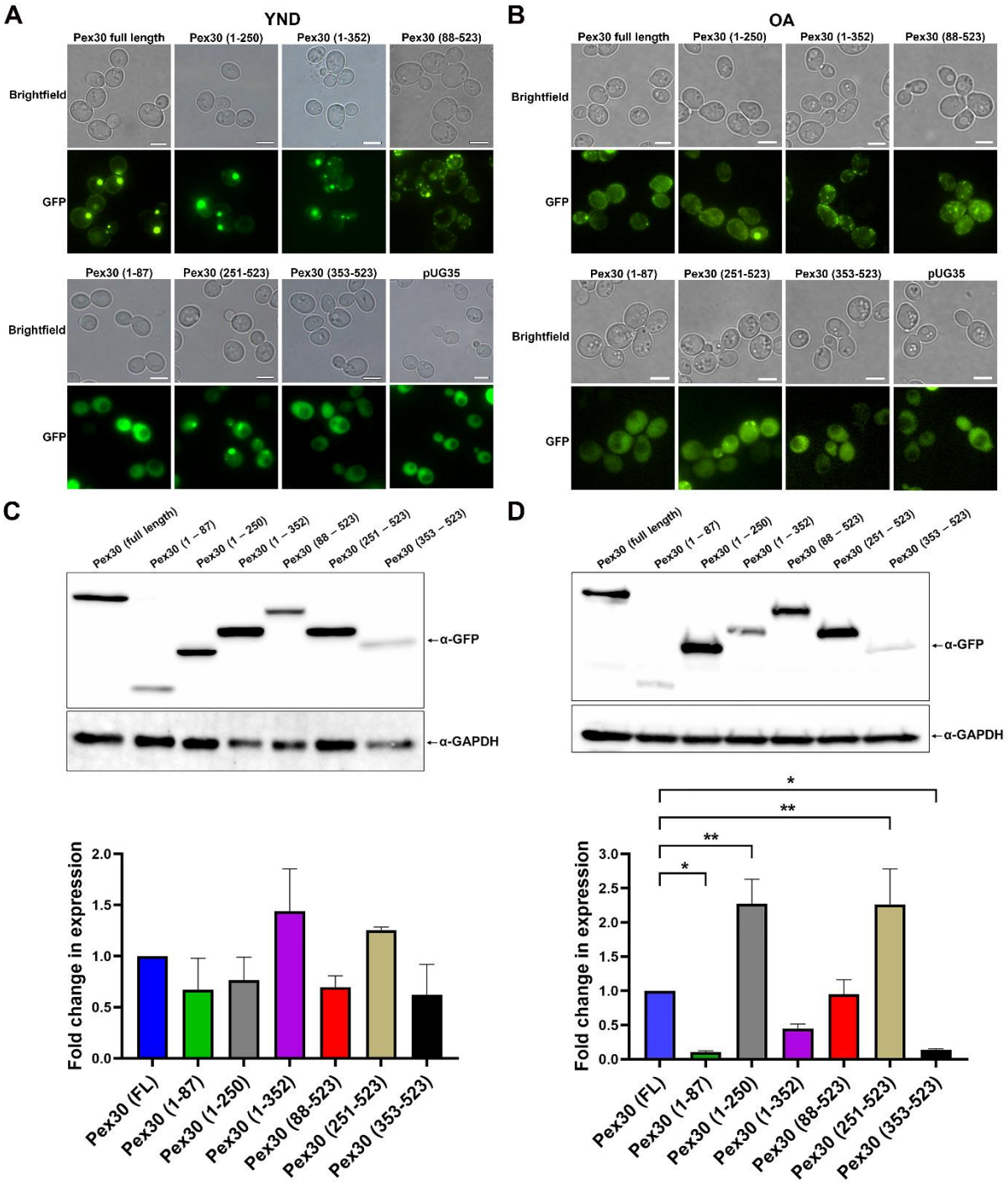

Fig. 5.3 Expression analysis of truncated variants of Pex30

(A) & **(B)**. Different phenotypes exhibited by truncated variants of Pex30 was examined by fluorescence microscopy. pex30Δ cells expressing FL Pex30 and the empty vector pUG35 was taken as control. Cells cultured in both YND and OA media were analyzed. Brightfield and fluorescence images corresponding to a group of cells from each strain are represented. Scale bar, 5 μm.

(C) & **(D)**. Analysis of protein expression levels of FL Pex30 and its truncated variants cultured in YND and oleic acid-containing media. Cells at the exponential growth phase were harvested by measuring the optical density that corresponds to 3 OD units. The whole cell extracts were separated by SDS-PAGE and subsequently analyzed via western blotting. Equal protein amounts were loaded into each lane. FL Pex30 and the truncated variants were detected by α-GFP antibody and GAPDH, used as a loading control, was probed using α-GAPDH antibody. Quantification of protein expression was performed by normalizing the GFP blots with GAPDH and the obtained data is represented in the form of bar graph. Data from two independent experiments were analysed and the SEM is displayed as error bars. The statistical difference was determined by using two-way ANOVA with multiple comparisons. $P < 0.05$ were significant (*); $P < 0.01$very significant (**).

The FL Pex30 exhibits discrete GFP puncta along with reticular distribution of GFP around the cell boundary in most cells cultured in YND media (Fig. 5.3A). On the contrary, cells cultured in OA media displayed two distinguishable phenotypes such as only reticulate and both reticulate and punctate (Fig. 5.3B) [180]. As reported in a previous study, the phenotype displayed by Pex30 (1-250) is similar to that exhibited by the FL protein [131] (Fig. 5.3A and 5.3B). Cells expressing Pex30 (1-352) and Pex30 (88-523) displayed an increase in GFP puncta that preferentially targeted to the cell periphery. Interestingly, it was observed that cells expressing the dysferlin domain, Pex30 (251-523) displayed both punctate as well as substantial cytosolic fluorescence. On the other hand, exclusively cytosolic fluorescence was observed in Pex30 (1-87) and Pex30 (353-523) expressing cells (Table 5.1). Expression of the truncated variants were also analyzed and compared with the FL protein by western blot analysis. (Fig. 5.3C and 5.3D). The difference in expression level was quantified and is illustrated as a fold change in protein expression. In YND cultured cells, expression levels of the truncated forms of Pex30 remain unaltered in comparison to FL Pex30 (Fig. 5.3C). On the other hand, in peroxisome-inducing OA media, cells expressing Pex30 (1-250) and Pex30 (251-523) displayed a significant increase in protein expression whereas cells expressing Pex30 (1-87) and Pex30 (353-523) depicted reduced expression when compared to the FL protein (Fig. 5.3D).

To understand if the altered expression levels of Pex30 truncations influences cell growth, the growth kinetics of cells expressing the truncated variants and FL Pex30 was analyzed (Fig. 5.4A and 5.4B). Cells expressing truncated variants of Pex30 did not differ in growth from cells expressing the FL Pex30 in both the YND and OA growth conditions.

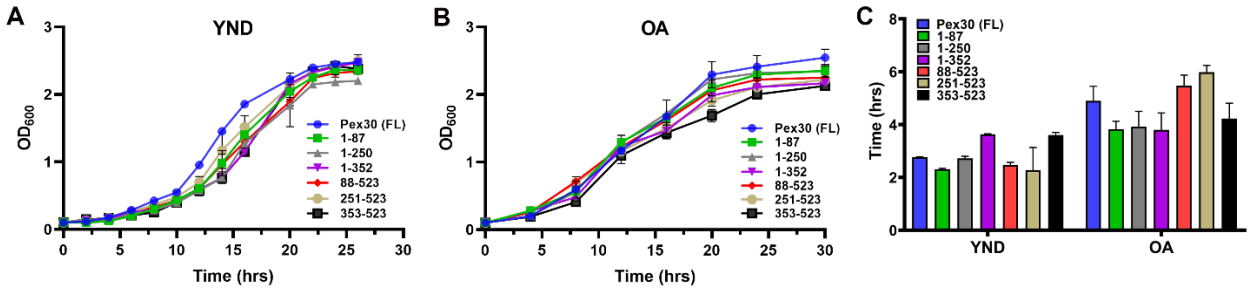

Fig. 5.4 Growth kinetics of cells expressing truncated variants of Pex30
Cells expressing truncated varaints of Pex30 were pre-cultured in glucose-containing YND media. The growth kinetics of yeast cells were then examined by shifting the cells to either fresh YND **(A)** or OA **(B)** media. Optical density (OD_{600}) of cells were measured at the indicated time-points. Doubling time was estimated by calculating the difference in growth rate of cells during exponential phase **(C)** Data from two independent experiments were analysed and the SEM is displayed as error bars.

5.2.2 Targeting of Pex30 to peroxisomes and ER is domain-dependent

To examine whether the domains of Pex30 have a role in the localization of the protein, the cells bearing truncated variants of the protein were co-transformed with plasmids that label peroxisomes or ER specifically and were cultured in both YND and OA media. GFP puncta signal of the FL Pex30 was observed in close proximity with the DsRed.SKL marked peroxisomes (Fig. 5.5A and 5.5.B). In addition, a partial co-localization was also observed between the Pex30 puncta and peroxisomes in some cells. Intensity line profiles depict the association between peroxisomes and the Pex30 puncta (Fig. 5.5A and 5.5.B). Similar co-localization between Pex30 and peroxisomes was reported earlier by David and co-workers [129]. The puncta exhibited by Pex30 (1-250), Pex30 (1-352), Pex30 (88-523) and Pex30 (251-523) displayed similar association with peroxisomes as observed in cells expressing FL Pex30 (Fig. 5.5A and 5.5.B).

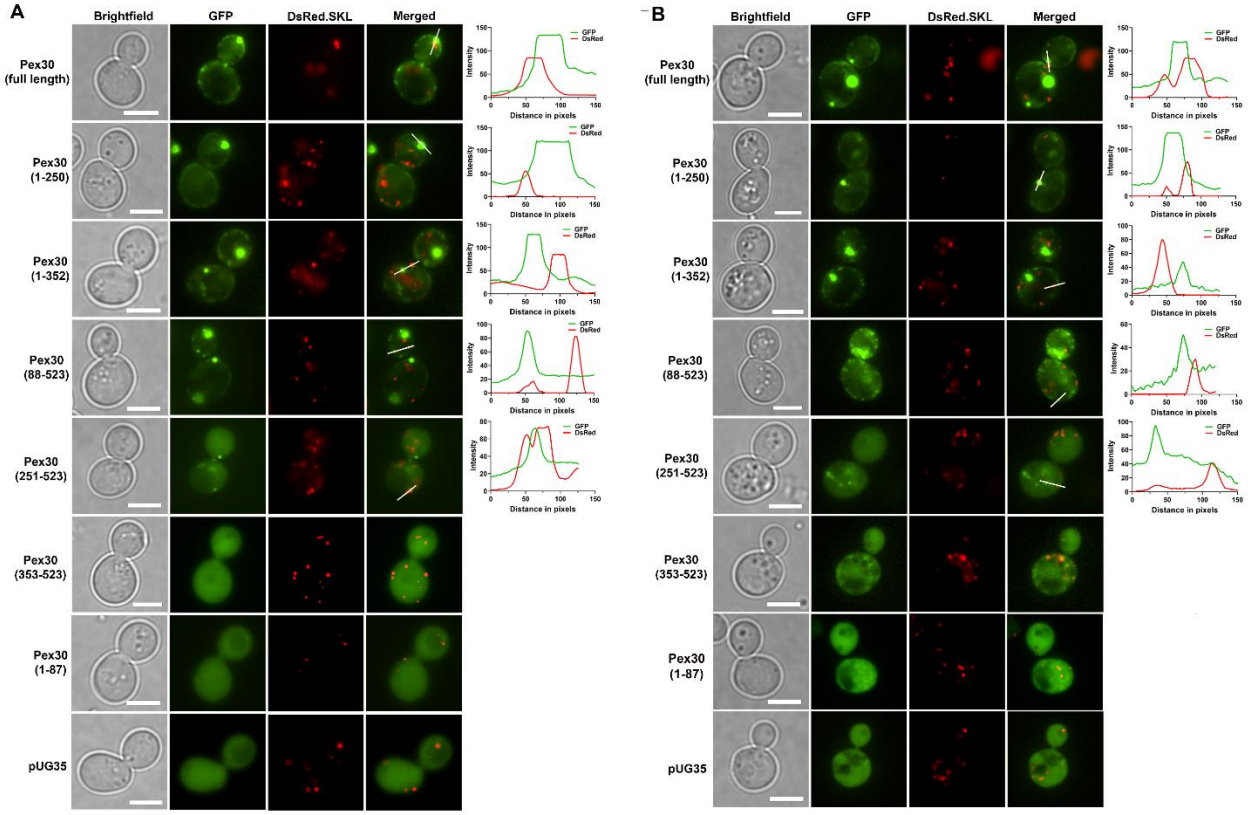

Fig. 5.5 Targeting of Pex30 truncated variants to peroxisomes
Cells of Δpex30 strain consisting truncated variants of Pex30 were co-expressed with DsRed.SKL to mark peroxisomes. The cells were cultured in both YND **(A)** and OA **(B)** media and subsequently, co-localization between GFP and DsRed was analyzed by fluorescence microscopy. Δpex30 cells containing the FL protein and the empty vector pUG35 co-expressed with DsRed.SKL were taken as control. The graph depicts relative fluorescence intensities of Pex30 (green) and peroxisomes (red) obtained from a single focal plane. ImageJ was used to measure the fluorescence intensities by a line drawn in the merged panel. Scale bar, 5 μm.

The targeting of Pex30 and its truncated forms to ER was analyzed by co-expressing Sec63-mRFP (Fig. 5.6). In accordance with previous study, the reticulate structure exhibited by FL Pex30 co-localizes with the cortical ER at the cell periphery [129] (Fig. 5.6). Our microscopy analysis also revealed similar association of the cortical ER with the reticulate-like phenotype of Pex30 (1-250) and the GFP puncta of Pex30 (1-352) and Pex30 (88-523). Moreover, the exclusive cytosolic fluorescence exhibited by cells expressing Pex30 (1-87) and Pex30 (353-523) indicates in-efficient targeting of the truncated protein to both peroxisomes and ER.

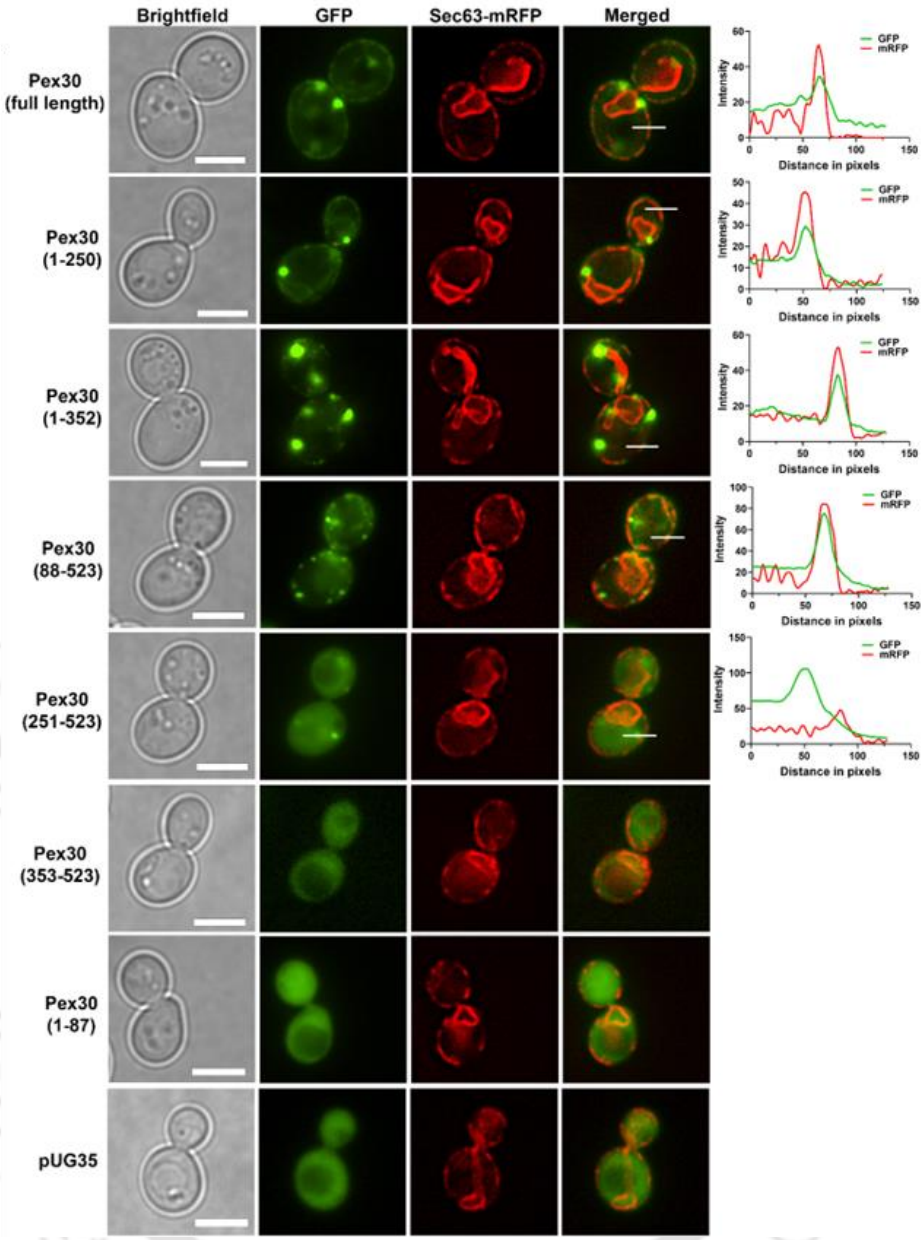

Fig. 5.6 Targeting of Pex30 truncated variants to ER
Sec63-mRFP (ER marker) was co-expressed in Δpex30 cells consisting Pex30 truncations and co-localization was analyzed by culturing the cells in YND media. Δpex30 cells containing the FL protein and the empty vector pUG35 co-expressed with Sec63-mRFP was taken as control. The graph depicts relative fluorescence intensities of Pex30 (green) and ER (red) obtained from a single focal plane. ImageJ was used to measure the fluorescence intensities by a line drawn in the merged panel. Scale bar, 5 μm.

5.2.3 Pex30 truncation results in altered peroxisome number

Earlier studies have reported a role for Pex30 in the regulation of peroxisome number [14, 18, 31]. Hence, we analysed if this regulation is particularly dependent on any domain of the protein. For this, peroxisome number was quantitatively determined in both YND and OA grown cells expressing the truncated variants (Fig. 5A and 5B). Cells expressing FL Pex30

depicted on an average 7.1 ± 1.4 peroxisomes on YND and 10.6 ± 2.6 peroxisomes when cultured in OA media. In comparison to cells expressing the FL Pex30, the Pex30 (1-250) and Pex30 (1-352) expressing cells displayed a significant increase in peroxisome number in both YND (8.7 ± 2.1, $p<0.001$ and 7.6 ± 2, $p<0.05$ respectively) and OA (12 ± 3.3, $p<0.001$ and 11.4 ± 2.7, $p<0.05$ respectively) medium. On the other hand, cells bearing Pex30 (353-523) displayed a significant reduction in peroxisome number in both YND and OA (6.2 ± 1.7, $p<0.05$; 9.5 ± 1.8; $p<0.01$) in comparison to cells expressing the FL Pex30 (Fig. 5A and 5B; Table 1). No significant change in peroxisome number was observed in cells expressing the truncated forms (1-87), (1-352), (88-523) and (251-523) when compared to FL Pex30 (Table 5.1). Similarly, the average number of peroxisomes observed in cells expressing the empty vector pUG35-GFP did not differ significantly in comparison to cells expressing the FL Pex30 (Fig. 5A and 5B).

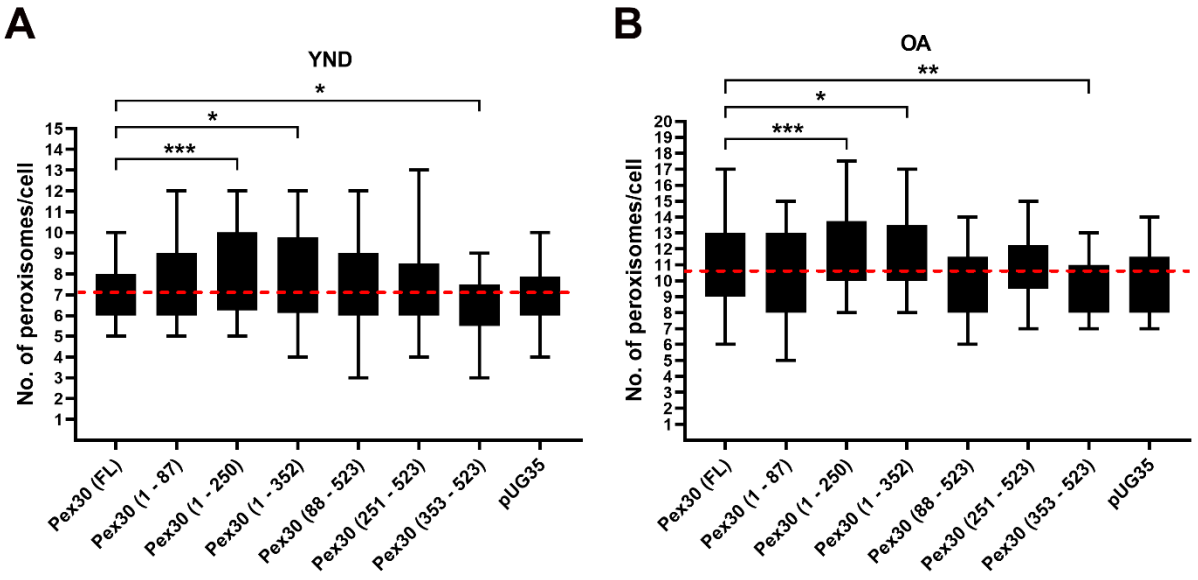

Fig. 5.7 Expression of truncated variants of Pex30 results in altered number of peroxisomes

A, B Peroxisome number in cells expressing truncated variants of Pex30 was examined and compared with cells expressing FL Pex30 in YND and OA growth conditions. Cell expressing pUG35-GFP (vector only) were taken as control. Peroxisomes were labelled with the marker protein DsRed.SKL. 40 cells from each strain were quantified from the merged Z-stack images using Image J. Data from two independent experiments were analyzed and illustrated as box and whisker plot. The mean peroxisome number of cells expressing FL Pex30 is shown as the red dashed line. Two-way ANOVA with multiple comparisons was used to obtain the statistical difference. $P < 0.05$ were significant (*); $P < 0.01$ very significant (**) and $P < 0.001$ extremely significant (***).

Table 5.1 Effect of Pex30 truncations on the distribution of the protein and regulation of peroxisome number

Sl. No.	Truncation	Distribution			Peroxisome number
		Punctate	Reticulate	Cytosolic	
1	Pex30 (1-87)	-	-	✓	NA
2	Pex30 (1-250)	✓	✓	-	↑
3	Pex30 (1-352)	✓	✓	-	↑
4	Pex30 (88-523)	✓	✓	-	NA
5	Pex30 (251-523)	✓	-	✓	NA
6	Pex30 (353-523)	-	-	✓	↓

Note: ✓: distribution exhibited by the particular truncated form, ↑: increase in peroxisome number, ↓: decrease in peroxisome number, NA: not altered

5.3 Discussion

Previous studies have highlighted the role of *S. cerevisiae* Pex30 in the formation of peroxisomes and regulation of their number [129, 130, 172]. Several interacting proteins and the complexes formed by Pex30 at the domains of ER have also been reported [87, 106, 129, 130]. Two important domains namely RHD and dysferlin domain have been identified in the protein and their role in protein interactions have been reported [87, 106]. However, the role of the various domains in the targeting of the protein to peroxisomes and ER and in regulating the peroxisome number has not been completely analyzed. To further study the role of the protein in peroxisome biogenesis we generated truncations of the protein namely 1-87, 1-250, 1-352, 88-523, 251-523 and 353-523 and analyzed these for the localization of the protein and role in regulating peroxisome number.

Recent studies by Ferreira and Carvalho also looked at truncations of Pex30 and studied the effect of these on the interaction of the protein with other peroxins such as Pex28, Pex29 and Pex32 [106]. Similar to earlier studies this study also showed that lack of dysferlin domain resulted in a peroxisome phenotype similar to Δpex30 [129, 131]. Interestingly, two truncations Δ60-160 and Δ161-190 that lack part of the RHD domain reported lower expression levels of Pex30 and its interacting proteins [106]. Earlier studies by Vizeacoumar and colleagues also looked at various truncations of the protein, however these were not analyzed for their targeting

to ER [131]. No alteration in the peroxisome targeting of the truncations that lack dysferlin domain was reported in this study. David and colleagues also reported an important role for the C-Dysf domain in regulating peroxisome number. This study however, did not look at the localization of the protein [129].

In this study all the generated truncations were tagged with GFP at their C-terminals and analyzed for their localization to peroxisomes and ER. Two truncations 1-87 and 353-523 displayed exclusively cytosolic fluorescence highlighting no role for these residues in the reticulate or punctate distribution of the protein. As expected, 251-523 that lacks the RHD domain did not show any reticulate distribution. This variant also exhibited cytosolic fluorescence along with punctate distribution suggesting that interactions needed for the localization of the protein at the ER may be lost resulting in cytosolic fluorescence signal. Surprisingly, 353-523 variant that in addition lacks the N-dysf domain (compared to 251-523) did not show any punctate distribution signifying its role in protein distribution. Two truncations 1-352 and 88-523 showed significant increase in the distribution of the protein (increased number of puncta) at the cell periphery. The distribution of the protein in all the truncations was observed to be similar in YND and OA grown cells. However, the expression of 1-87 and 353-523 was significantly reduced and 1-250 and 251-523 was significantly increased in OA. This could be due to altered interactions that may influence the steady state level of the protein. As reported earlier, 1-250 showed a significant increase in peroxisome number in both YND and OA cultured cells albeit no affect on the localization of the protein was observed. Interestingly, Ferreira and Carvalho also reported unaltered interactions of a similar construct with other peroxins belonging to this family [106]. On the other hand, increased number of peroxisomes was observed in 1-352 that lacks C-Dysf domain only, suggesting a role for these domains in regulating peroxisome number. Interestingly, this truncation also showed marked reduction in protein expression in OA cultured cells when

compared to the FL expressing cells. Though cytosolic fluorescence to some extent was observed in 251-523, the peroxisome number did not alter in this variant. Reduced number of peroxisomes was observed in 353-523 which lacks the N-Dysf domain additionally when compared to 251-523.

Our results suggest that RHD is indispensable for the proper localization of the protein and dysferlin domain may contribute meagerly to this. A role for Pex30 in membrane-contact site formation required for organelle biogenesis has been reported [106, 160]. Further studies can unravel if MCS are altered in these truncations.

Chapter 6

Conclusion and future perspectives

6.1 Conclusion

Peroxisome proliferation is governed by a set of proteins called peroxins that exerts an array of functions in the regulation of peroxisome dynamics. The growth and division and *de novo* biogenesis of peroxisomes occurs independent of each other. However, peroxins involved in different events of these two pathways may co-ordinate and intricately be linked. In this thesis, our study aims to characterize the function and localization of the peroxisomal membrane protein Pex30. The role of Pex30 as a negative regulator of peroxisome number has been reported by previous studies [129, 172]. Regulation of peroxisome proliferation by Pex30 varies among different yeast species. In *S. cerevisiae*, cells lacking Pex30 display an increase in normal-sized peroxisomes; while in *K. phaffii* the absence of this protein results in the appearance of fewer and enlarged peroxisomes [123, 172]. Most PMPs involved in the formation of peroxisomes are targeted to peroxisomes by mPTS that involves the receptor protein, Pex19 [68]. Pex30 also consists of putative Pex19 binding sites but instead it mostly localizes to specific ER subdomains and associates with the reticulon proteins in maintaining the tubular structure of ER [87, 131]. Pex30 in association with various ER-resident proteins regulates the formation of PPVs and nascent LDs [142]. Co-localization experiments have demonstrated that in addition to its localization to peroxisomes and ER, Pex30 also associates with mature LDs, indicating the dynamic localization of this protein to multiple organelles [151]. The interaction of Pex30 with proteins belonging to the same group is crucial in its targeting to MCSs between different organelles [106]. Pex30 has not yet been identified as a tether that facilitates the formation of MCSs between organelles but its dynamic association with different organelles and localization to multiple MCSs render it as a potential candidate protein that might function as a tether.

To decipher the mechanisms that regulate the function of Pex30, our study emphasised in understanding different facets involved in the regulation of this protein:

- Characterizing the phenotype of interacting partners of Pex30
- Characterizing the phosphorylation status of Pex30
- Characterizing the different domains of Pex30

To achieve our objectives, we first investigated the role of Pex30 interacting proteins in distribution and expression of the protein. Our data indicates that the distribution and expression of Pex30 is independent of its interacting proteins such as Mdm10, Pet10 and Erg6. As the function of Pex30 in regulation of peroxisome number is identified and proven and accepted by previous studies, we speculated whether the interacting proteins of Pex30 might also be involved in regulation of peroxisome proliferation. Quantification analysis indicates that cells lacking Mdm10 exhibits significant increase in peroxisome number as compared to WT cells. Taken together, our results suggest that although the distribution Pex30 is not affected by the deletion of Mdm10, the peroxisome abundance is altered in cell lacking Mdm10 which indicates that Mdm10 might associate with Pex30 or other peroxisomal proteins and regulate of peroxisome dynamics.

The effect of the PTM phosphorylation, on the targeting and function of Pex30 was studied. Pex30 was first purified to identify the presence of phosphorylated sites by mass spectrometry. The identified phosphorylated sites were subsequently mutated to non-phosphorylatable and phosphomimetic variants and the effect on localization and function of the protein was analyzed. Our results demonstrated that phosphorylation has no effect on the localization of Pex30 to both peroxisome and ER. Interestingly, a reduction in peroxisome number was displayed by the phosphomimetic variants when cultured in peroxisome-inducing media. Altogether our data indicates a role for phosphorylation of Pex30 in the regulation of peroxisome number.

The role of various domains of Pex30 in its sub-cellular localization and regulation of peroxisome number was studied. For this, we created six truncations of the protein (1-87, 1-

250, 1-352, 88-523, 251-523 and 353-523) and tagged GFP at the C-terminus. The truncated variants displayed differences in expression and localization patterns in both peroxisome inducing and non-inducing media. A variation in distribution patterns such as punctate, reticulate and cytosolic fluorescence was observed. Our results suggest that RHD is indispensable for the proper localization of the protein as truncations lacking this domain exhibit cytosolic fluorescence indicating mislocalization to cytosol. Intriguingly, lack of the complete dysferlin domain or C-Dysf resulted in an increase in peroxisome number similar to as observed in cells lacking Pex30. No contribution of this domain in the reticulate distribution of the proteins was also observed. In summary, our findings demonstrated interesting role for the various domains of Pex30 in localization and regulation of peroxisome number.

Our study has answered certain important questions with regard to the function of Pex30. These results have taken our understanding on this topic a step further. We do acknowledge few shortcomings in our study, that however may not alter the results significantly. Despite several attempts we were not successful in cloning the Pex30 fusion proteins under its native promoter. Earlier studies have also reported very faint signal when the protein was cloned under its own promoter [129]. However, the distribution of the full-length protein in our study was similar to that as published earlier [87, 129].

Global phospho-proteome studies have identified 17 putative sites that may undergo phosphorylation in *S. cerevisiae* Pex30. Interestingly, our experimental data identified only 3 residues (T60, S61 and S511) of which T60 and S61 have been reported earlier. This difference can be due to technical variations or growth conditions of the cells (media/cell-age/lysis conditions) as phosphorylation can be a very labile modification. Indeed, it would be interesting to study if the other sites also effect the phosphorylation status of the protein.

6.2 Future perspectives

- Our data indicates that phosphorylation most likely does not play an important role in the localization of Pex30 to peroxisomes or ER. Other mechanisms needed for this targeting should be investigated.
- Future studies can decipher if any Pex30 interactions are regulated by phosphorylation and the kinase that phosphorylates Pex30 can be identified.
- Whether the interaction of Pex30 with other proteins is influenced by the truncations generated in this study needs to be examined. In addition, whether the targeting of Pex30 to specific MCSs is altered in these truncations can also be investigated.
- Pex30 belongs to an important class of proteins that possess dysferlin domain. In humans, errors in proteins belonging to this family may lead to disease conditions called dysferlinopathies. Surprisingly, not much is known about the precise function of this domain. Thus, structural and functional analysis of proteins that contain this domain in other model systems such as yeast may contribute to the understanding of molecular aspects of these proteins.
- As in this study phosphorylation of Pex30 was analyzed only in the context of peroxisomal phenotype, it cannot be ruled out that this modification may have an effect on LD biogenesis.
- Finally, it is very intriguing to speculate that Pex30 might act as a tether or it might be a member of a tethering complex. However, this needs to be verified experimentally.
- The role of Pex30 in the formation of membrane contact sites during *de novo* biogenesis of peroxisomes and interaction of mature peroxisome with the ER needs to be investigated in detail. Peroxisomes are formed by two main pathways viz. growth and division of pre-existing peroxisome and de-novo biogenesis from the ER. The import of matrix and membrane proteins then facilitates the maturation of nascent peroxisomes

to a functional organelle. Proteins belonging to the Pex11 family proteins involved in the division of peroxisomes are expressed in both YND and OA-containing media. Notably, the expression of Pex11 is induced in oleic acid resulting in enhanced proliferation of peroxisomes. In the absence of functional peroxisomes, the ER plays an important role in the de-novo formation of peroxisomes by trafficking the peroxisomal membrane proteins that eventually pinch off in the form of PPVs. The ER-resident protein, Pex30 that negatively regulates peroxisome number associates with the ER-reticulon proteins and helps in maintaining the tubular structure of ER. An increase in peroxisome number was observed in cells lacking Pex30 when cultured in OA-containing media. However, a basal level of peroxisome proliferation was also observed in Δpex30 cells grown in YND media. A close association between Pex30 and peroxisomes was also observed in media containing oleic acid as the sole carbon source thereby suggesting the implication of carbon source supplemented in growth media in peroxisome dynamics. The maturation of nascent peroxisomes by the import of matrix and membrane proteins is facilitated by receptor proteins. One such protein is Pex9, a paralog of Pex5 that is responsible for the import of a limited number of PTS1 containing proteins to peroxisomes. Pex9 is induced in cells grown in OA-containing media and regulates the import of malate synthase to peroxisomes.

Further studies may aim to study the fate of other peroxins in both peroxisome inducing and non-inducing conditions and how such proteins influence peroxisome proliferation when cultured in media differing in carbon sources.

Bibliography

Bibliography

1. Schrader, M. and H.D. Fahimi, *The peroxisome: still a mysterious organelle.* Histochem Cell Biol, 2008. **129**(4): p. 421-40.
2. Waterham, H.R., S. Ferdinandusse, and R.J.A. Wanders, *Human disorders of peroxisome metabolism and biogenesis.* Biochimica et Biophysica Acta (BBA) - Molecular Cell Research, 2016. **1863**(5): p. 922-933.
3. Sibirny, A.A., *Yeast peroxisomes: structure, functions and biotechnological opportunities.* FEMS Yeast Research, 2016. **16**(4).
4. Bonekamp, N.A., et al., *Reactive oxygen species and peroxisomes: struggling for balance.* Biofactors, 2009. **35**(4): p. 346-55.
5. Fransen, M., et al., *Role of peroxisomes in ROS/RNS-metabolism: implications for human disease.* Biochim Biophys Acta, 2012. **1822**(9): p. 1363-73.
6. Poirier, Y., et al., *Peroxisomal beta-oxidation--a metabolic pathway with multiple functions.* Biochim Biophys Acta, 2006. **1763**(12): p. 1413-26.
7. Demarquoy, J. and F. Le Borgne, *Crosstalk between mitochondria and peroxisomes.* World J Biol Chem, 2015. **6**(4): p. 301-9.
8. Wanders, R.J., *Metabolic functions of peroxisomes in health and disease.* Biochimie, 2014. **98**: p. 36-44.
9. Hajra, A.K. and A.K. Das, *Lipid biosynthesis in peroxisomes.* Annals of the New York Academy of Sciences, 1996. **804**(1): p. 129-141.
10. Nagan, N. and R.A. Zoeller, *Plasmalogens: biosynthesis and functions.* Prog Lipid Res, 2001. **40**(3): p. 199-229.
11. Thai, T.P., et al., *Ether lipid biosynthesis: isolation and molecular characterization of human dihydroxyacetonephosphate acyltransferase.* FEBS Lett, 1997. **420**(2-3): p. 205-11.
12. Gallego-García, A., et al., *A bacterial light response reveals an orphan desaturase for human plasmalogen synthesis.* Science, 2019. **366**(6461): p. 128-132.
13. Werner, E.R., et al., *The TMEM189 gene encodes plasmanylethanolamine desaturase which introduces the characteristic vinyl ether double bond into plasmalogens.* 2020. **117**(14): p. 7792-7798.
14. Deb, R. and S. Nagotu, *Versatility of peroxisomes: An evolving concept.* Tissue and Cell, 2017. **49**: p. 209-226.
15. Wanders, R.J.A., H.R. Waterham, and S. Ferdinandusse, *Metabolic Interplay between Peroxisomes and Other Subcellular Organelles Including Mitochondria and the Endoplasmic Reticulum.* Frontiers in Cell and Developmental Biology, 2016. **3**(83).
16. Gunkel, K., et al., *Selective peroxisome degradation in Yarrowia lipolytica after a shift of cells from acetate/oleate/ethylamine into glucose/ammonium sulfate-containing media.* FEBS Lett, 1999. **451**(1): p. 1-4.
17. Deb, R. and S. Nagotu, *Versatility of peroxisomes: An evolving concept.* Tissue Cell, 2017. **49**(2, Part B): p. 209-226.
18. Kunze, M., et al., *A central role for the peroxisomal membrane in glyoxylate cycle function.* Biochim Biophys Acta, 2006. **1763**(12): p. 1441-52.
19. McCammon, M.T., et al., *Association of glyoxylate and beta-oxidation enzymes with peroxisomes of Saccharomyces cerevisiae.* J Bacteriol, 1990. **172**(10): p. 5816-27.
20. Yurimoto, H., M. Oku, and Y. Sakai, *Yeast methylotrophy: metabolism, gene regulation and peroxisome homeostasis.* Int J Microbiol, 2011. **2011**: p. 101298.
21. van der Klei, I.J., et al., *The significance of peroxisomes in methanol metabolism in methylotrophic yeast.* Biochim Biophys Acta, 2006. **1763**(12): p. 1453-62.
22. Dixit, E., et al., *Peroxisomes are signaling platforms for antiviral innate immunity.* Cell, 2010. **141**(4): p. 668-81.

23. Xu, Z., et al., *MicroRNAs upregulated during HIV infection target peroxisome biogenesis factors: Implications for virus biology, disease mechanisms and neuropathology.* PLOS Pathogens, 2017. **13**(6): p. e1006360.
24. Delmaghani, S., et al., *Hypervulnerability to Sound Exposure through Impaired Adaptive Proliferation of Peroxisomes.* Cell, 2015. **163**(4): p. 894-906.
25. Berger, J., et al., *Peroxisomes in brain development and function.* Biochim Biophys Acta, 2016. **1863**(5): p. 934-55.
26. Li, X., et al., *PEX11 beta deficiency is lethal and impairs neuronal migration but does not abrogate peroxisome function.* Mol Cell Biol, 2002. **22**(12): p. 4358-65.
27. Fransen, M., et al., *Aging, age-related diseases and peroxisomes.* Subcell Biochem, 2013. **69**: p. 45-65.
28. Goth, L., P. Rass, and A. Pay, *Catalase enzyme mutations and their association with diseases.* Mol Diagn, 2004. **8**(3): p. 141-9.
29. Hong, H. and B.S. Kim, *Pathophysiological Role of Neuroinflammation in Neurodegenerative Diseases and Psychiatric Disorders.* 2016. **20**(Suppl 1): p. S2-7.
30. Trompier, D., et al., *Brain peroxisomes.* Biochimie, 2014. **98**: p. 102-10.
31. Wright, J.J. and T.S. Tylee, *Pharmacologic Therapy of Type 2 Diabetes.* Med Clin North Am, 2016. **100**(4): p. 647-63.
32. Thorrez, L., et al., *Tissue-specific disallowance of housekeeping genes: the other face of cell differentiation.* Genome research, 2010. **21**: p. 95-105.
33. Elsner, M., W. Gehrmann, and S. Lenzen, *Peroxisome-generated hydrogen peroxide as important mediator of lipotoxicity in insulin-producing cells.* Diabetes, 2011. **60**(1): p. 200-8.
34. Gehrmann, W., M. Elsner, and S. Lenzen, *Role of metabolically generated reactive oxygen species for lipotoxicity in pancreatic beta-cells.* Diabetes Obes Metab, 2010. **12 Suppl 2**: p. 149-58.
35. Gehrmann, W., et al., *Antagonism Between Saturated and Unsaturated Fatty Acids in ROS Mediated Lipotoxicity in Rat Insulin-Producing Cells.* Cell Physiol Biochem, 2015. **36**(3): p. 852-65.
36. Plotz, T., et al., *The role of lipid droplet formation in the protection of unsaturated fatty acids against palmitic acid induced lipotoxicity to rat insulin-producing cells.* Nutr Metab (Lond), 2016. **13**: p. 16.
37. Hwang, I., et al., *Catalase deficiency accelerates diabetic renal injury through peroxisomal dysfunction.* Diabetes, 2012. **61**(3): p. 728-738.
38. Vasko, R., et al., *Endothelial peroxisomal dysfunction and impaired pexophagy promotes oxidative damage in lipopolysaccharide-induced acute kidney injury.* Antioxidants & redox signaling, 2013. **19**(3): p. 211-230.
39. Kim, D., et al., *Peroxisomal dysfunction is associated with up-regulation of apoptotic cell death via miR-223 induction in knee osteoarthritis patients with type 2 diabetes mellitus.* Bone, 2014. **64**: p. 124-131.
40. Lindfors, E., et al., *Detection of molecular paths associated with insulitis and type 1 diabetes in non-obese diabetic mouse.* PloS one, 2009. **4**(10): p. e7323.
41. Montagner, A., W. Wahli, and N.S. Tan, *Nuclear receptor peroxisome proliferator activated receptor (PPAR) beta/delta in skin wound healing and cancer.* Eur J Dermatol, 2015. **25 Suppl 1**: p. 4-11.
42. Syed, D.N. and H. Mukhtar, *Gender bias in skin cancer: role of catalase revealed.* Journal of Investigative Dermatology, 2012. **132**(3): p. 512-514.
43. Frederiks, W.M., et al., *Renal cell carcinoma and oxidative stress: the lack of peroxisomes.* Acta histochemica, 2010. **112**(4): p. 364-371.
44. Benjamin, D.I., et al., *Ether lipid generating enzyme AGPS alters the balance of structural and signaling lipids to fuel cancer pathogenicity.* Proceedings of the National Academy of Sciences, 2013. **110**(37): p. 14912-14917.

45. Rubin, M.A., et al., *α-Methylacyl coenzyme A racemase as a tissue biomarker for prostate cancer.* Jama, 2002. **287**(13): p. 1662-1670.
46. Doherty, J.R. and J.L. Cleveland, *Targeting lactate metabolism for cancer therapeutics.* The Journal of clinical investigation, 2013. **123**(9): p. 3685-3692.
47. Valença, I., et al., *Localization of MCT2 at peroxisomes is associated with malignant transformation in prostate cancer.* Journal of cellular and molecular medicine, 2015. **19**(4): p. 723-733.
48. Lloyd, M.D., et al., *α-Methylacyl-CoA racemase (AMACR): metabolic enzyme, drug metabolizer and cancer marker P504S.* Progress in lipid research, 2013. **52**(2): p. 220-230.
49. Uyama, T., et al., *Regulation of peroxisomal lipid metabolism by catalytic activity of tumor suppressor H-rev107.* Journal of Biological Chemistry, 2012. **287**(4): p. 2706-2718.
50. Uyama, T., et al., *Interaction of Phospholipase A/Acyltransferase-3 with Pex19p A POSSIBLE INVOLVEMENT IN THE DOWN-REGULATION OF PEROXISOMES.* Journal of Biological Chemistry, 2015. **290**(28): p. 17520-17534.
51. Luo, J., et al., *α-methylacyl-CoA racemase.* Cancer research, 2002. **62**(8): p. 2220-2226.
52. Tripathi, D.N. and C.L. Walker, *The peroxisome as a cell signaling organelle.* Curr Opin Cell Biol, 2016. **39**: p. 109-12.
53. Xi, J., et al., *A Nanozyme-Based Artificial Peroxisome Ameliorates Hyperuricemia and Ischemic Stroke.* 2021. **31**(9): p. 2007130.
54. Kulagina, N., et al., *Peroxisomes: A New Hub for Metabolic Engineering in Yeast.* 2021. **9**.
55. Hasan, S., H.W. Platta, and R. Erdmann, *Import of proteins into the peroxisomal matrix.* Front Physiol, 2013. **4**: p. 261.
56. Subramani, S., A. Koller, and W.B. Snyder, *Import of peroxisomal matrix and membrane proteins.* Annu Rev Biochem, 2000. **69**: p. 399-418.
57. Nötzel, C., et al., *Identification of New Fungal Peroxisomal Matrix Proteins and Revision of the PTS1 Consensus.* 2016. **17**(10): p. 1110-1124.
58. Petriv, O.I., et al., *A New Definition for the Consensus Sequence of the Peroxisome Targeting Signal Type 2.* Journal of Molecular Biology, 2004. **341**(1): p. 119-134.
59. Kempiński, B., et al., *The Peroxisomal Targeting Signal 3 (PTS3) of the Budding Yeast Acyl-CoA Oxidase Is a Signal Patch.* Front Cell Dev Biol, 2020. **8**: p. 198.
60. Effelsberg, D., et al., *Pex9p is a new yeast peroxisomal import receptor for PTS1-containing proteins.* Journal of Cell Science, 2016. **129**(21): p. 4057-4066.
61. Yifrach, E., et al., *Characterization of proteome dynamics during growth in oleate reveals a new peroxisome-targeting receptor.* Journal of Cell Science, 2016. **129**(21): p. 4067-4075.
62. Gabay-Maskit, S., et al., *A piggybacking mechanism enables peroxisomal localization of the glyoxylate cycle enzyme Mdh2 in yeast.* J Cell Sci, 2020. **133**(24).
63. Thoms, S., *Import of proteins into peroxisomes: piggybacking to a new home away from home.* 2015. **5**(11): p. 150148.
64. Kim, P.K. and E.H. Hettema, *Multiple pathways for protein transport to peroxisomes.* J Mol Biol, 2015. **427**(6 Pt A): p. 1176-90.
65. Santos, M.J., et al., *Peroxisomal Membrane Ghosts in Zellweger Syndrome--Aberrant Organelle Assembly.* Science, 1988. **239**(4847): p. 1536-1538.
66. Wendland, M. and S. Subramani, *Presence of cytoplasmic factors functional in peroxisomal protein import implicates organelle-associated defects in several human peroxisomal disorders.* The Journal of Clinical Investigation, 1993. **92**(5): p. 2462-2468.
67. van der Zand, A., et al., *Biochemically Distinct Vesicles from the Endoplasmic Reticulum Fuse to Form Peroxisomes.* Cell, 2012. **149**(2): p. 397-409.
68. Jansen, R.L.M. and I.J. van der Klei, *The peroxisome biogenesis factors Pex3 and Pex19: multitasking proteins with disputed functions.* 2019. **593**(5): p. 457-474.

69. Jones , J.M., J.C. Morrell , and S.J. Gould *PEX19 is a predominantly cytosolic chaperone and import receptor for class 1 peroxisomal membrane proteins.* Journal of Cell Biology, 2004. **164**(1): p. 57-67.
70. Hettema, E.H., et al., *Saccharomyces cerevisiae pex3p and pex19p are required for proper localization and stability of peroxisomal membrane proteins.* Embo j, 2000. **19**(2): p. 223-33.
71. Fang, Y., et al., *PEX3 functions as a PEX19 docking factor in the import of class I peroxisomal membrane proteins.* J Cell Biol, 2004. **164**(6): p. 863-75.
72. Dahan, N., et al., *Peroxisome function relies on organelle-associated mRNA translation.* 2022. **8**(2): p. eabk2141.
73. Mayerhofer, P.U., *Targeting and insertion of peroxisomal membrane proteins: ER trafficking versus direct delivery to peroxisomes.* Biochimica et Biophysica Acta (BBA) - Molecular Cell Research, 2016. **1863**(5): p. 870-880.
74. Agrawal, G. and S. Subramani, *De novo peroxisome biogenesis: Evolving concepts and conundrums.* Biochim Biophys Acta, 2016. **1863**(5): p. 892-901.
75. Wróblewska, J.P., et al., *Saccharomyces cerevisiae cells lacking Pex3 contain membrane vesicles that harbor a subset of peroxisomal membrane proteins.* Biochimica et Biophysica Acta (BBA) - Molecular Cell Research, 2017. **1864**(10): p. 1656-1667.
76. Knoops, K., et al., *Preperoxisomal vesicles can form in the absence of Pex3.* Journal of Cell Biology, 2014. **204**(5): p. 659-668.
77. Agrawal, G. and S. Subramani, *Emerging role of the endoplasmic reticulum in peroxisome biogenesis.* 2013. **4**.
78. Haan, G.-J., et al., *Reassembly of peroxisomes in Hansenula polymorpha pex3 cells on reintroduction of Pex3p involves the nuclear envelope.* FEMS Yeast Research, 2006. **6**(2): p. 186-194.
79. Hoepfner, D., et al., *Contribution of the Endoplasmic Reticulum to Peroxisome Formation.* Cell, 2005. **122**(1): p. 85-95.
80. van der Zand, A., I. Braakman, and H.F. Tabak, *Peroxisomal membrane proteins insert into the endoplasmic reticulum.* Mol Biol Cell, 2010. **21**(12): p. 2057-65.
81. Mast, F.D., et al., *ESCRT-III is required for scissioning new peroxisomes from the endoplasmic reticulum.* J Cell Biol, 2018. **217**(6): p. 2087-2102.
82. Munck, J.M., et al., *A dual function for Pex3p in peroxisome formation and inheritance.* J Cell Biol, 2009. **187**(4): p. 463-71.
83. Chang, J., et al., *Pex3 peroxisome biogenesis proteins function in peroxisome inheritance as class V myosin receptors.* J Cell Biol, 2009. **187**(2): p. 233-46.
84. Neuspiel, M., et al., *Cargo-Selected Transport from the Mitochondria to Peroxisomes Is Mediated by Vesicular Carriers.* Current Biology, 2008. **18**(2): p. 102-108.
85. Sugiura, A., et al., *Newly born peroxisomes are a hybrid of mitochondrial and ER-derived pre-peroxisomes.* Nature, 2017. **542**(7640): p. 251-254.
86. Zientara-Rytter, K.M., et al., *Recognition and Chaperoning by Pex19, Followed by Trafficking and Membrane Insertion of the Peroxisome Proliferation Protein, Pex11.* 2022. **11**(1): p. 157.
87. Joshi, A.S., et al., *A family of membrane-shaping proteins at ER subdomains regulates pre-peroxisomal vesicle biogenesis.* J Cell Biol, 2016. **215**(4): p. 515-529.
88. Opaliński, Ł., et al., *Membrane curvature during peroxisome fission requires Pex11.* Embo j, 2011. **30**(1): p. 5-16.
89. Huber, A., et al., *A Subtle Interplay Between Three Pex11 Proteins Shapes De Novo Formation and Fission of Peroxisomes.* 2012. **13**(1): p. 157-167.
90. Tower, R.J., et al., *The peroxin Pex34p functions with the Pex11 family of peroxisomal divisional proteins to regulate the peroxisome population in yeast.* 2011. **22**(10): p. 1727-1738.
91. Hoepfner , D., et al., *A role for Vps1p, actin, and the Myo2p motor in peroxisome abundance and inheritance in Saccharomyces cerevisiae.* Journal of Cell Biology, 2001. **155**(6): p. 979-990.

92. Kuravi, K., et al., *Dynamin-related proteins Vps1p and Dnm1p control peroxisome abundance in Saccharomyces cerevisiae.* J Cell Sci, 2006. **119**(Pt 19): p. 3994-4001.
93. Motley, A.M., G.P. Ward, and E.H. Hettema, *Dnm1p-dependent peroxisome fission requires Caf4p, Mdv1p and Fis1p.* J Cell Sci, 2008. **121**(Pt 10): p. 1633-40.
94. Nagotu, S., et al., *Peroxisome proliferation in Hansenula polymorpha requires Dnm1p which mediates fission but not de novo formation.* Biochimica et Biophysica Acta (BBA) - Molecular Cell Research, 2008. **1783**(5): p. 760-769.
95. Williams, C., et al., *The membrane remodeling protein Pex11p activates the GTPase Dnm1p during peroxisomal fission.* 2015. **112**(20): p. 6377-6382.
96. Motley , A.M. and E.H. Hettema *Yeast peroxisomes multiply by growth and division.* Journal of Cell Biology, 2007. **178**(3): p. 399-410.
97. Nagotu, S., et al., *Peroxisome Fission in Hansenula polymorpha Requires Mdv1 and Fis1, Two Proteins Also Involved in Mitochondrial Fission.* 2008. **9**(9): p. 1471-1484.
98. Krikken, A.M., M. Veenhuis, and I.J. van der Klei, *Hansenula polymorpha pex11 cells are affected in peroxisome retention.* 2009. **276**(5): p. 1429-1439.
99. Fagarasanu, A., et al., *The Peroxisomal Membrane Protein Inp2p Is the Peroxisome-Specific Receptor for the Myosin V Motor Myo2p of Saccharomyces cerevisiae.* Developmental Cell, 2006. **10**(5): p. 587-600.
100. Thomas, A.S., et al., *Phosphorylation of Pex11p does not regulate peroxisomal fission in the yeast Hansenula polymorpha.* Sci Rep, 2015. **5**(1): p. 11493.
101. Joshi, S., G. Agrawal, and S. Subramani, *Phosphorylation-dependent Pex11p and Fis1p interaction regulates peroxisome division.* 2012. **23**(7): p. 1307-1315.
102. Chang, J., et al., *An ancestral role in peroxisome assembly is retained by the divisional peroxin Pex11 in the yeast Yarrowia lipolytica.* Journal of Cell Science, 2015. **128**(7): p. 1327-1340.
103. Carmichael, R.E. and M. Schrader, *Determinants of Peroxisome Membrane Dynamics.* 2022. **13**.
104. Mast, F.D., R.A. Rachubinski, and J.D. Aitchison, *Peroxisome prognostications: Exploring the birth, life, and death of an organelle.* Journal of Cell Biology, 2020. **219**(3).
105. Farré, J.-C., et al., *Peroxisome biogenesis, membrane contact sites, and quality control.* 2019. **20**(1): p. e46864.
106. Ferreira, J.V. and P. Carvalho, *Pex30-like proteins function as adaptors at distinct ER membrane contact sites.* J Cell Biol, 2021. **220**(10): p. e202103176.
107. Koch, J. and C. Brocard, *Membrane elongation factors in organelle maintenance: the case of peroxisome proliferation.* Biomol Concepts, 2011. **2**(5): p. 353-364.
108. Akşit, A. and I.J. van der Klei, *Yeast peroxisomes: How are they formed and how do they grow?* Int J Biochem Cell Biol, 2018. **105**: p. 24-34.
109. Kiel, J.A.K.W., M. Veenhuis, and I.J. van der Klei, *PEX Genes in Fungal Genomes: Common, Rare or Redundant.* 2006. **7**(10): p. 1291-1303.
110. Küberl, A., et al., *High-quality genome sequence of Pichia pastoris CBS7435.* Journal of Biotechnology, 2011. **154**(4): p. 312-320.
111. van Zutphen, T., et al., *Adaptation of Hansenula polymorpha to methanol: a transcriptome analysis.* BMC Genomics, 2010. **11**(1): p. 1.
112. Farré, J.-C., et al., *A New Yeast Peroxin, Pex36, a Functional Homolog of Mammalian PEX16, Functions in the ER-to-Peroxisome Traffic of Peroxisomal Membrane Proteins.* Journal of Molecular Biology, 2017. **429**(23): p. 3743-3762.
113. Erdmann, R. and G. Blobel, *Giant peroxisomes in oleic acid-induced Saccharomyces cerevisiae lacking the peroxisomal membrane protein Pmp27p.* Journal of Cell Biology, 1995. **128**(4): p. 509-523.
114. Cepińska, M.N., et al., *Peroxisome Fission is Associated with Reorganization of Specific Membrane Proteins.* 2011. **12**(7): p. 925-937.

115. Su, J., et al., *The N-terminal amphipathic helix of Pex11p self-interacts to induce membrane remodelling during peroxisome fission.* Biochimica et Biophysica Acta (BBA) - Biomembranes, 2018. **1860**(6): p. 1292-1300.
116. Mindthoff, S., et al., *Peroxisomal Pex11 is a pore-forming protein homologous to TRPM channels.* Biochimica et Biophysica Acta (BBA) - Molecular Cell Research, 2016. **1863**(2): p. 271-283.
117. Rottensteiner, H., et al., *Conserved function of pex11p and the novel pex25p and pex27p in peroxisome biogenesis.* Mol Biol Cell, 2003. **14**(10): p. 4316-28.
118. Marelli , M., et al., *Quantitative mass spectrometry reveals a role for the GTPase Rho1p in actin organization on the peroxisome membrane.* Journal of Cell Biology, 2004. **167**(6): p. 1099-1112.
119. Agrawal, G., et al., *Functional regions of the peroxin Pex19 necessary for peroxisome biogenesis.* J Biol Chem, 2017. **292**(27): p. 11547-11560.
120. Infant, T., et al., *Post-translational modifications of proteins associated with yeast peroxisome membrane: An essential mode of regulatory mechanism.* Genes Cells, 2021. **00**: p. 1-18.
121. Knoblach, B. and R.A. Rachubinski, *Phosphorylation-dependent activation of peroxisome proliferator protein PEX11 controls peroxisome abundance.* J Biol Chem, 2010. **285**(9): p. 6670-80.
122. Wu, F., et al., *Pex24 and Pex32 are required to tether peroxisomes to the ER for organelle biogenesis, positioning and segregation in yeast.* Journal of Cell Science, 2020. **133**(16).
123. Yan, M., et al., *Dysferlin domain-containing proteins, Pex30p and Pex31p, localized to two compartments, control the number and size of oleate-induced peroxisomes in Pichia pastoris.* Molecular biology of the cell, 2008. **19**(3): p. 885-898.
124. Jansen, R.L.M., et al., *Comparative Genomics of Peroxisome Biogenesis Proteins: Making Sense of the PEX Proteins.* 2021. **9**.
125. Vizeacoumar, F.J., et al., *Pex30p, Pex31p, and Pex32p Form a Family of Peroxisomal Integral Membrane Proteins Regulating Peroxisome Size and Number in Saccharomyces cerevisiae.* 2004. **15**(2): p. 665-677.
126. Vizeacoumar , F.J., et al., *YHR150w and YDR479c encode peroxisomal integral membrane proteins involved in the regulation of peroxisome number, size, and distribution in Saccharomyces cerevisiae.* Journal of Cell Biology, 2003. **161**(2): p. 321-332.
127. Brown, T.W., V.I. Titorenko, and R.A. Rachubinski, *Mutants of the Yarrowia lipolytica PEX23 gene encoding an integral peroxisomal membrane peroxin mislocalize matrix proteins and accumulate vesicles containing peroxisomal matrix and membrane proteins.* Mol Biol Cell, 2000. **11**(1): p. 141-52.
128. Tam, Y.Y. and R.A. Rachubinski, *Yarrowia lipolytica cells mutant for the PEX24 gene encoding a peroxisomal membrane peroxin mislocalize peroxisomal proteins and accumulate membrane structures containing both peroxisomal matrix and membrane proteins.* Mol Biol Cell, 2002. **13**(8): p. 2681-91.
129. David, C., et al., *A combined approach of quantitative interaction proteomics and live-cell imaging reveals a regulatory role for endoplasmic reticulum (ER) reticulon homology proteins in peroxisome biogenesis.* Mol Cell Proteomics, 2013. **12**(9): p. 2408-25.
130. Mast, F.D., et al., *Peroxins Pex30 and Pex29 Dynamically Associate with Reticulons to Regulate Peroxisome Biogenesis from the Endoplasmic Reticulum.* J Biol Chem, 2016. **291**(30): p. 15408-27.
131. Vizeacoumar, F.J., et al., *Pex19p Binds Pex30p and Pex32p at Regions Required for Their Peroxisomal Localization but Separate from Their Peroxisomal Targeting Signals *.* Journal of Biological Chemistry, 2006. **281**(21): p. 14805-14812.
132. Helle, S.C.J., et al., *Organization and function of membrane contact sites.* Biochimica et Biophysica Acta (BBA) - Molecular Cell Research, 2013. **1833**(11): p. 2526-2541.

133. Prinz, W.A., A. Toulmay, and T. Balla, *The functional universe of membrane contact sites.* Nature Reviews Molecular Cell Biology, 2020. **21**(1): p. 7-24.
134. Sargsyan, Y. and S. Thoms, *Staying in Healthy Contact: How Peroxisomes Interact with Other Cell Organelles.* Trends in Molecular Medicine, 2020. **26**(2): p. 201-214.
135. Shai, N., M. Schuldiner, and E. Zalckvar, *No peroxisome is an island — Peroxisome contact sites.* Biochimica et Biophysica Acta (BBA) - Molecular Cell Research, 2016. **1863**(5): p. 1061-1069.
136. Silva, B.S.C., et al., *Maintaining social contacts: The physiological relevance of organelle interactions.* Biochimica et Biophysica Acta (BBA) - Molecular Cell Research, 2020. **1867**(11): p. 118800.
137. Agrawal, G. and S. Subramani, *De novo peroxisome biogenesis: Evolving concepts and conundrums.* Biochimica et biophysica acta, 2016. **1863**(5): p. 892-901.
138. Raychaudhuri, S. and W.A. Prinz, *Nonvesicular phospholipid transfer between peroxisomes and the endoplasmic reticulum.* 2008. **105**(41): p. 15785-15790.
139. Petrova, V.Y., et al., *Dual targeting of yeast catalase A to peroxisomes and mitochondria.* Biochem J, 2004. **380**(Pt 2): p. 393-400.
140. Cohen, Y., et al., *Peroxisomes are juxtaposed to strategic sites on mitochondria.* Molecular BioSystems, 2014. **10**(7): p. 1742-1748.
141. Binns , D., et al., *An intimate collaboration between peroxisomes and lipid bodies.* Journal of Cell Biology, 2006. **173**(5): p. 719-731.
142. Wang, S., et al., *Seipin and the membrane-shaping protein Pex30 cooperate in organelle budding from the endoplasmic reticulum.* Nat Commun, 2018. **9**(1): p. 2939.
143. Wanders, R.J.A., H.R. Waterham, and S. Ferdinandusse, *Metabolic Interplay between Peroxisomes and Other Subcellular Organelles Including Mitochondria and the Endoplasmic Reticulum.* 2016. **3**.
144. Walton, P., *Effects of peroxisomal catalase inhibition on mitochondrial function.* 2012. **3**.
145. Lismont, C., et al., *Redox interplay between mitochondria and peroxisomes.* 2015. **3**.
146. Farre, J.-C., et al., *OXPHOS deficiencies affect peroxisome proliferation by downregulating genes controlled by the SNF1 signaling pathway.* eLife, 2022. **11**: p. e75143.
147. Mattiazzi Ušaj, M., et al., *Genome-Wide Localization Study of Yeast Pex11 Identifies Peroxisome–Mitochondria Interactions through the ERMES Complex.* Journal of Molecular Biology, 2015. **427**(11): p. 2072-2087.
148. Liu, X., X. Wen, and D.J. Klionsky, *ER-mitochondria contacts are required for pexophagy in Saccharomyces cerevisiae.* Contact (Thousand Oaks), 2018. **2**.
149. Esposito, M., S. Hermann-Le Denmat, and A. Delahodde, *Contribution of ERMES subunits to mature peroxisome abundance.* PLOS ONE, 2019. **14**(3): p. e0214287.
150. Shai, N., et al., *Systematic mapping of contact sites reveals tethers and a function for the peroxisome-mitochondria contact.* Nature Communications, 2018. **9**(1): p. 1761.
151. Choudhary, V., et al., *Seipin and Nem1 establish discrete ER subdomains to initiate yeast lipid droplet biogenesis.* Journal of Cell Biology, 2020. **219**(7).
152. Novikoff , P.M. and A.B. Novikoff *PEROXISOMES IN ABSORPTIVE CELLS OF MAMMALIAN SMALL INTESTINE.* Journal of Cell Biology, 1972. **53**(2): p. 532-560.
153. Joshi, A.S., H. Zhang, and W.A. Prinz, *Organelle biogenesis in the endoplasmic reticulum.* Nature Cell Biology, 2017. **19**(8): p. 876-882.
154. Tabak, H.F., I. Braakman, and A.v.d. Zand, *Peroxisome Formation and Maintenance Are Dependent on the Endoplasmic Reticulum.* 2013. **82**(1): p. 723-744.
155. Knoblach, B., et al., *An ER-peroxisome tether exerts peroxisome population control in yeast.* The EMBO journal, 2013. **32**(18): p. 2439-2453.
156. Joshi, A.S., *Peroxisomal Membrane Contact Sites in Yeasts.* 2021. **9**.
157. Yuan, W., et al., *Yeast Vps13 is Crucial for Peroxisome Expansion in Cells With Reduced Peroxisome-ER Contact Sites.* 2022. **10**.

158. Bascom, R.A., H. Chan, and R.A. Rachubinski, *Peroxisome Biogenesis Occurs in an Unsynchronized Manner in Close Association with the Endoplasmic Reticulum in Temperature-sensitiveYarrowia lipolytica Pex3p Mutants.* 2003. **14**(3): p. 939-957.
159. Pu, J., et al., *Interactomic study on interaction between lipid droplets and mitochondria.* Protein & Cell, 2011. **2**(6): p. 487-496.
160. Joshi, A.S., et al., *Lipid droplet and peroxisome biogenesis occur at the same ER subdomains.* Nat Commun, 2018. **9**(1): p. 2940.
161. Sandager, L., et al., *Storage Lipid Synthesis Is Non-essential in Yeast*.* Journal of Biological Chemistry, 2002. **277**(8): p. 6478-6482.
162. Wang, W. and B.A. Malcolm, *Two-stage PCR protocol allowing introduction of multiple mutations, deletions and insertions using QuikChange Site-Directed Mutagenesis.* Biotechniques, 1999. **26**(4): p. 680-2.
163. Gietz, R.D. and A. Sugino, *New yeast-Escherichia coli shuttle vectors constructed with in vitro mutagenized yeast genes lacking six-base pair restriction sites.* Gene, 1988. **74**(2): p. 527-34.
164. Haridhasapavalan, K.K., et al., *Generation of cell-permeant recombinant human transcription factor GATA4 from E. coli.* Bioproc Biosyst Eng, 2021. **44**(6): p. 1131-1146.
165. Micsonai, A., et al., *BeStSel: a web server for accurate protein secondary structure prediction and fold recognition from the circular dichroism spectra.* Nucleic Acids Res, 2018. **46**(W1): p. W315-W322.
166. Micsonai, A., et al., *Accurate secondary structure prediction and fold recognition for circular dichroism spectroscopy.* Proc Natl Acad Sci USA, 2015. **112**(24): p. E3095-103.
167. Olsen, J.V., et al., *Parts per Million Mass Accuracy on an Orbitrap Mass Spectrometer via Lock Mass Injection into a C-trap.* Mol Cell Proteomics, 2005. **4**(12): p. 2010-2021.
168. Kinoshita, E., E. Kinoshita-Kikuta, and T. Koike, *Separation and detection of large phosphoproteins using Phos-tag SDS-PAGE.* Nat Protoc, 2009. **4**(10): p. 1513-21.
169. Baerends, R.J., et al., *A stretch of positively charged amino acids at the N terminus of Hansenula polymorpha Pex3p is involved in incorporation of the protein into the peroxisomal membrane.* J Biol Chem, 2000. **275**(14): p. 9986-95.
170. Lowry, O., et al., *PROTEIN MEASUREMENT WITH THE FOLIN PHENOL REAGENT.* J Biol Chem, 1951. **193**(1): p. 265-275.
171. Metzger, M.B., et al., *Degradation of a cytosolic protein requires endoplasmic reticulum-associated degradation machinery.* J Biol Chem, 2008. **283**(47): p. 32302-16.
172. Vizeacoumar, F.J., et al., *Pex30p, Pex31p, and Pex32p form a family of peroxisomal integral membrane proteins regulating peroxisome size and number in Saccharomyces cerevisiae.* Mol Biol Cell, 2004. **15**(2): p. 665-77.
173. Yanagida, M., *Functional proteomics; current achievements.* Journal of Chromatography B, 2002. **771**(1): p. 89-106.
174. Lv, Q., et al., *Genome-wide protein-protein interactions and protein function exploration in cyanobacteria.* Scientific Reports, 2015. **5**(1): p. 15519.
175. von Mering, C., et al., *Comparative assessment of large-scale data sets of protein–protein interactions.* Nature, 2002. **417**(6887): p. 399-403.
176. Gao, Q., et al., *Pet10p is a yeast perilipin that stabilizes lipid droplets and promotes their assembly.* J Cell Biol, 2017. **216**(10): p. 3199-3217.
177. Jordá, T. and S. Puig, *Regulation of Ergosterol Biosynthesis in Saccharomyces cerevisiae.* Genes (Basel), 2020. **11**(7).
178. Meisinger, C., et al., *The Mitochondrial Morphology Protein Mdm10 Functions in Assembly of the Preprotein Translocase of the Outer Membrane.* Developmental Cell, 2004. **7**(1): p. 61-71.
179. Ellenrieder, L., et al., *Separating mitochondrial protein assembly and endoplasmic reticulum tethering by selective coupling of Mdm10.* Nature Communications, 2016. **7**(1): p. 13021.
180. Deori, N.M., et al., *Pex30 undergoes phosphorylation and regulates peroxisome number in Saccharomyces cerevisiae.* Molecular Genetics and Genomics, 2022.

181. Kunau, W.-H., V. Dommes, and H. Schulz, *β-Oxidation of fatty acids in mitochondria, peroxisomes, and bacteria: A century of continued progress.* Prog Lipid Res, 1995. **34**(4): p. 267-342.
182. Poirier, Y., et al., *Peroxisomal β-oxidation—A metabolic pathway with multiple functions.* BBA-Mol Cell Res, 2006. **1763**(12): p. 1413-1426.
183. Cohen, P., *The origins of protein phosphorylation.* Nat Cell Biol, 2002. **4**(5): p. E127-E130.
184. Taylor, S.S., et al., *Evolution of the eukaryotic protein kinases as dynamic molecular switches.* Philos Trans R Soc Lond Ser B Biol Sci, 2012. **367**(1602): p. 2517-28.
185. Hunter, T., *Why nature chose phosphate to modify proteins.* Philos Trans R Soc Lond Ser B Biol Sci, 2012. **367**(1602): p. 2513-2516.
186. Johnson, L.N. and D. Barford, *The Effects of Phosphorylation on the Structure and Function of Proteins.* Annu Rev Biophys Biomol Struct, 1993. **22**(1): p. 199-232.
187. Balta, E.-A., et al., *Phosphorylation Modulates the Subcellular Localization of SOX11.* Front Mol Neurosci, 2018. **11**(211).
188. Nishi, H., K. Hashimoto, and Anna R. Panchenko, *Phosphorylation in Protein-Protein Binding: Effect on Stability and Function.* Structure, 2011. **19**(12): p. 1807-1815.
189. Vlastaridis, P., et al., *Estimating the total number of phosphoproteins and phosphorylation sites in eukaryotic proteomes.* GigaScience, 2017. **6**(2): p. 1-11.
190. Deori, N.M., et al., *Peroxisomes: role in cellular ageing and age related disorders.* Biogerontology, 2018. **19**(5): p. 303-324.
191. Zutphen, T., M. Veenhuis, and I.J. van der Klei, *Pex14 is the sole component of the peroxisomal translocon that is required for pexophagy.* Autophagy, 2008. **4**(1): p. 63-6.
192. Zhang, J., et al., *ATM functions at the peroxisome to induce pexophagy in response to ROS.* Nat Cell Biol, 2015. **17**(10): p. 1259-1269.
193. Saleem, R.A., et al., *Integrated phosphoproteomics analysis of a signaling network governing nutrient response and peroxisome induction.* Mol Cell Proteomics, 2010. **9**(9): p. 2076-88.
194. Oeljeklaus, S., et al., *Regulation of peroxisome dynamics by phosphorylation.* BBA-Mol. Cell Res., 2016. **1863**(5): p. 1027-37.
195. Schummer, A., et al., *Pex14p Phosphorylation Modulates Import of Citrate Synthase 2 Into Peroxisomes in Saccharomyces cerevisiae.* Front Cell Dev Biol, 2020. **8**: p. 955.
196. Okumoto, K., et al., *The peroxisome counteracts oxidative stresses by suppressing catalase import via Pex14 phosphorylation.* Elife, 2020. **9**.
197. Joshi, S., G. Agrawal, and S. Subramani, *Phosphorylation-dependent Pex11p and Fis1p interaction regulates peroxisome division.* Mol Biol Cell, 2012. **23**(7): p. 1307-15.
198. Lanz, M.C., et al., *In-depth and 3-dimensional exploration of the budding yeast phosphoproteome.* EMBO Rep, 2021. **22**(2): p. e51121.
199. Swaney, D.L., et al., *Global analysis of phosphorylation and ubiquitylation cross-talk in protein degradation.* Nat Methods, 2013. **10**(7): p. 676-82.
200. Albuquerque, C.P., et al., *A multidimensional chromatography technology for in-depth phosphoproteome analysis.* Mol Cell Proteomics, 2008. **7**(7): p. 1389-96.
201. Kelly, S.M., T.J. Jess, and N.C. Price, *How to study proteins by circular dichroism.* BBA-Proteins Proteomics, 2005. **1751**(2): p. 119-39.
202. Greenfield, N.J., *Using circular dichroism spectra to estimate protein secondary structure.* Nat Protoc, 2006. **1**(6): p. 2876-2890.
203. Jumper, J., et al., *Highly accurate protein structure prediction with AlphaFold.* Nature, 2021. **596**(7873): p. 583-589.
204. Hildebrand, A., et al., *Fast and accurate automatic structure prediction with HHpred.* Proteins, 2009. **77 Suppl 9**: p. 128-32.
205. Sievers, F., et al., *Fast, scalable generation of high-quality protein multiple sequence alignments using Clustal Omega.* Mol Syst Biol, 2011. **7**(1): p. 539.

206. Léger, J., et al., *Conversion of Serine to Aspartate Imitates Phosphorylation-induced Changes in the Structure and Function of Microtubule-associated Protein Tau *.* J Biol Chem, 1997. **272**(13): p. 8441-8446.
207. Sula, A., et al., *Crystal structures of the human Dysferlin inner DysF domain.* BMC Struct Biol, 2014. **14**: p. 3-3.
208. Pan, R., et al., *Peroxisomes: versatile organelles with diverse roles in plants.* 2020. **225**(4): p. 1410-1427.
209. Ferdinandusse, S. and S.M. Houten, *Peroxisomes and bile acid biosynthesis.* Biochimica et Biophysica Acta (BBA) - Molecular Cell Research, 2006. **1763**(12): p. 1427-1440.
210. Lodhi, Irfan J. and Clay F. Semenkovich, *Peroxisomes: A Nexus for Lipid Metabolism and Cellular Signaling.* Cell Metabolism, 2014. **19**(3): p. 380-392.
211. Hayashi, S., S. Fujiwara, and T. Noguchi, *Evolution of urate-degrading enzymes in animal peroxisomes.* Cell Biochemistry and Biophysics, 2000. **32**(1): p. 123-129.
212. Islinger, M., et al., *The peroxisome: an update on mysteries 2.0.* Histochemistry and Cell Biology, 2018. **150**(5): p. 443-471.
213. Fujiki, Y., et al., *Recent insights into peroxisome biogenesis and associated diseases.* Journal of Cell Science, 2020. **133**(9).
214. Braverman, N.E., M.D. D'Agostino, and G.E. MacLean, *Peroxisome biogenesis disorders: Biological, clinical and pathophysiological perspectives.* 2013. **17**(3): p. 187-196.
215. Walter, T. and R. Erdmann, *Current Advances in Protein Import into Peroxisomes.* The Protein Journal, 2019. **38**(3): p. 351-362.
216. Aziz, M.F. and G. Caetano-Anollés, *Evolution of networks of protein domain organization.* Scientific Reports, 2021. **11**(1): p. 12075.
217. Basu, M.K., E. Poliakov, and I.B. Rogozin, *Domain mobility in proteins: functional and evolutionary implications.* Briefings in Bioinformatics, 2009. **10**(3): p. 205-216.
218. Forslund, S.K., M. Kaduk, and E.L.L. Sonnhammer, *Evolution of Protein Domain Architectures*, in *Evolutionary Genomics: Statistical and Computational Methods*, M. Anisimova, Editor. 2019, Springer New York: New York, NY. p. 469-504.
219. Yang, Y.S. and S.M. Strittmatter, *The reticulons: a family of proteins with diverse functions.* Genome biology, 2007. **8**(12): p. 234-234.
220. Lek, A., et al., *Phylogenetic analysis of ferlin genes reveals ancient eukaryotic origins.* BMC Evolutionary Biology, 2010. **10**(1): p. 231.
221. D'Eletto, M., S. Oliverio, and F. Di Sano, *Reticulon Homology Domain-Containing Proteins and ER-Phagy.* 2020. **8**.
222. Okumura, Y., et al., *The Dysferlin Domain-Only Protein, Spo73, Is Required for Prospore Membrane Extension in Saccharomyces cerevisiae.* 2016. **1**(1): p. e00038-15.
223. Liu, J., et al., *Dysferlin, a novel skeletal muscle gene, is mutated in Miyoshi myopathy and limb girdle muscular dystrophy.* Nature Genetics, 1998. **20**(1): p. 31-36.

List of Publications, Conferences & Workshops attended, Awards and Achievements

Publications from Ph.D thesis:

- **Deori NM**, Infant T, Thummer RP, Nagotu S (2022) Characterization of multiple domains of Pex30 involved in subcellular localization of the protein and regulation of peroxisome number. Cell Biochem Biophys. https://doi.org/10.1007/s12013-022-01122-z
- **Deori NM**, Nagotu S (2022) Peroxisome biogenesis and inter-organelle communication: an indispensable role for Pex11 and Pex30 family proteins in yeast. Current Genetics 68, 537–550. https://doi.org/10.1007/s00294-022-01254-y
- **Deori NM**, Infant T, Sundaravadivelu PK, Thummer RP, Nagotu S (2022) Pex30 undergoes phosphorylation and regulates peroxisome number in *Saccharomyces cerevisiae*. Molecular Genetics and Genomics 297:573-590. 10.1007/s00438-022-01872-8
- **Deori NM**, Kale A, Maurya PK, Nagotu S (2018) Peroxisomes: role in cellular ageing and age-related disorders. Biogerontology 19:303-324. 10.1007/s10522-018-9761-9

Publications from collaborative research:

- Glingston S, Rajpoot J, **Deori NM**, Deb R, Kumar S, Nagotu S (2021) Characterization of nucleocapsid and matrix proteins of Newcastle disease virus in yeast. 3 Biotech 11:65. 10.1007/s13205-020-02624-4
- Pathak S, Tripathi S, **Deori NM**, Ahmad B, Verma H, Lokhande R, Nagotu S, Kale A (2021) Effect of tetracycline family of antibiotics on actin aggregation, resulting in the formation of Hirano bodies responsible for neuropathological disorders. J Biomol Struct Dyn 39:236-253. 10.1080/07391102.2020.1717629
- Pathak S, **Deori NM**, Sharma A, Nagotu S, Kale A (2020) In vitro, in vivo and in silico rationale for the muscle loss due to therapeutic drugs used in the treatment of

Mycobacterium tuberculosis infection. J Biomol Struct Dyn:1-17. 10.1080/07391102.2020.1806928

- **Deori NM**, Deb R, Banerjee R, Nagotu S (2017). Yeast: A multifaceted eukaryotic microbe and its biotechnological applications. Advances in Microbial Biotechnology: Current Trends and Future Prospects.

Conferences and Workshops attended:

- National Conference on Advances in Microbiology (MiCON), Yenepoya Research Center, India (2022) (Oral presentation).
- Research and Industrial Conclave-22, Indian Institute of Technology Guwahati, Guwahati, India (2022) (Oral presentation).
- International Conference on Yeast Biology and Filamentous Fungi, University of Hyderabad, Hyderabad, India (2019) (Poster presentation).
- 20th Indo-Us Flow Cytometry Symposium Cum Workshop on Applications of Flow Cytometry in Biotechnology, organized by Indian Institute of Technology Guwahati, Guwahati, India (2019).
- Research Conclave-19 organized by Students' Academic Board, Indian Institute of Technology Guwahati, Guwahati, India (2019) (Poster presentation).
- 10th Conference on Yeast Biology-2018, Jawaharlal Nehru University, New Delhi (Poster Presentation).
- Advanced microscopy and imaging techniques, jointly organized by DSS imagetech Pvt. Ltd., Olympus medical systems India Pvt. Ltd. and supported by Indian Institute of Technology Guwahati at IIT Guwahati, Guwahati (2017).
- Research Conclave-17 organized by Students' Academic Board, Indian Institute of Technology Guwahati, 2017 (Poster presentation).

Awards and Achievements:

- Received best oral presentation award at **Research and Industrial Conclave,** IIT-Guwahati, Guwahati, India (2022).
- Received best poster presentation award at **International Conference on Yeast Biology and Filamentous Fungi**, University of Hyderabad, Hyderabad, India (2019).